AD_____

Award Number: W81XWH-08-1-0405

TITLE: 9th Annual UC Systemwide Bioengineering Symposium

PRINCIPAL INVESTIGATOR: Victor G. J. Rodgers

CONTRACTING ORGANIZATION: University of California
Riverside, CA, 92521

REPORT DATE: August 2008

TYPE OF REPORT: Final Proceedings

PREPARED FOR: U.S. Army Medical Research and Materiel Command
Fort Detrick, Maryland 21702-5012

DISTRIBUTION STATEMENT: Approved for Public Release;
Distribution Unlimited

REPORT DOCUMENTATION PAGE

Form Approved
OMB No. 0704-0188

1. REPORT DATE *(DD-MM-YYYY)*	**2. REPORT TYPE**	**3. DATES COVERED** *(From - To)*
01-08-2008	Final Proceedings	20 JUN 2008-22 JUN 2008

4. TITLE AND SUBTITLE

9th Annual UC Systemwide Bioengineering Symposium

5a. CONTRACT NUMBER

5b. GRANT NUMBER
W81XWH-08-1-0405

5c. PROGRAM ELEMENT NUMBER

6. AUTHOR(S)
Victor G. J. Rodgers

E-Mail: vrodgers@engr.ucr.edu

5d. PROJECT NUMBER

5e. TASK NUMBER

5f. WORK UNIT NUMBER

7. PERFORMING ORGANIZATION NAME(S) AND ADDRESS(ES)

University of California
Riverside, CA, 92521

8. PERFORMING ORGANIZATION REPORT NUMBER

9. SPONSORING / MONITORING AGENCY NAME(S) AND ADDRESS(ES)
U.S. Army Medical Research and Materiel Command
Fort Detrick, Maryland 21702-5012

10. SPONSOR/MONITOR'S ACRONYM(S)

11. SPONSOR/MONITOR'S REPORT NUMBER(S)

12. DISTRIBUTION / AVAILABILITY STATEMENT
Approved for Public Release; Distribution Unlimited

13. SUPPLEMENTARY NOTES

14. ABSTRACT
No abstract provided.

15. SUBJECT TERMS
No subject terms provided.

16. SECURITY CLASSIFICATION OF:			**17. LIMITATION OF ABSTRACT**	**18. NUMBER OF PAGES**	**19a. NAME OF RESPONSIBLE PERSON**
a. REPORT	**b. ABSTRACT**	**c. THIS PAGE**			USAMRMC
U	U	U	UU	149	**19b. TELEPHONE NUMBER** *(include area code)*

UNIVERSITY OF CALIFORNIA
UC RIVERSIDE
BOURNS COLLEGE OF ENGINEERING

9th Annual UC Systemwide Bioengineering Symposium

Final Report, GOR W81XWH-08-1-0405

Principal Investigator
Victor G. J. Rodgers
Professor,
Bioengineering
A237
University of California
Riverside, CA, 92521
Phone: (951) 827- 6241
951) 827-6416
E-mail: vrodgers@engr.ucr.edu

Staff Contact
Denise Sanders
Management Services Officer
A220 Bourns Hall
University of
California
Riverside, CA, 92521
Phone: (951) 827-5025
Fax: (951) 827-6416
E-mail: denise@engr.ucr.edu

July 30, 2008

Prepared for:
Commander
U.S. Army Medical Research and Material Command
Attn: MCRR-ZC-I
504 Scott Street
Fort Detrick, MD 21702-9218

1. Summary

The Bourns College of Engineering thanks the USA Med Research ACQ (TATRC) program for supporting the 9th Annual UC Systemwide Bioengineering Symposium. The theme of this conference was to increase the synergistic interaction of the University of California's vast biomedical engineering research expertise with the practical medical and healthcare engineering undertaken by biomedical firms and government agencies. The symposium had 204 attendees representing all ten UC campuses as well as interested corporate and government agencies and individuals in the community. The symposium was supported by seven corporate sponsors and had four partnerships with industrial and government agencies.

The symposium had twelve tracks that covered a broad range of topics to represent most research in Bioengineering at the University of California. In all, 48 talks and 49 posters were presented. In addition, five major presentations were given including three keynote speakers and two speakers representing TATRC.

Through our generous corporate support, twelve cash awards totaling $5,000 were given to student oral and poster presenters who were judged to be outstanding. Judges were members of the UC, TATRC and our corporate sponsors. The program schedule is attached.

2. Attendance

Total attendance at the two-day event was 204 persons with representation from community organizations, local high schools, government agencies, industry, and academia.

3. Academic Institution Representation

All ten University of California campuses were represented. In addition students in the National Science Foundation BRITE (Bioengineering Research Institute for Technical Excellence) REU at UCR were also present. The attendance list is attached.

4. Industry and Government Representation

In addition to the UC Bioengineering campuses, seven corporate sponsors were also represented at the symposium. These include: Genentech, Gilead, ResMed, Abbott Vascular, Boston Scientific, BioRad and Penguin Computing. In addition, government representation from TATRC (Telemedicine Advanced Technology Research Center), and the UC Discovery Grant were present and CHI (California Healthcare Institute) and the Southern California Biomedical Council were represented.

5. Significant Achievements

General

The goals of the 9th Annual Systemwide Bioengineering Symposium (www.bioeng.ucr.edu/2008UCBES) was to increase stronger government and industrial connections with bioengineering research at UC and increase the involvement of the UC researchers in the symposium. The 9th Annual Symposium at UC Riverside included industrial interactions from biotech firms, a published conference proceedings and a special addition of Biotechnology Progress that focuses on the highest quality presented work. In addition, twelve student prizes totaling $5,000 cash were awarded.

To help increase the synergistic interaction of the UC campuses, industry and the government agencies, representatives from various components on these groups volunteered to help with the student poster and presentation judging. In addition the scientific subcommittee included members from both UCR and UC Merced. Information tables manned by representatives were available for the sponsors.

We were particularly fortunate to have a slate of keynote speakers who are national leaders in our field. Included as keynote or special guest were: John Anderson, President of Illinois Institute of Technology; Don Giddens, Dean of Engineering of Georgia Tech; Christine Kelley, Director of Discovery Science and Technology at NIBIB at NIH, Eva Lai from TATRC and Song Li from UC Berkeley representing TATRC.

Student Awards

The corporate sponsors provided support for twelve student awards. The award recipients for the podium competition were (recipient is underlined for each award);

- Genentech 1st Place Award ($750)
    - Improving the spatial resolution and sensitivity of small animal PET scanners. Sara St. James, Yongfeng Yang, Yibao Wu, Richard Farrell, Purushottam Dokhale, Kanai, S. Shah and Simon R. Cherry, UCD/Radiation Monitoring Devices Inc., Watertown, MA
- Genentech 2nd Place Award ($500)
    - Engineering Transferrin Mutants to Enhance Targeted Drug Delivery. Dennis J. Yoon David S. H. Chu, Christopher W. Ng, Edward A. Pham, Anne B. Mason, David Hudson, Valerie C. Smith, Ross T. A. MacGillivray and Daniel T. Kamei, UCLA/U Vermont/UBC
- Boston Scientific 2nd Place Award ($500)
    - Thermal Modeling and Experimental Validation of Hair and Skin Tissue Heated by Intense Pulsed Light. Feng Sun, Alex Chaney and Guillermo Aguilar, UCR
- Genentech 3rd Place Award ($250)
    - Microfabricated Cylindrical Wells Facilitate Single-Molecule Enzymology of Bovine α-Chymotrypsin. Angela Y. Chen, A.S. Jani, L. Zheng, P.J. Burke and James P. Brody, UCI
- Boston Scientific 3rd Place Award ($250)

    - Bioengineering of Polymeric Drug Carriers for Cancer Therapeutics Using Computational Modeling. Lili X. Peng, Robert Swift, Anthony Ivetac, Sang Van, J. Andrew McCammon, Lei Yu, Stephen B. Howell and David A. Gough, UCSD/Nitto Denko Technology Corporation
- Genentech 3rd Place Award ($250)
    - A Novel AC Electrokinetic Cell and Nanoparticle Separation Device for Cancer Diagnostics. Rajaram Krishnan, Benjamin D. Sullivan, Jason Steiner, Sergio Sandoval, Sadik C. Esener and Michael J. Heller, UCSD.

The award recipients for the poster competition were (recipient is underlined for each award);

- Genentech 1st Place Award ($750)
    - Assembly of Micropatterned Co-Cultures on Conductive and Optically Transparent ITO Substrates. Sunny Shah, Ji Youn Lee and Alexander Revzin. UCD
- ResMed 2nd Place Award ($500)
    - Computational Investigation of Transient Heat Transport through a Porous Filled Heat Exchanger Applicable in Biological Sciences. Shadi Mahjoob. UCR
- Abbott Vascular 2nd Place Award ($500)
    - Quantitative Conversion of Alcohols to Aldehydes Using Alcohol Dehydrogenase. Sean Guthrie and Valentine I. Vullev. UCR
- Abbott Vascular 3rd Place Award ($250)
    - Self-Assembly and DNA Binding Properties of bZip Peptide Amphiphiles. Rachel Marullo, Raymond Tu and Matthew Tirrell,UCSB
- Genentech 3rd Place Award ($250)
    - Temperature Measurements of Laser Irradiation for Tissue Protection During Cryosurgery. L. Martínez-Suástegui, G. Aguilar, F. Godinez and A. M. Walker. UCR
- ResMed 3rd Place Award ($250)
    - Prospective Study of the Effectiveness of Thermal Imaging in the Diagnosis of Arthritis: Can a Radiometric Thermal Imager Detect Pre-clinical Stages of Arthritisin a Quick and Noninvasive Test? Shay Edwards. Norco High School

Exit Evaluation

In addition, an exit survey was available for all attendees. The evaluation form is attached. A total of 31 evaluations were completed. The question that summarized this specific symposium the most asked to rate the conference on "Overall Conference, Organization, Structure and Execution". The results were a 4.8 $\pm$ 0.57 out of 5, indicating that this symposium was very successful.

Attachment: Program Summary

Final Conference Agenda

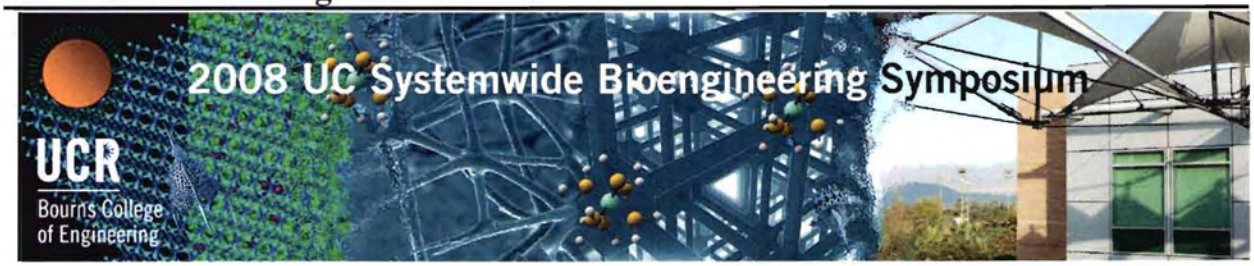

Time and Date	Event
Friday, June 20, 2008	*All events will be held at the Historic Mission Inn & Spa*
5:00 – 8:00 pm	**Check–In and Registration** *(Spanish Art Galley in the Mission Inn)*
6:00 – 8:00 pm	**Reception** *(Spanish Art Galley in the Mission Inn)*
6:00 – 7:00 pm	**Welcome & Introduction of Keynote Speaker: Reza Abbaschian** **Keynote Speaker: Don P. Giddens** **Dean, College of Engineering, Georgia Institute of Technology** ***"Know Your Arteries, Know Thyself"*** *(Spanish Art Galley in the Mission Inn)*
Saturday, June 21, 2008	*All events will be held at the UC Riverside Commons*
6:30 – 7:00 am	**Highlander Trolley to UCR Campus from Mission Inn and Marriott** *(Hotel Entrances)*
7:00 – 8:00 am	**Check–In and Registration** *(Lobby of 302 Commons)*
7:00 – 8:00 am	**Breakfast** *(Lobby and 302A Commons)*
7:00 – 8:00 am	**Bioengineering Institute of California Steering Committee Meeting** *(260 Commons)*
7:00 – 8:00 am	**Exhibitor Set-Up** *(302B Commons)*
7:00 – 7:30 am	**Poster Session I Set-Up** *(302B Commons)*
7:00 – 8:00 am	**Judges Check–In** *(268 Commons)*
8:00 am– 6:00 pm	**Exhibitor Tables Open** *(302B Commons)*
8:00 – 8:10 am	**Welcome & Introduction: Jerome Schultz** *(302A Commons)*
8:15 – 9:00 am	**TATRC Presentation** **Eva Lai, PhD (TATRC)** ***"Introduction to TATRC"*** **Song Li, PhD (UCB)** ***"Nanofibers for Nerve Regeneration"*** *(302A Commons)*
9:15 – 9:30 am	*Coffee Break* *(Lobby of 302 Commons)*

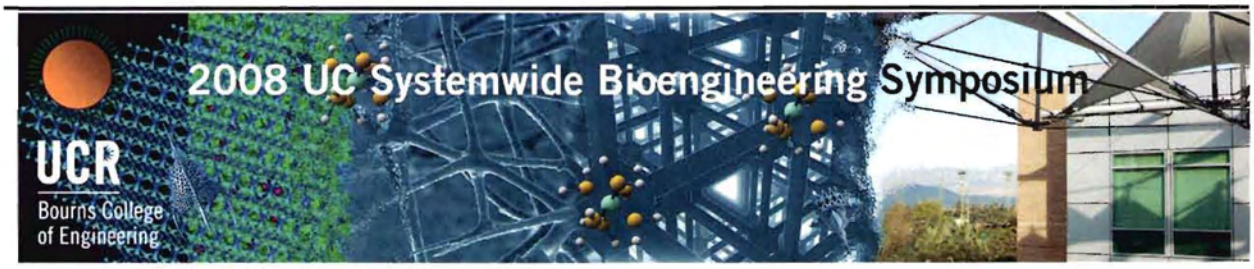

Time and Date	Event		
		Podium Session I	
9:30 – 11:00 am	Track 1 Bioinformatics & Genomics Chair: J. Liao (UCR) *(379 Commons)*	Track 2 Biomedical Imaging I Chair: J. Lyubovitsky (UCR) *(355 Commons)*	Track 3 Nanotechnology & BioMEMS Chair: M. Khine (UCM) *(367 Commons)*
Saturday, June 21, 2008	*All events will be held at the UC Riverside Commons*		
11:00 am – 12:00 pm		**Poster Session I** Chair: B. Anvari (UCR) *(302B Commons)*	
12:00 pm – 1:00 pm		**Lunch** *(Lobby and 302A Commons)*	
		Podium Session II	
1:00 – 2:30 pm	Track 4 Biocomputation, *in Silico* & Biosystems Modeling Chair: D. Morikis (UCR) *(379 Commons)*	Track 5 Tissue Engineering Chair: G. Aguilar (UCR) *(367 Commons)*	Track 6 Biomaterials Chair: V. Vullev (UCR) *(355 Commons)*
2:30 - 2:45 pm		*Coffee Break* *(Lobby of 302 Commons)* **Judges Meeting** *(268 Commons)*	
		Podium Session III	
2:45 – 4:15 pm	Track 7 Molecular & Cellular Engineering Chair: J. Liao (UCR) *(355 Commons)*	Track 8 Drug Delivery & Targeting Chair: G. Aguilar (UCR) *(379 Commons)*	Track 9 Biomechanics & Biodevices Chair: M. Khine (UCM) *(367 Commons)*
4:30 – 6:00 pm		**Reception** *(Lobby of 302 Commons)*	
6:00 – 6:15 pm		**Poster Session I Removal** *(302B Commons)*	
6:15 – 6:30 pm		**Poster Session II Setup** *(302B Commons)*	
6:30 – 8:30 pm		**Dinner** *(302A Commons)*	

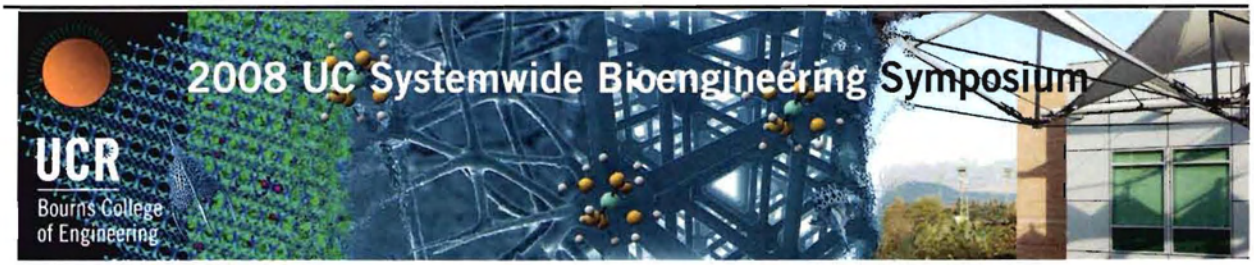

Time and Date	Event		
7:15 – 8:00 pm	**Introduction of Keynote Speaker: Shu Chien** **Keynote Speaker: John Anderson** **President, Illinois Institute of Technology** ***"Biomedical Engineering, Bioengineering, Biological Engineering, Biotechnology - What's in a Name?"*** *(302A Commons)*		
8:00 – 8:30 pm	**Judges Meeting** *(268 Commons)*		
8:10 – 8:45 pm	**Highlander Trolley from UCR Campus to Mission Inn and Marriott** *(Hinderaker Loop UCR Campus)*		
Sunday, June 22, 2008	*All events will be held at the UC Riverside Commons*		
6:00 – 8:00 am	**Highlander Trolley to UCR Campus from Mission Inn and Marriott** *(Hotel Entrances)*		
7:00 – 8:00 am	**Breakfast** *(Lobby and 302A Commons)*		
8:00 am– 2:00 pm	**Exhibits Tables Open** *(302B Commons)*		
8:00 – 8:10 am	**Welcome & Introduction of Keynote Speaker: Jerome Schultz** *(302A Commons)*		
8:30 – 9:15 am	**Keynote Speaker: Christine Kelley, PhD** **Director, Division of Discovery Science and Technology at the NIBIB (NIH)** ***"Research and Training Programs and Funding Opportunities at the National Institute of Biomedical Imaging and Bioengineering"*** *(302A Commons)*		
9:15 - 9:30 am	*Coffee Break* *(Lobby of 302 Commons)*		
9:45 – 11:15 am	**Podium Session IV**		
	Track 10 Biomedical Imaging II Chair: J. Lyubovitsky (UCR) *(355 Commons)*	Track 11 Biophysics Chair: V. Vullev (UCR) *(379 Commons)*	Track 12 New Frontiers Chair: D. Morikis (UCR) *(367 Commons)*
11:15 am – 12:15 pm	**Poster Session II** Chair: B. Anvari (UCR) *(302B Commons)*		
12:30 m – 1:00 pm	**Judges Meeting** *(268 Commons)*		
12:30 pm – 2:00pm	**Lunch and Award Ceremony** *(302A Commons)*		
2:00 pm --	**Poster Session II and Exhibit Removal** *(302B Commons)*		
1:10 – 3:00 pm	**Highlander Trolley from UCR Campus to Mission Inn and Marriott** *(Hotel Entrances)*		

Attachment: Attendees List

First	*Last Name*	*Affiliation*
Trenton	Baker	Centennial High School
Kevin	Baker	Alliance for Education
Michael	Lee	UCLA
Joseph	Clift	UC Riverside
Caryn	Urbanczyk	UC San Diego
Steven	George	UC Irvine
Eric	Matthys	UC Santa Barbara
Jeff	Sausman	UC Riverside
Jay	Kao	Abbott Vascular
Mohammed	Yousef	Bio-Rad
Jennifer	Griffin	UC San Diego
Rowella	Garcia	UC San Diego
Corena	Valencia	UC Riverside
Gabrielle	Goodman	UC Riverside
Elias	Wilson	Telemedicine and Advanced Tech. Research Center
Eva	Lai	Telemedicine and Advanced Tech. Research Center
Jessica	Kenyon	Telemedicine and Advanced Tech. Research Center
Shruthi	Balasubramanian	UC Riverside
Naubahar	Agha	UC Riverside
Vince	Nunez	UC Riverside
Katie	Peterson	UC Riverside
David	Sheldon	UC Riverside
Dane	Soholt	Colorado State University
Reza	Abbaschian	UC Riverside
Jane	Schultz	UC Riverside
John	Anderson	Illinois Institute of Technology
Christine	Kelley	National Institute of Biomedical Imaging & Bioeng.
Don	Giddens	Georgia Institute of Technology
Deborah	Vasquez	UC Riverside
Sylvie	Bryant	Genentech
Dan	Abramzon	Genentech
Tony	Casadonte	Abbott Vascular
Kelly	Russell	Abbott Vascular
Jana	Buccola	Abbott Vascular
Brandon	Wong	Abbott Vascular
Robert	Peralta	Abbott Vascular
Anthony	Oshinuga	Abbott Vascular
Heriberto (Berto)	Moya	Abbott Vascular
Mahboubeh	Hashemi	Abbott Vasular

First	Last Name	Affiliation
Saleha	Ahmed	Abbott Vascular
Edward	Roberts	UC Riverside
Mathew-Alexander	Roberts	UC Riverside
Ann	Daugherty	Genentech
Bryant	Mclaughlin	Genentech
Joe	Hess	Genentech
Shadi	Mahjoob	UC Riverside
Zhenshan	Chen	UC Riverside
Mariela	Anguelov	Winchester Associates Inc
Entcho	Anguelov	Winchester Associates Inc
Georgia	Thomas	UC Riverside
Hong	Xu	UC Riverside
Jim	Dexter	Bourns College of Engineering
Linda	Parker	UCR
Judith	Chappell	UC Riverside
James	Taylor	Courant Institute, New York University
Anton	Nekrutenko	Penn State University
Roger	Canales	Biosystems
Reza	Safa	Penguin Computing
Won Hyuk	Suh	UC Santa Barbara
Sarah	Nelson	UCSF
John	Shyy	UC Riverside
Adam	Feinman	UCLA
Rajaram	Krishnan	UC San Diego
Woonggyu	Jung	Beckman Laser Institute in UC Irvine
Diep	Nguyen	University of California, Merced
YONGFENG	ZHAO	UC Riverside
Chi-Shuo	Chen	UC, Merced
Fang	Wei	UCLA, MAE Department
KANDICE	TANNER	UNIVERSITY OF CALIFORNIA, IRVINE
Hayri	AKIN	UC Riverside
Zhen	Chen	UCR
Michelle	Khine	UC Merced
PRIYAMVADA	TEWARI	University of California Los Angeles
Nzola	De Magalhaes	University of California, Irvine
Shivani	Singh	UCLA
Jason	Poulos	UCLA
YI	FU	DR. John Shyy's LAB
Wei	Wu	UC-Riverside
George	Shackelford	UC, Santa Cruz
Huiqing	Ma	UC Riverside
Noah	Wilson	University of California, Santa Cruz
Aaron	Newman	University of California, Santa Barbara
Sara	St. James	UC Davis

First	*Last Name*	*Affiliation*
Robert	LeMoyne	UCLA
Philippos	Tsourkas	University of California, Davis
Perla	Ayala	UC San Francisco
Shyam	Natarajan	University of California, Los Angeles
Feng	Sun	University of California, Riverside
Navid	Amini	University of California, Los Angeles
BING	WU	UNIVERSITY OF CALIFORNIA, SAN FRANCISCO
Francisco G.	Perez-Gutierrez	UCR
Guillermo	Aguilar	University of California Riverside
Lorenzo	Martinez	University of California Riverside
Robert	Tan	UCLA
Nazgul	Tuleuova	UCDavis
Yu	Zhang	University of California, Riverside
Elizabeth	Gillard	UCR
Jinxiu	Cheng-Liao	University of California, Davis
Devin	McBride	University of California, Riverside
Sara	Farahmand	UCSF
Huini	Du	University of California, Davis
Rania	Elkeeb	University of California San Francisco
Gulnaz	Stybayeva	UCDavis
Shay	Edwards	Norco High School
Marshall	Levesque	University of California, San Diego
MIN-HO	KIM	UC Davis
Mark	Kastantin	UCSB
Song	Li	UC Berkeley
Gurneet	Singh	UCLA
Kanaka	Hettiarachchi	University of California, Irvine
Dimitrios	Morikis	UCR
CHUNSHENG	WANG	University of California San Francisco
Christopher	Druzgalski	PAHCE
Jeffrey	Chen	UC Riverside BRITE
Adriana	Aguirre	UC Riverside BRITE
Olga	Jennings	UC Riverside BRITE
Benjamin	Steyer	UC Riverside BRITE
Aleksandr	Gerasimenko	UC Riverside BRITE
Melissa	Sy	UC Riverside BRITE
James	Gutierrez	UC Riverside BRITE
Yasmine	Salas	UC Riverside BRITE
Sean	Culver	UC Riverside BRITE
Alexander	Chen	UC Riverside BRITE
Ioannis	Mountziaris	UC Riverside BRITE
Nicholas	Novak	UC Riverside BRITE
Rachel	Rattner	UC Riverside BRITE
Robert	Purnell	UCLA

First	*Last Name*	*Affiliation*
Rainya	Bridges	UC Riverside BRITE
Justin	Creel	UC Davis
Roy	Lefkowitz	UCSD
Marlon	Thomas	UC Riverside
Bongsu	Jung	UCR
Chang	Lee	University of California, Irvine
Sunny	Shah	UC Davis
Aydogan	Ozcan	UCLA
Andrew	Vu	UCR
Carlos	Huang	University of California, Irvine
Alicia	Blancas	University of California, Merced
Warren	Grundfest	UCLA
Peter	Chen	University of California, San Diego
Xiulin	Shen	UCR
Antonio	Contreras	UCR
Yiheng	Wang	University of California, Riverside
Sarah	Stolberg	University of California, Merced
Nima	Khatibzadeh	Mechanical Engineering
Ryan	Honda	UCR
Ilwoo	Park	University of California, Berkeley/San Francisco
Yan	Liu	UC-Riverside
Prashanthi	Vandrangi	University of California Riverside
Sean	Guthrie	University of California, Riverside
Yang	Song	University of California, Riverside
Chris	Kieslich	University of California, Riverside
Aliana	LÃ³pez De Victoria	UCR
Matthew	Valdez	Univeristy of California Riverside
Noriko	Sausman	UCR
Cheng-Yuk	Lee	University of California, Davis
Jonathan	Lam	University of California, Davis
David	Gough	UC San Diego
Valentine	Vullev	University of California, Riverside
Bahman	Anvari	UC Riverside
Yobed	Woldeabzghi	University of California
Elizabeth	Zielins	UC Riverside
Simon	Hu	UCSF/UCB Join Graduate Group in Bioengineering
Jacob	Vasquez	UCR
Chih-Huei	Cheung	n/a
Alexander	Cheung	UC Riverside
Lili	Peng	UCSD
Angela	Chen	University of California, Irvine
Kara	McCloskey	UC, Merced
So Hyun	Chung	University of California, Irvine
Laura	Marcu	UC Davis

First	*Last Name*	*Affiliation*
Jiayu	Liao	UC Riverside
Sergio	Rodriquez	UCLA
Erica	Andreozzi	University of California, Davis
Heather	Palko	UC Davis
angelique	louie	UC Davis
Chadwick	Shrum	UCLA
Dong Soo	HWANG	University of California, Santa Barbara
Nora	Hackett	University of California, Riverside
Andrea	Kasko	UCLA
Yi ng	Wang	University of California, Davis
Md.	Ashraf	University of California, Riverside
Foad	Mashayekhi	University of California, Los Angeles
Matthew	Black	University of California, Santa Barbara
Victor	Sun	UCLA
Jacob	Schmidt	UCLA
Uh-Joo	Choe	University of California, Los Angeles
Amanda	Trent	UCSB
Ben	Wu	UCLA
Yu-Jer	Hwang	UC Riverside
Julia	Lyubovitsky	UC Riverside
Brent	Millare	UC Riverside
Rachel	Marullo	University of California, Santa Barbara
Dennis	Yoon	University of California, Los Angeles
Daniel	Kamei	UCLA
Srigokul	Upadhyayula	UC Riverside
Duoduo	Bao	UC Riverside
Victor	Rodgers	UC Riverside
Jerome	Schultz	UC Riverside
Surekha	Gajria	UC Santa Barbara
Thorsten	Neumann	University of California Santa Barbara
Kaveh	Azartash	University of California Irvine
Shu	Chien	UCSD

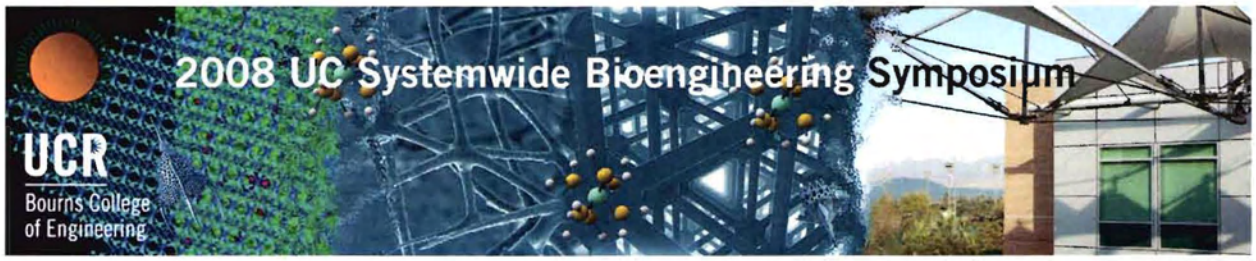

Symposium Evaluation Form

(Results are shown in red. n=31)

Thank you for taking the time to complete this evaluation form. The results of this survey will be used to help improve future programming.

When you have completed the survey, please place the folded form in the blue box on the UCR table in 302B Commons.

Please use numbers between 1 and 5 to answer each item below. Excellent = 5, Poor = 1

	Value
1. Overall Rating of the Symposium	**4.5 ± 0.67**
2. Overall Quality of Oral Presentations	**4.3 ± 0.68**
3. Overall Quality of Poster Presentations	**4.2 ± 0.71**
4. Overall Quality of Exhibits	**4.1 ± 0.89**
5. Overall Conference Organization, Structure and Execution Rating	**4.8 ± 0.57**
6. Conference Amenities / Facilities Rating	**4.4 ± 0.49**

Please comment on what you liked /or did not like at this 9th Annual Symposium.

Please comment on what you would like to see/or not see at upcoming UC Systemwide Bioengineering Symposiums.

Bioengineering Institute of California

9th Annual
UC Systemwide Bioengineering Symposium

20-22 June, 2008

Hosted by

The Department of Bioengineering

UNIVERSITY OF CALIFORNIA
UCRIVERSIDE | Bourns College of Engineering

9th Annual UC Systemwide Bioengineering Symposium
UC Riverside , 20-22 June, 2008

Welcome,

The Bourns College of Engineering is delighted to host the 9th Annual UC Systemwide Bioengineering Symposium. After only two decades, the Bourns College of Engineering has achieved significant growth in its enrollment, research holdings and reputation. The number of our faculty and students has more than tripled since 2000, with a similar growth in state-of-the-art laboratories, equipment and technological capabilities. A new Materials Science and Engineering building is underway on campus that will greatly expand our capabilities in nanotechnology and bioengineering, including a 10-fold increase in clean room space. And while the Department of Bioengineering is less than three years old, you will, nevertheless, see their tremendous energy in the results of this symposium.

This year's symposium effort is focused on increased UC Bioengineering interaction and improved collaborations with California's vast biomedical firms as well as government agencies. According to the California Life Sciences Action Plan, over 40% of the world's 6,250 life sciences firms are located in California and 25% of the nation's life sciences industry claims California as the location of their headquarters.

Thus, our organizing committees have put a tremendous effort into increasing the symposium's corporate connection as well as improving the synergism of the Bioengineering UC components. Throughout this year's program you will see judges and session chairs, not only from UCR, but from a number of other UC and other campuses, TATRC and the biotech industry.

Given this we would like to also especially thank our sponsors and partners for this year's symposium. Our corporate response has been outstanding, with generous gifts from Genentech and substantial financial support from Gilead, ResMed, Abbott Vascular, Boston Scientific Neuromodulation Group, BioRad and Penguin Computing. We are also extremely appreciative of the TATRC partnership and an award from the UC Discovery Grant Program.

All together, we believe this year's symposium will provide the catalyst for increased interaction and opportunity for years to come.

Finally, we hope you enjoy the symposium, and, again, welcome to UCR!

Sincerely

Reza Abbaschian
Dean
Bourns College of Engineering

Dear Guests,

The faculty and students of the Bioengineering Department welcome you to Riverside for this important event.

We are delighted to have the opportunity to host the 2008 UC Systemwide Bioengineering Symposium. This symposium is the signature event for the Bioengineering Institute of California that represents the largest academic organization of bioengineering faculty and students in the country. This talent pool, along with our sister University of California campuses, has been the creative engine that has lifted the California bioengineering and biotechnology industry to a leadership position that accounts for about ¼ of the sales in the United States.

We are particularly fortunate to have a slate of keynote speakers who are national leaders in our field. John Anderson has been a moving force in the development of bioengineering in various roles, starting as Chairman of Chemical Engineering at Carnegie Mellon, then Dean, and continuing his involvement as Provost at Case Western; he is currently President of Illinois Institute of Technology. John Anderson's personal research contributions have been recognized by his election to the National Academy of Engineering and the National Academy of Science.

Dean Don Giddens is nationally known for his contributions to the understanding of the influence of fluid mechanic phenomena on the development of vascular disease. As previous Dean of Engineering at Johns Hopkins and current Dean of Engineering at Georgia Tech, and consultant to the National Academy of Engineering, Don Giddens has had a major impact on engineering education. In addition, as Founding Chair of the Biomedical Engineering Department at Georgia Tech, he had a major role in the development of this highly-ranked department.

As Director of Discovery Science and Technology at NIBIB, Christine Kelley has pioneered the formulation of new initiatives in our field. Through her efforts, in cooperation with her colleagues at NIH, she has organized workshops that have identified new opportunities for bioengineers to contribute to the advancement of health care. She has energetically promoted new paradigms for the application of technology to facilitate translational research.

These presentations, along with the excellent contributions from students and faculty of our 10 UC Campuses, will make important contributions to an exciting and stimulating Symposium.

Sincerely yours,

Jerome S. Schultz
Chairman, Bioengineering
UC Riverside

Dear Friends and Colleagues of the University of California,

On behalf of the UC Systemwide *Bioengineering Institute of California*, I would like to express our warmest welcome to you for attending the 9th UC Systemwide Bioengineering Symposium held on the beautiful campus of UC Riverside on June 20-22, 2008. This Symposium has become a wonderful tradition after outstanding meetings at eight other UC campuses, with the purpose of fostering exchange and discussions on bioengineering research performed on the ten UC campuses. Bioengineering at the UC campuses has strong representation in many different areas and offers almost limitless opportunities for new interactions. This meeting is designed to foster such interactions, with the motto of, "Ten Campuses United as One. Learning and Growing Together."

I wish to express our warmest appreciation to our colleagues at UC Riverside, led by Drs. Jerry Schultz and Victor Rodgers, with wonderful collaborations of faculty, staff and students. They have done a marvelous job in organizing this Symposium, which will have outstanding scientific and social programs. On Friday, June 20, there will be a welcome reception in the Spanish Art Galley in the beautiful Mission Inn, which is a national historical landmark hotel; Dr. Don Giddens, Dean of Engineering of Georgia Tech, will give a keynote speech. The meetings on June 21 and 22 will be held on UCR Commons. In the morning of June 21, after opening remarks by Dr. Schultz, we will have plenary lectures by Dr. Eva Lai of the U.S. Army Telemedicine & Advanced Technology Research Center (TATRC), which is a major partner of this meeting, and Dr. Song Li of UC Berkeley. The remainder of the day and the morning of June 22 will have podium and poster sessions with excellent presentations by students and faculty from the various campuses. President John Anderson of the Illinois Institute of Technology will give a Keynote Speech after dinner on June 21. The morning of June 22 will start with a keynote speech by Dr. Christine Kelley, Director of Division of Discovery Science and Technology at the NIBIB. I wish to thank the panel of judges, who will select the top presentations for awards sponsored by Genentech, Gilead, Boston Scientific Neuromodulation, ResMed, and Abbott Vascular, whose generous support is very much appreciated.

The meeting will have an excellent participation by industry, with exhibits throughout the meeting. There will be breakfasts, lunches, and coffee breaks on June 21 and 22, in addition to the dinners, which will provide ample opportunities for all participants to interact, getting to know our colleagues from other campuses and initiating new collaborations.

I look forward to seeing you at this Symposium, which will be most stimulating and enjoyable. I wish to thank once again our organizers, sponsors, speakers, poster presenters, exhibitors, and all the participants at this meeting.

With best regards,

Sincerely yours,
Shu Chien
Director, UC Bioengineering Institute of California

Acknowledgements

Corporate Sponsors

Genentech
IN BUSINESS FOR LIFE

GILEAD
Advancing Therapeutics.
Improving Lives.

ResMed

Abbott
Vascular

Boston Scientific

BIO-RAD

Penguin Computing

Partnerships

the UC Discovery Grant
Success is a great investment

TATRC

CHI
California Healthcare Institute

SoCalBio
Southern California Biomedical Council

UCR | Bourns College of Engineering

This symposium is being held in collaborative partnership with the Telemedicine Advanced Technology Research Center (TATRC), and is made possible by a conference support grant administered by the U.S. Army Medical Research Materiel Command (USAMRMC). Conference Support Grant #08324001. *The views, opinions and findings presented at this event are those of the organizers and should not be construed as an official Department of the Army position, policy or decision unless so designated by other documentation.*

Table of Contents

Executive Program Chair

Jerome S. Schultz

Program Organizing Chair

Victor G. J. Rodgers

Scientific Program Subcommittee

Dimitrios Morikis, Chair (UCR)
Julia Lyubovitsky (UCR)
Michelle Khine (UCM)
Guillermo Aquilar (UCR)
Jiayu Liao (UCR)
Valentine Vullev (UCR)

Fundraising Subcommittee

Jerome S. Schultz, Chair (UCR)
Richard Chute (UCR)
Linda Parker (UCR)
Denise Sanders (UCR)
Mitch Boretz (UCR)
Warren Grumfest (UCLA)
Shu Chien (UCSD)

Judging & Awards Subcommittee

Bahman Anvari, Chair (UCR)
Marilu Chavez (SACNAS)
Val Vullev (UCR)
Jacob Schmidt (UCLA)
Laura Marcu (UCD)
Kara McCloskey (UCM)
Mohammed Yousef (BioRad)
Eva Lai (TATRC)
Anton Nekrutenko (Penguin/Penn State)
Warren Grumfest (UCLA)
Bryant Mclaughlin (Genentech)
Anthony Oshinuga (Abbott Vascular)
Jiayu Liao (UCR)

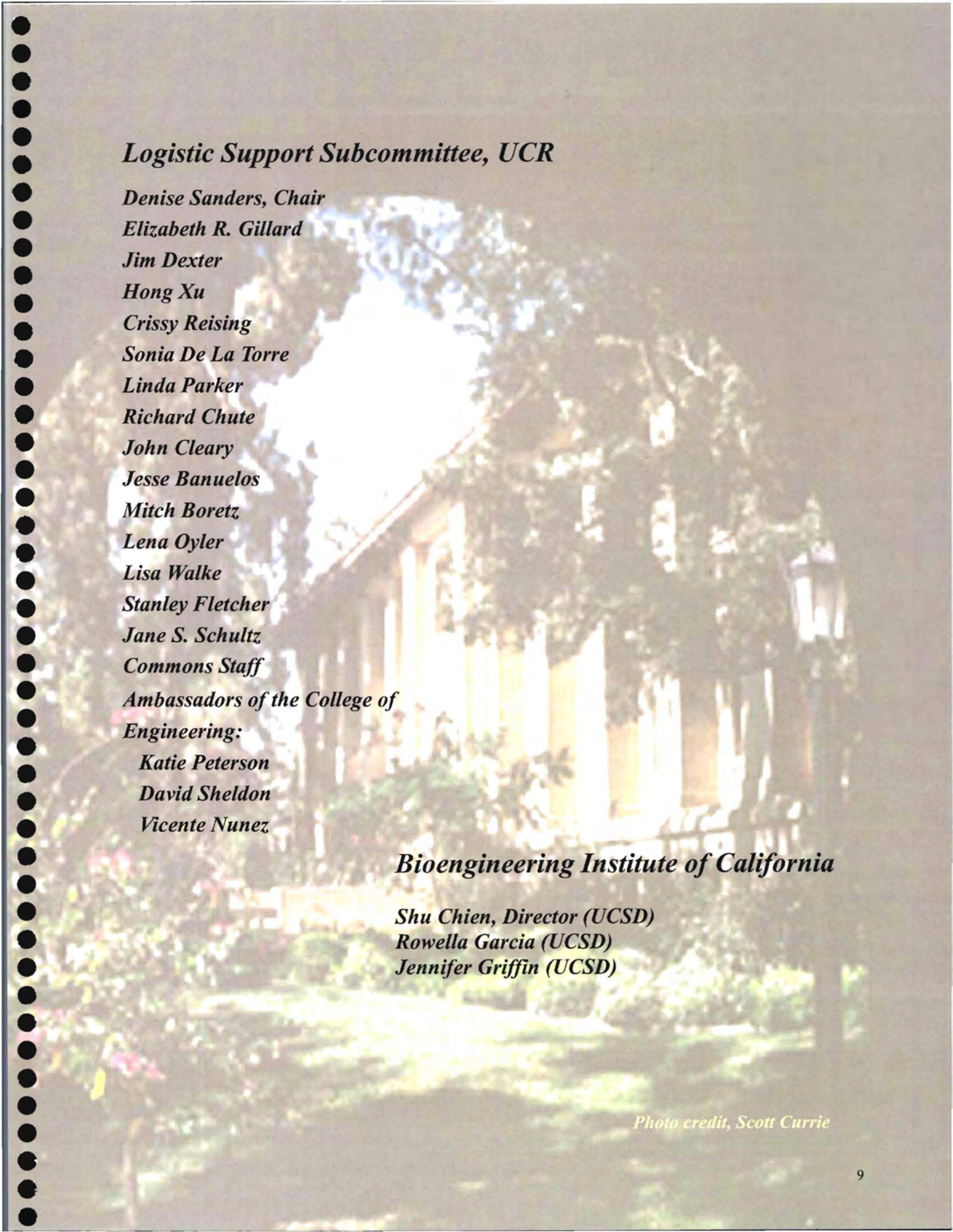

Logistic Support Subcommittee, UCR

Denise Sanders, Chair
Elizabeth R. Gillard
Jim Dexter
Hong Xu
Crissy Reising
Sonia De La Torre
Linda Parker
Richard Chute
John Cleary
Jesse Banuelos
Mitch Boretz
Lena Oyler
Lisa Walke
Stanley Fletcher
Jane S. Schultz
Commons Staff
Ambassadors of the College of Engineering:
Katie Peterson
David Sheldon
Vicente Nunez

Bioengineering Institute of California

Shu Chien, Director (UCSD)
Rowella Garcia (UCSD)
Jennifer Griffin (UCSD)

Photo credit, Scott Currie

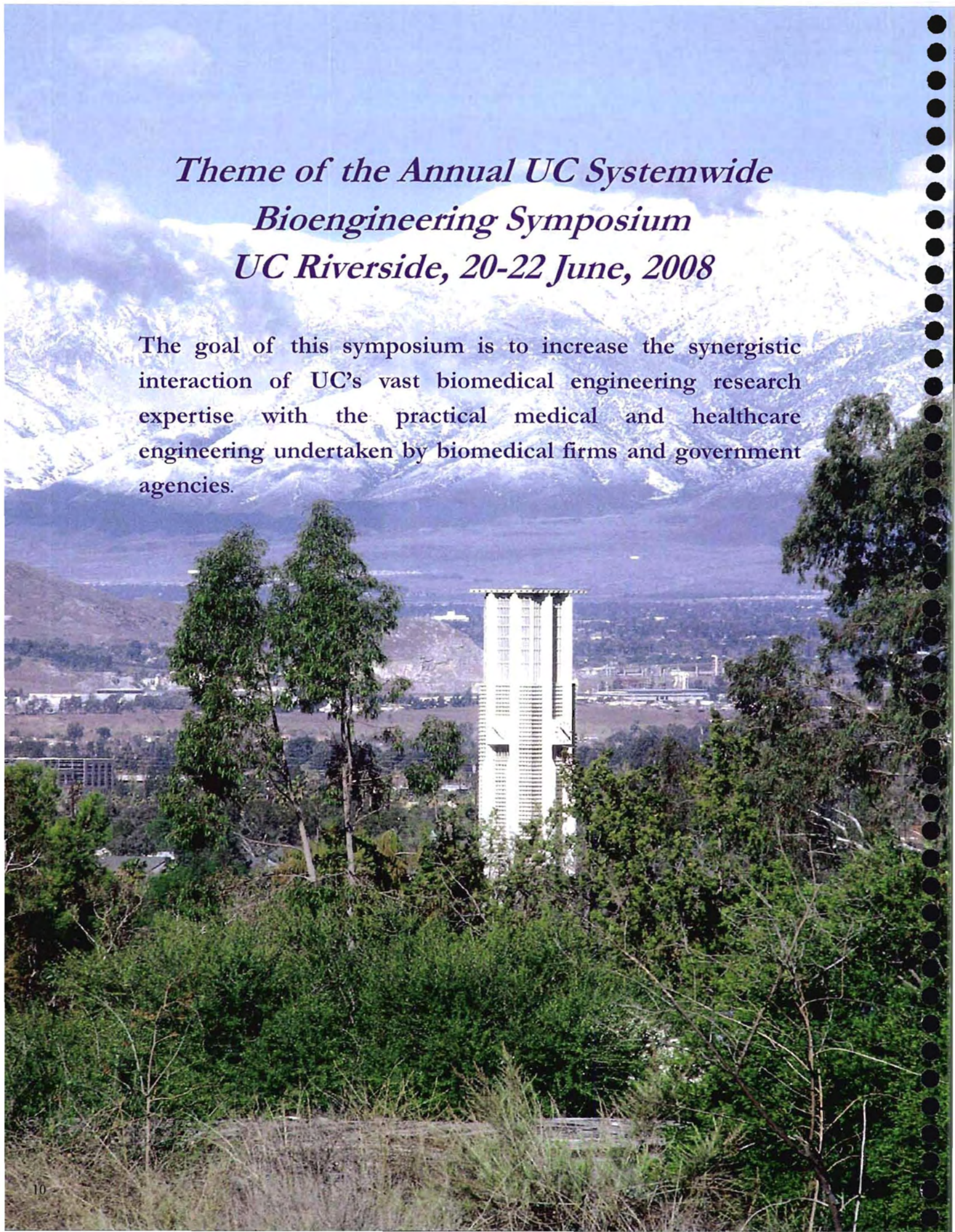

Theme of the Annual UC Systemwide Bioengineering Symposium UC Riverside, 20-22 June, 2008

The goal of this symposium is to increase the synergistic interaction of UC's vast biomedical engineering research expertise with the practical medical and healthcare engineering undertaken by biomedical firms and government agencies.

Distinguished Keynote Speakers

This year's symposium is honored to have three distinguished keynote speakers who are leaders and pioneers in the fields of bioengineering and biomedical engineering.

FRIDAY 20 June
6-7 pm
Spanish Art Gallery

"Know Thy Arteries, Know Thyself"

DR. DON P. GIDDENS, Ph.D. is the Dean of the College of Engineering and the Lawrence L. Gellerstedt, Jr. Chair in Bioengineering & Georgia Research Alliance Eminent Scholar at Georgia Institute of Technology. His research is in the areas of biofluid mechanics, Blood velocity and spectral estimations from Doppler ultrasound, hemodynamics of the carotid bifurcation, effects of fluid dynamics on vascular function and vessel adaptation, and patency of small caliber vascular grafts.

Selected Awards include; Elected into the National Academy of Engineering in 1999; and recipient of the H.R. Lissner Award, American Society of Mechanical Engineers, Winter Annual Meeting 1993.

SUNDAY 22 June
8:30-9:15 am
302 A Commons

"Research and Training Programs and Funding Opportunities at the National Institute of Biomedical Imaging and Bioengineering"

DR. CHRISTINE A. KELLEY is the Director of the Division of Discovery Science and Technology at the NIBIB. She received her Ph.D. degree in Cell Biology from Boston University in 1988. Her graduate research focused on the role of pericytes in the microvasculature. From 1988-1996 Dr. Kelley conducted postdoctoral and independent research on the function and regulation of smooth muscle and nonmuscle myosin isoforms in the Laboratory of Molecular Cardiology in the National Heart, Lung, and Blood Institute (NHLBI). In 1996 Dr. Kelley became a Health Scientist Administrator in the Vascular Biology Research Group at the NHLBI, before moving in 1998 to a position as a Health Scientist Administrator in the Bioengineering and Genomic Applications Research Group within the same Division. Dr. Kelley assumed her current position in NIBIB in March, 2002.

SATURDAY 21 June
7:15-8 pm
302 A Commons

Biomedical Engineering, Bioengineering, Biological Engineering, Biotechnology - What's in a Name?"

DR. JOHN L. ANDERSON is the President of Illinois Institute of Technology and Professor of Chemical Engineering. He received his BChE degree from the University of Delaware and PhD in Chemical Engineering from the University of Illinois. He served on the faculty of Cornell University before joining the faculty at Carnegie Mellon University in 1976. At Carnegie Mellon he was University Professor of Chemical Engineering and held the positions Director of Biomedical Engineering (1980-85), Head of the Chemical Engineering Department (1983-94), and Dean of the College of Engineering (1996-2004). He was Provost and University Vice President at Case Western Reserve University during 2004-2007.

Dr. Anderson is a member of the National Academy of Engineering and has chaired the NAE section for Chemical Engineering as well as several study committees of the National Research Council. He is a Fellow of the American Academy of Arts and Sciences, the American Association for the Advancement of Science (AAAS), and the American Institute of Medical and Biological Engineering. He received the Professional Progress Award of the American Institute of Chemical Engineers (AIChE), and a John Simon Guggenheim Fellowship. He has published in areas of membrane separations, electrokinetics, dynamics of polymer chains and colloidal particles in porous media and near surfaces, and fluid dynamics.

Tour the Historic Mission Inn!

Friday 20 June
4:30 pm

Convene in the Main Hotel Lobby just inside the Orange Street entrance (across from the Public Library and Pagoda) to meet your Tour Guide. You will see the Presidential Lounge once you are in the Lobby.

Transportation Schedule:

Saturday, 21 June, 2008

6:30am, 7:00am	pick up at Marriott Hotel Entrance
6:40am, 7:10am	pick up at Mission Inn Orange Street Entrance
6:55am, 7:25am	arrival at UCR Hinderaker Loop
8:10pm, 8:45pm	depart from UCR Hinderaker Loop
8:20pm, 8:55pm	drop off at Marriott Hotel Entrance
8:30pm, 9:00pm	drop off at Mission Inn Orange Street Entrance

Sunday, 22 June, 2008

6:30am, 7:00am	pick up at Marriott Hotel Entrance
6:40am, 7:10am	pick up at Mission Inn Orange Street Entrance
6:55am, 7:25am	arrival at UCR Hinderaker Loop
1:10pm, 1:40pm	depart from UCR Hinderaker Loop
1:20pm, 1:50pm	drop off at Marriott Hotel Entrance
1:25pm, 2:00pm	drop off at Mission Inn Orange Street Entrance
	Final Departure to Hotels
2:15pm	depart from UCR Hinderaker Loop
2:25pm	drop off at Marriott Hotel Entrance
2:35pm	drop off at Mission Inn Orange Street Entrance

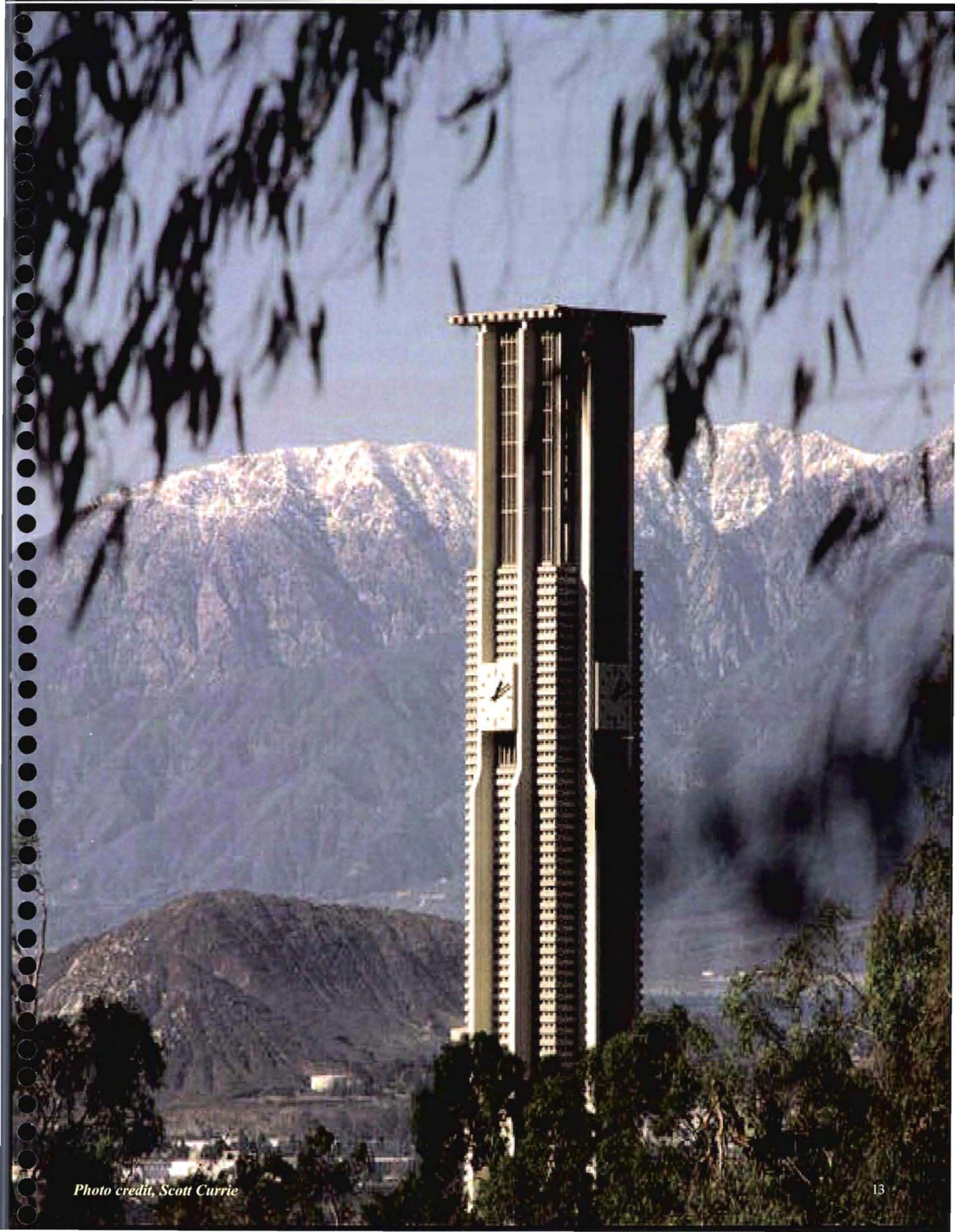

Photo credit, Scott Currie

Final Conference Agenda

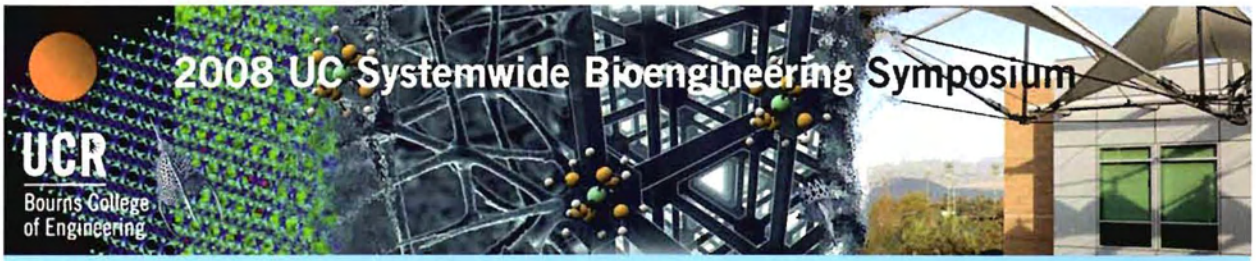

Friday, June 20, 2008	*All events will be held at the Historic Mission Inn & Spa*		
5:00 – 8:00 pm	**Check–In and Registration** *(Spanish Art Galley in the Mission Inn)*		
6:00 – 8:00 pm	**Reception** *(Spanish Art Galley in the Mission Inn)*		
6:00 – 7:00 pm	**Welcome & Introduction of Keynote Speaker: Reza Abbaschian** **Keynote Speaker: Don P. Giddens** **Dean, College of Engineering, Georgia Institute of Technology** ***"Know Your Arteries, Know Thyself"*** *(Spanish Art Galley in the Mission Inn)*		
Saturday, June 21, 2008	*All events will be held at the UC Riverside Commons*		
6:30 – 7:00 am	**Highlander Trolley to UCR Campus from Mission Inn and Marriott** *(Hotel Entrances)*		
7:00 – 8:00 am	**Check–In and Registration** *(Lobby of 302 Commons)*		
7:00 – 8:00 am	**Breakfast** *(Lobby and 302A Commons)*		
7:00 – 8:00 am	**Bioengineering Institute of California Steering Committee Meeting** *(260 Commons)*		
7:00 – 8:00 am	**Exhibitor Set-Up** *(302B Commons)*		
7:00 – 7:30 am	**Poster Session I Set-Up** *(302B Commons)*		
7:00 – 8:00 am	**Judges Check–In** *(268 Commons)*		
8:00 am– 6:00 pm	**Exhibitor Tables Open** *(302B Commons)*		
8:00 – 8:10 am	**Welcome & Introduction: Jerome Schultz** *(302A Commons)*		
8:15 – 9:00 am	**TATRC Presentation** **Eva Lai, PhD (TATRC)** ***"Introduction to TATRC"*** **Song Li, PhD (UCB)** ***"Nanofibers for Nerve Regeneration"*** *(302A Commons)*		
9:15 – 9:30 am	*Coffee Break* *(Lobby of 302 Commons)*		
	Podium Session I		
9:30 – 11:00 am	Track 1 Bioinformatics & Genomics Chair: J. Liao (UCR) *(379 Commons)*	Track 2 Biomedical Imaging I Chair: J. Lyubovitsky (UCR) *(355 Commons)*	Track 3 Nanotechnology & BioMEMS Chair: M. Khine (UCM) *(367 Commons)*

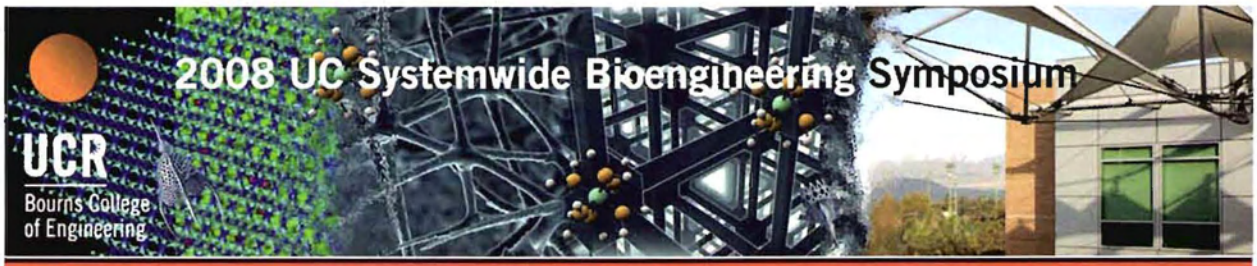

Saturday, June 21, 2008 — *All events will be held at the UC Riverside Commons*

11:00 am – 12:00 pm		**Poster Session I** Chair: B. Anvari (UCR) *(302B Commons)*	
12:00 pm – 1:00 pm		**Lunch** *(Lobby and 302A Commons)*	
		Podium Session II	
1:00 – 2:30 pm	Track 4 Biocomputation, *in Silico* & Biosystems Modeling Chair: D. Morikis (UCR)	Track 5 Tissue Engineering Chair: G. Aguilar (UCR) *(367 Commons)*	Track 6 Biomaterials Chair: V. Vullev (UCR) *(355 Commons)*
2:30 - 2:45 pm		*Coffee Break* *(Lobby of 302 Commons)* **Judges Meeting** *(268 Commons)*	
		Podium Session III	
2:45 – 4:15 pm	Track 7 Molecular & Cellular Engineering Chair: J. Liao (UCR) *(355 Commons)*	Track 8 Drug Delivery & Targeting Chair: G. Aguilar (UCR) *(379 Commons)*	Track 9 Biomechanics & Biodevices Chair: M. Khine (UCM) *(367 Commons)*
4:30 – 6:00 pm		**Reception** *(Lobby of 302 Commons)*	
6:00 – 6:15 pm		**Poster Session I Removal** *(302B Commons)*	
6:15 – 6:30 pm		**Poster Session II Setup** *(302B Commons)*	
6:30 – 8:30 pm		**Dinner** *(302A Commons)*	
7:15 – 8:00 pm		**Introduction of Keynote Speaker: Shu Chien** **Keynote Speaker: John Anderson** **President, Illinois Institute of Technology** ***"Biomedical Engineering, Bioengineering, Biological Engineering, Biotechnology - What's in a Name?"*** *(302A Commons)*	
8:00 – 8:30 pm		**Judges Meeting** *(268 Commons)*	
8:10 – 8:45 pm		**Highlander Trolley from UCR Campus to Mission Inn and Marriott** *(Hinderaker Loop UCR Campus)*	

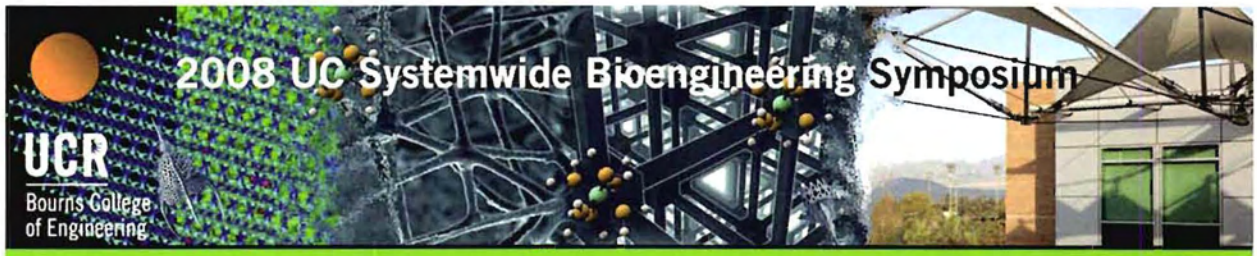

Sunday, June 22, 2008	*All events will be held at the UC Riverside Commons*		
6:00 – 8:00 am	**Highlander Trolley to UCR Campus from Mission Inn and Marriott** *(Hotel Entrances)*		
7:00 – 8:00 am	**Breakfast** *(Lobby and 302A Commons)*		
8:00 am– 2:00 pm	**Exhibits Tables Open** *(302B Commons)*		
8:00 – 8:10 am	**Welcome & Introduction of Keynote Speaker: Jerome Schultz** *(302A Commons)*		
8:30 – 9:15 am	**Keynote Speaker: Christine Kelley, PhD Director, Division of Discovery Science and Technology at the NIBIB (NIH)** ***"Research and Training Programs and Funding Opportunities at the National Institute of Biomedical Imaging and Bioengineering"*** *(302A Commons)*		
9:15 - 9:30 am	*Coffee Break (Lobby of 302 Commons)*		
9:45 – 11:15 am	**Podium Session IV**		
	Track 10 Biomedical Imaging II Chair: J. Lyubovitsky (UCR) *(355 Commons)*	Track 11 Biophysics Chair: V. Vullev (UCR) *(379 Commons)*	Track 12 New Frontiers Chair: D. Morikis (UCR) *(367 Commons)*
11:15 am – 12:15 pm	**Poster Session II** Chair: B. Anvari (UCR) *(302B Commons)*		
12:30 m – 1:00 pm	**Judges Meeting** *(268 Commons)*		
12:30 pm – 2:00pm	**Lunch and Award Ceremony** *(302A Commons)*		
2:00 pm –	**Poster Session II and Exhibit Removal** *(302B Commons)*		
1:10 – 3:00 pm	**Highlander Trolley from UCR Campus to Mission Inn and Marriott** *(Hotel Entrances)*		

Maps & Layout of Conference Locations

Symposia on Friday will be held at the Mission Inn Hotel & Spa

MISSION INN
A NATIONAL HISTORIC LANDMARK HOTEL & SPA

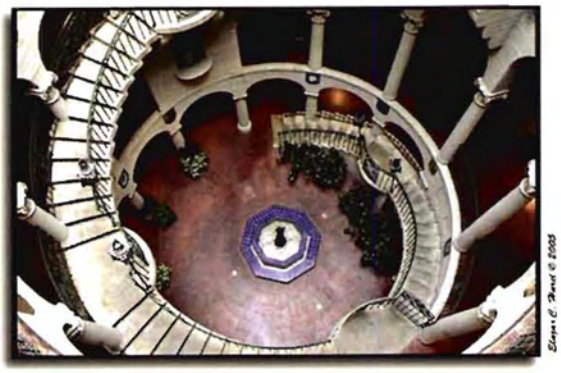

Spanish Art Gallery

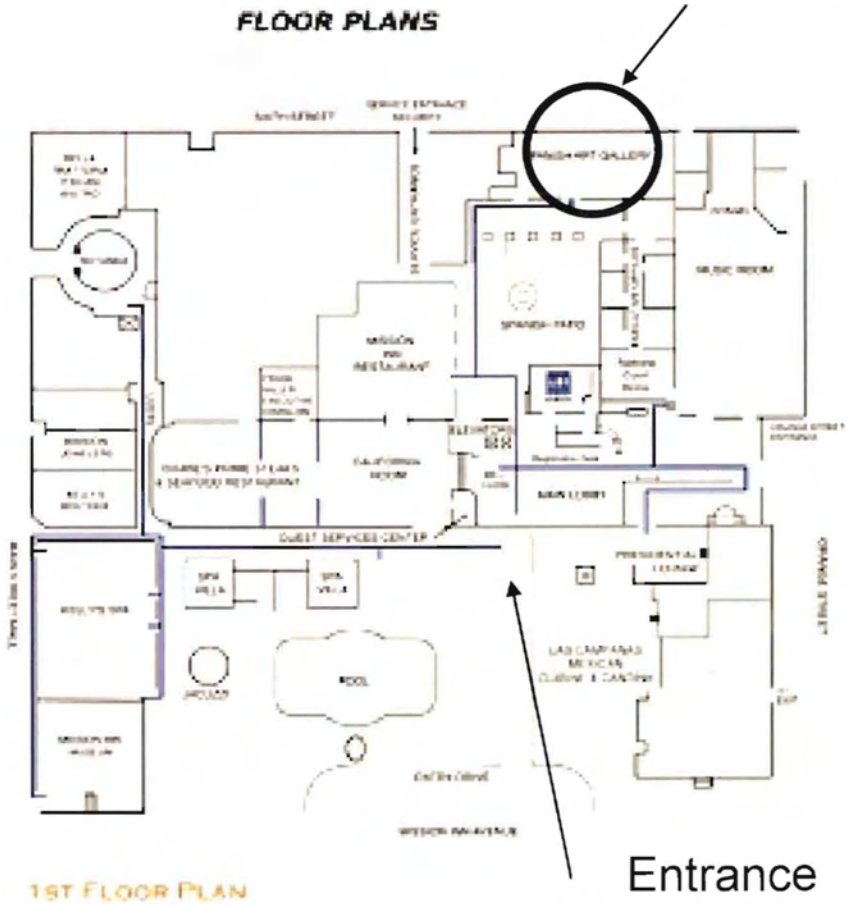

Maps & Layout of Conference Locations

Symposia on Saturday and Sunday will be held at the UCR Campus

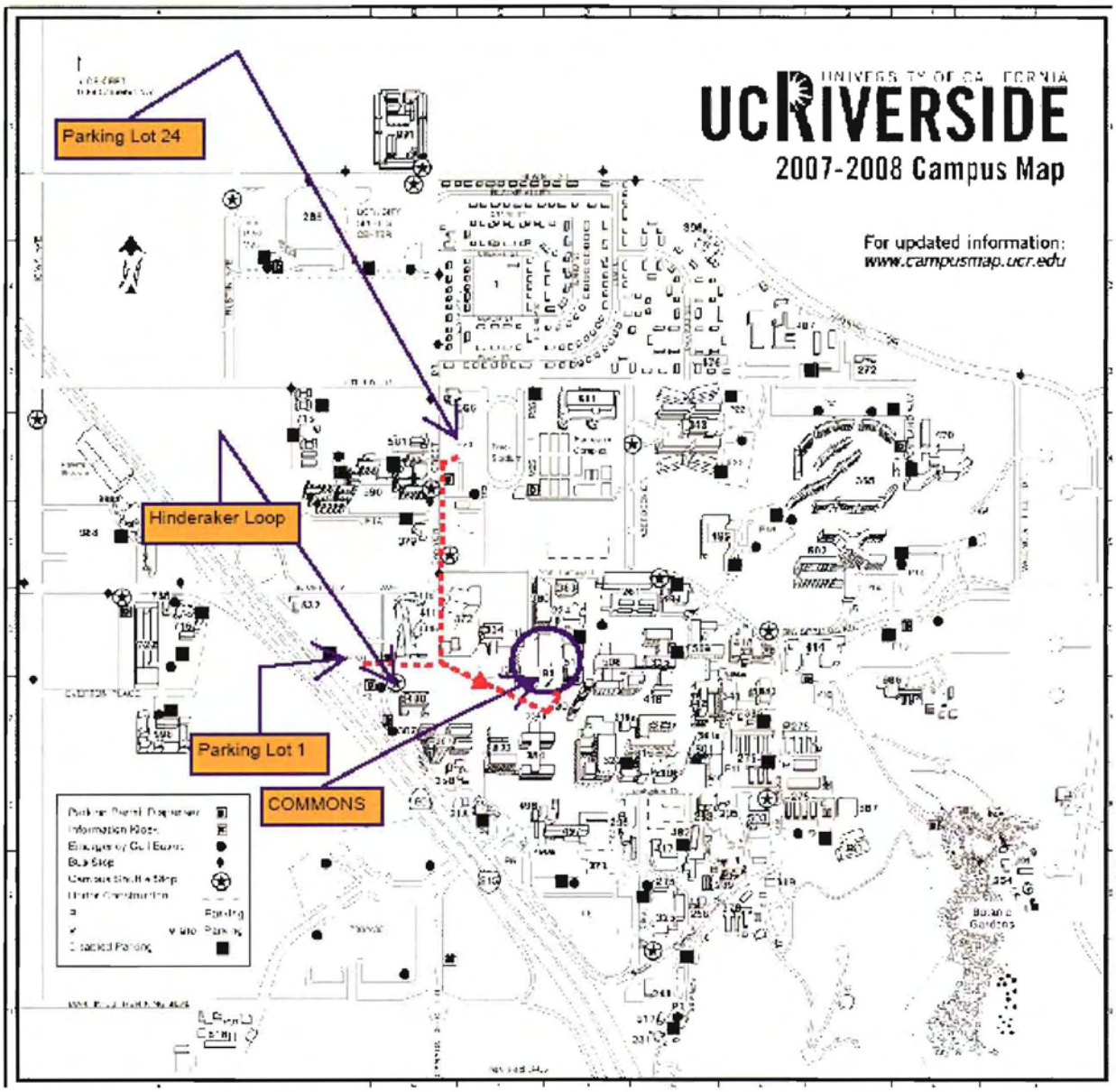

Maps & Layout of Conference Locations

Symposia on Saturday and Sunday will be held at the UCR Campus

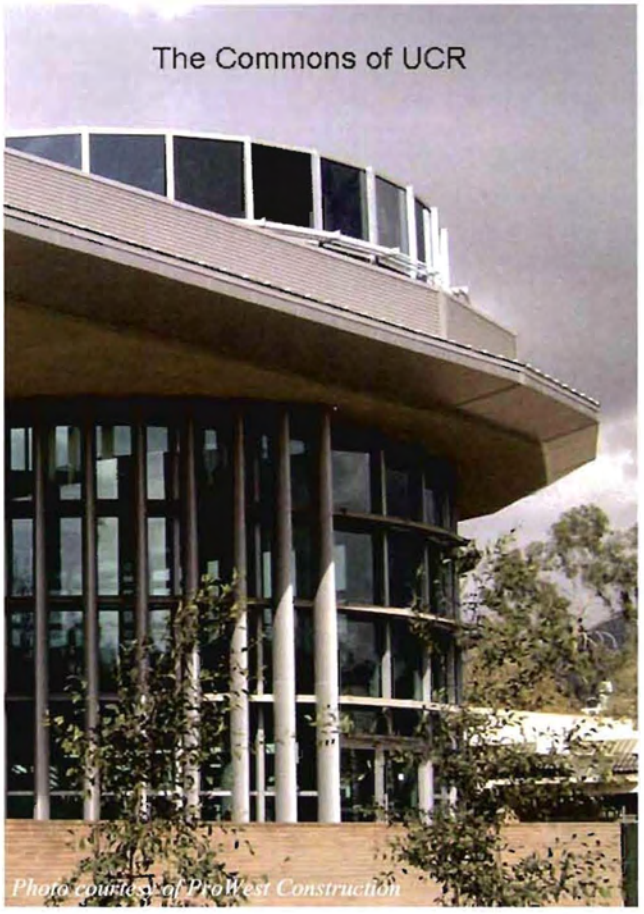

Symposium Floor Plan in the Commons

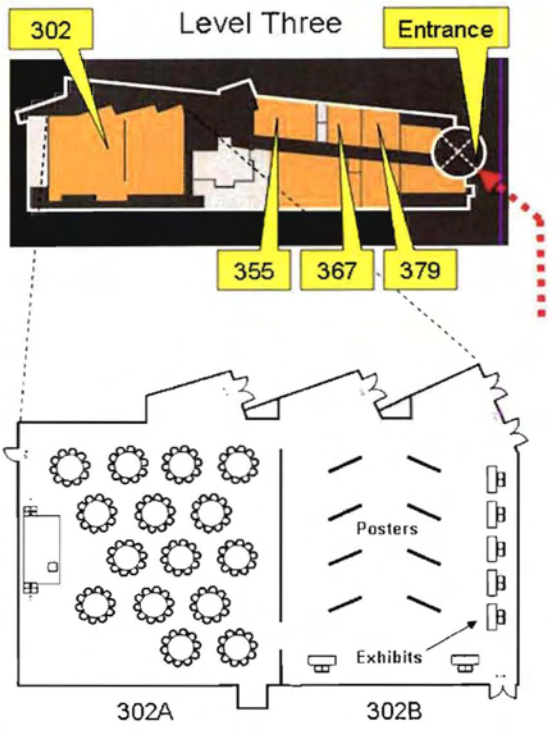

Commons entrance is at the rotunda pictured above. Following the red path on the previous page will take you to the red path to the rotunda entrance, as shown on this page.

Podium Session I

9:30 am-11 am
SATURDAY

Track 1	Track 2	Track 3
Bioinformatics & Genomics	Biomedical Imaging I	Nanotechnology & BioMEMS
Chair: J. Liao (UCR)	Chair: J. Lyubovitsky (UCR)	Chair: M. Khine (UCM)
(379 Commons)	*(355 Commons)*	*(367 Commons)*

Oral Track 1 — *Bioinformatics & Genomics*

Oral Track 2 — *Biomedical Imaging I*

Podium Session I

9:30 am-11 am
SATURDAY

Track 1	Track 2	Track 3
Bioinformatics & Genomics	Biomedical Imaging I	Nanotechnology & BioMEMS
Chair: J. Liao (UCR)	Chair: J. Lyubovitsky (UCR)	Chair: M. Khine (UCM)
(379 Commons)	*(355 Commons)*	*(367 Commons)*

Oral Track 3 — *Nanotechnology & BioMEMS*

Poster Session I

11 am-12 pm SATURDAY *302 B Commons* *Chair: B. Anvari, UCR*

Poster Track 3 *Nanotechnology & BioMEMS*

Poster Session I

11 am-12 pm SATURDAY *302 B Commons* *Chair: B. Anvari, UCR*

Poster Track 4 *Biocomputation, in Silico & Biosystems*

Poster Track 5 *Tissue Engineering*

Poster Track 7 *Molecular & Cellular Engineering*

Poster Session I

11 am-12 pm SATURDAY *302 B Commons* *Chair: B. Anvari, UCR*

Poster Track 8 *Drug Delivery & Targeting*

		Page
A18	Recombinant mussel adhesive protein as a gene delivery material. Dong Soo Hwang, Hyung Joon Cha and Matthew Tirrell. UCSB/Pohang University of Science and Technology	118
A19	ATR Analysis of Nucleic Acid-Lipid Self-Assembling Complexes for Drug Delivery on Biochips. Thorsten Neumann, Surekha Gajria, Wirasak Smitthipong, Luc Jaeger and Matthew Tirrell. UCSB	119

Poster Track 9 *Biomechanics & Biodevices*

A20	The Atheroprotective Pulsatile Flow Activates the AMP-activated Protein Kinase-Krüppel-like factor 2 in Vascular Endothelial Cells. Wei Wu, Angela Young, Wei Sun, Yi-Shuan Li, John Y Shyy and Shu Chien. UCR/UCSD	121
A21	Translocation of ATP synthase β chain by laminar versus oscillatory flow. Yi Fu, Yingjian Hou, Yi Zhu and John Y-J. Shyy. UCR	122
A22	Electrostatic Contributions in Binary Protein Ultrafiltration. Yiheng Wang and Victor G. J. Rodgers. UCR	123
A23	Pump-probe imaging of nanosecond laser-induced bubbles in agar gel F. Pérez-Gutiérrez, R. Evans, S. Camacho-López and G. Aguilar. UCR	124
A24	Energy-Aware Heart Rate Monitoring During Stair Climbing Navid Amini, Mahsan Rofouei, William J. Kaiser, Majid Sarrafzadeh. UCLA	125

Podium Session II

1 pm-2:30 pm
SATURDAY

Track 4
Biocomputation,
in Silico & Biosystems
Modeling
Chair: D. Morikis (UCR)
(379 Commons)

Track 5
Tissue Engineering
Chair: G. Aguilar (UCR)
(367 Commons)

Track 6
Biomaterials
Chair: V. Vullev (UCR)
(355 Commons)

Oral Track 4 — *Biocomputation, in Silico & Biosystems*

Oral Track 5 — *Tissue Engineering*

Podium Session II

1 pm-2:30 pm
SATURDAY

Track 4
Biocomputation,
in Silico & Biosystems
Modeling
Chair: D. Morikis (UCR)
(379 Commons)

Track 5
Tissue Engineering
Chair: G. Aguilar (UCR)
(367 Commons)

Track 6
Biomaterials
Chair: V. Vullev (UCR)
(355 Commons)

Oral Track 6 — *Biomaterials*

Podium Session III

2:45-4:15 pm
SATURDAY

Track 7	Track 8	Track 9
Molecular & Cellular Engineering	Drug Delivery & Targeting	Biomechanics & Biodevices
Chair: J. Liao (UCR)	Chair: G. Aguilar (UCR)	Chair: M. Khine (UCM)
(355 Commons)	*(379 Commons)*	*(367 Commons)*

Oral Track 7 — *Molecular & Cellular Engineering*

Oral Track 8 — *Drug Delivery & Targeting*

Podium Session III

2:45-4:15 pm
SATURDAY

Track 7	Track 8	Track 9
Molecular & Cellular Engineering	Drug Delivery & Targeting	Biomechanics & Biodevices
Chair: J. Liao (UCR)	Chair: G. Aguilar (UCR)	Chair: M. Khine (UCM)
(355 Commons)	*(379 Commons)*	*(367 Commons)*

Oral Track 9 — *Biomechanics & Biodevices*

Podium Session IV

9:45 am - 11:15 am SUNDAY

Track 10	Track 11	Track 12
Biomedical Imaging II	Biophysics	New Frontiers
Chair: J. Lyubovitsky (UCR)	Chair: V. Vullev (UCR)	Chair: D. Morikis (UCR)
(355 Commons)	*(379 Commons)*	*(367 Commons)*

Oral Track 10 — *Biomedical Imaging II*

Oral Track 11 — *Biophysics*

Podium Session IV

9:45 am - 11:15 am
SUNDAY

Track 10	Track 11	Track 12
Biomedical Imaging II	Biophysics	New Frontiers
Chair: J. Lyubovitsky (UCR)	Chair: V. Vullev (UCR)	Chair: D. Morikis (UCR)
(355 Commons)	*(379 Commons)*	*(367 Commons)*

Oral Track 12 — *New Frontiers*

Poster Session II

11:15 am – 12:15 pm *302 B* *Chair: B. Anvari, UCR*

SUNDAY *Commons*

Poster Track 2 — *Biomedical Imaging*

		Page
B1	Novel Scintillation Detector for A Laboratory PET Scanner. Huini Du, Yongfeng Yang, Jarek Glodo, Yibao Wu, Kanai Shah and Simon R. Cherry. UCD/Radiation Monitoring Devices	82
B2	Towards a Flexible, Conformal Medical Ultrasound Imaging System. Shyam Natarajan, Rahul S. Singh, Michael Lee, Elliott R. Brown, Warren S. Grundfest, Hua Lee and Martin O. Culjat. UCSB	83
B3	Multi-Modal Approach for the Integrated Assessment of Activated Microglia with Plaques in Alzheimer's Disease Models. Erica Andreozzi, Ben Jarrett, Izumi Maezawa, Lee-way Jin and Angelique Louie. UCD	84
B4	Design and Development of Circumferential Image Reconstruction Algorithms for a Flexible, Conformal Ultrasound Array System. Michael Lee; Rahul S. Singh, Martin O. Culjat, Shyam Natarajan, Elliott R. Brown, Warren S. Grundfest and Hua Lee. UCSB/UCLA	85
B5	Personal Computer Based Multimodal Trainer. Gurneet Singh, William J. Kaiser and Eric A. Savitsky. UCLA	86
B6	A Practical Double-tuned 1H/13C Birdcage Resonator for MRI/MRS at 7T. Chunsheng Wang, Bing Wu and Xiaoliang Zhang. UCSF/UCB	87
B7	Multiple Reception Strategy and Extended GRAPPA for SNR Improvement at 7T. Bing Wu, Chunsheng Wang and Xiaoliang Zhang. UCSF/UCB	88
B8	Correlation of Transepidermal Water Loss with Skin Barrier Function In Vitro and Comparison of Three Evaporimeters. Rania Elkeeb, Xiaoying Hui, Heidi Chan, Lilian Tian and Howard I. Maibach. UCSF	89
B9	Understanding cellular responses: multi-photon imaging of actin filament formation and mitochondrial energetics of ACBT gliomas. Yu-Jer Hwang, Edgar I. Sanchez, Chung-ho Sun, Tatiana B. Krasieva, Bruce J. Tromberg and Julia G. Lyubovitsky. UCR/UCI	90
B10	Temperature Measurements of Laser Irradiation for Tissue Protection During Cryosurgery. L. Martínez-Suástegui, G. Aguilar, F. Godinez and A. M. Walker. UCR	91
B11	An fMRI study to correlate objective brain activations with subjective survey responses. Prashanthi Vandrangia, Angelika Dimoka. UCR	92
B12	Measuring Transepidermal Water Loss: A comparison between Conventional Bioengineering Techniques in vivo. S. Farahmand, L. Tien, X. Hui, and H.I. Maibach. UCSF	93
B13	Prospective Study of the Effectiveness of Thermal Imaging in the Diagnosis of Arthritis: Can a radiometric thermal imager detect pre-clinical stages of arthritis in a quick and noninvasive test? Shay Edwards. Norco High School	94

Poster Session II

11:15 am – 12:15 pm *302 B* *Chair: B. Anvari, UCR*

SUNDAY *Commons*

Poster Track 6 — *Biomaterials*

Poster Track 9 — *Biomechanics & Biodevices*

Poster Track 11 — *Biophysics*

Using Neural Networks for Residue-Residue Contact Predictions

George Shackelford and Kevin Karplus
University of California, Santa Cruz

Advances in genomic sequencing have resulted in the addition of millions of protein sequences, but experimentally determined protein structures still number in the tens of thousands. Knowing the structure of the protein is useful in determining protein function and the development of new drugs. There is increased interest in improving protein structure prediction, known as the protein folding problem. Much software has been developed for generating and evaluating 3-D or tertiary models of a protein.

However, examining all possible folds of a sequence is computationally infeasible; finding constraints to reduce the search is essential. Residue-residue contact prediction is the prediction that two residues, widely separated along the sequence, will be in close proximity when the protein folds. Using these predictions as constraints can help develop the tertiary prediction models.

The neural network is a commonly used machine learning tool for contact prediction. We have developed a new predictor using a neural network with 647 selected inputs that improves on our previous 449 input neural network. At the seventh international Critical Assessment of Structure Predictions (CASP7), the earlier predictor was assessed as the best contact predictor. The newer network is competing in this summer's CASP8 experiment.

We discuss the selection of the inputs, including a novel correlation statistic based on the significance of mutual information, the selection of RProp backpropagation, and our method for correcting the imbalance between positive and negative training examples. We conclude with test results showing the improvement.

New Machine Learning and Data Mining Strategies for Identifying and Clustering Biostructural Molecules

Aaron M. Newman[1] and James B. Cooper[1,2]

[1]Biomolecular Science and Engineering Program, University of California, Santa Barbara
[2]Molecular, Cellular, and Developmental Biology Department, University of California, Santa Barbara USA 93106

Through an iterative process of mutation and natural selection, diverse living organisms evolved on Earth to succeed in almost every conceivable niche. Within Earth's biodiversity, myriad structural biomolecules solve a variety of chemo-mechanical problems. One class of such molecules are modular structural proteins composed of tandemly repeated peptide motifs. These Tandem Repeat Proteins (TRPs) are known to compose a variety of important biomaterials, including insect and spider silks, animal collagens and keratins, bivalve mussel holdfasts, insect flight muscles, and plant cell wall matrices. To complement conventional biochemical approaches, we are pioneering computational strategies to identify and classify useful TRPs from the ever-expanding genome sequence databases. A repeat-recognition program, called XSTREAM[1], uses seed-extension coupled with post-processing algorithms to efficiently identify fundamental TR motifs in large sequence datasets (approximately 10% of the ~12M available protein sequences have some TR content). Several key features of XSTREAM, such as TR architecture modeling, merging of discontinuous TR domains, and the detection of complex hierarchical TR patterns are illustrated. To facilitate TRP studies at the multi-genome scale, a powerful graphical user interface, the TR Browser, was developed to navigate and analyze MySQL databases populated with output from XSTREAM. The TR Browser features novel machine-learning tools for *a priori* clustering of TRPs according to physico-chemical properties of their corresponding TR domains. We present examples of X-like structural TRP classes (where X = elastin, silk, collagen) and of natural AB diblock copolymer proteins found with the TR Browser. Using several common benchmark datasets, we provide validation results of our new clustering algorithms, which have utility for detecting clusters of diverse geometries within any discrete or continuous dataset without user specification of cluster number, shape, or size. Additional capabilities of the TR Browser, such as domain-based modular protein sorting, three-dimensional visualization of TR clusters, automatic taxonomy retrieval, and rapid collection of large multi-genome datasets statistics are also illustrated. Taken together, these approaches provide a valuable discovery platform for uncovering 'green' biomaterials with novel properties stemming from the precise nanoscale engineering evolved by Nature over the past 3.5 B years.

[1] Newman AM, Cooper JB. XSTREAM: a practical algorithm for identification and architecture modeling of tandem repeats in protein sequences. *BMC Bioinformatics* (2007) 8:382

Virtual Screening for Novel Phosphatase Inhibitors Using Grid Computing

Marshall J. Levesque[2], Kohei Ichikawa[3], Susumu Date[1], Shu Chien[2], Jason H. Haga[2]
[1] Cybermedia Center, Osaka University, Osaka, Japan
[2] Department of Bioengineering, University of California, San Diego, La Jolla, CA, USA
[3] The Research Center of Socionetwork Strategies, Kansai University, Osaka, Japan

Virtual screening has become an important part of the drug discovery process. Grid computing facilitates this process by providing shared computational resources across different international institutions to run computationally intensive, scientific applications without the need for a centralized supercomputer. This study designed and implemented a flexible, scalable platform to perform a large virtual screening experiment on the PRAGMA grid testbed using the molecular docking simulation software DOCK 5.4. Using Opal OP to wrap DOCK as a grid service and PERL for data manipulation purposes, the "druglike" subset of the ZINC database, which contains 2,066,906 compounds, was successfully screened against the catalytic site of a protein tyrosine phosphatase. The screening required 11.56 days laboratory time and utilized 200 processors over 7 clusters. A ranked list of the best binding compounds to the phosphatase was generated and is currently being tested in biological assays for their efficacy and specificity.

Deep Sequencing and Bioinformatics Analysis of Human Endothelial MicroRNA Profiling under Hypoxia Stress

Zhen Chen[1], Ruobai Sun[2], Chellappan Padmanabhan[3], Wei Sun[1], Thomas Girke[2], Shu Chien[4], Hailing Jin[3], and John Y-J. Shyy[1]

[1]Division of Biomedical Sciences, [2]Institute for Integrative Genome Biology, [3]Department of Plant Pathology and Microbiology, University of California, Riverside, CA.
[4]Department of Bioengineering, University of California, San Diego, La Jolla, CA.

MicroRNAs (miRNAs) are small non-coding RNAs that regulate gene expression by degrading or translationally repressing target messenger RNAs (mRNAs) with fully or partially complementary pairing match. Most miRNAs are evolutionarily conserved and have been identified to regulate a variety of developmental, physiological, and pathological processes. To date, ~ 500 human miRNAs have been identified. However, the relative abundance, expression specificity, and functional relevance of miRNAs in different tissues, especially under various pathophysiological conditions, remain to be investigated. Hypoxia, a pathological stress on the cardiovascular system, induces drastic functional changes in endothelium. We hypothesize that alternation of endothelial miRNA expression profile plays a critical role in hypoxia-induced endothelial responses. Cultured human umbilical vein endothelial cells (HUVECs) were stressed with <1% environmental O_2 hypoxia for 24 hours. Small RNAs extracted from hypoxia-stressed HUVECs or normoxia control cells were ligated with distinct RNA adaptors and reverse transcribed into cDNA. The PCR amplified small RNA cDNA libraries were subjected to SBS deep sequencing. Bioinformatics analyses, including consecutive BLAST of the sequences against human genome and Rfam and miRNA Registry databases matching, were performed on ~10^6 small RNA sequences. A total of 157 known miRNAs were identified, of which 58 were highly expressed in HUVECs. A cluster of potential new miRNAs expressed in endothelium was also analyzed. The differential expression profiles of miRNAs between hypoxia-stressed HUVECs and normoxia controls suggest that miRNAs expression is regulated by hypoxia stress, which would participate in hypoxia-induced endothelial response (see Table below). Based on the sequence homology, we were able to decipher the miRNA-targeted mRNAs. Our study represents a first bioinformatics analysis for large-scale and genome-wide characterization of human endothelial miRNAs expression profiling and differential expression in response to hypoxia stress.

Table: Changes of HUVEC miRNA expression profile in response to hypoxia stress

Response to Hypoxia	Number of miRNA	
Upregulated (>2 folds)	41	miR-151-5p, miR-107, miR-103, miR-31, miR-320, miR-36b, miR-221, etc
Downregulated (>2 folds)	16	miR-22, miR-101, miR-21, miR-411, miR-23a, miR-30c, etc
Unchanged	100	miR-222, miR-92b, miR-92a, miR-27a, miR-27b, miR-216a, miR-181b, miR-15b, etc

Serial Assessment of Lactate in GBM Patients Undergoing Treatment Using Lactate-Edited 3D ^{1}H MR Spectroscopic Imaging at 3T

I. Park[1], S. M. Chang[2], S. J. Nelson[1]

[1]UCSF/UCB Joint Graduate Group in Bioengineering, San Francisco, CA, United States,
[2]Department of Neurological Surgery, University of California, San Francisco, CA

Introduction: Assessment of lactate prior to the initiation of radiation/chemo treatment and over the course of treatment is of interest to test lactate as a predictive marker for treatment outcome. The purpose of this study is to evaluate and compare lactate values prior to radiation (preRT) and during treatment in GBM patients. The emphasis was on both quantitative and qualitative assessment of the patterns of lactate.

Materials and Methods: Eleven GBM patients (9 male, 2 female; median age 55, range 41-67), who underwent surgical resection and were treated with radiation/chemotherapy, were examined for this study. A lactate edited 3D MRSI (TR/TE=1104/144 ms with 1 cc nominal resolution, 16x16x16 for readout coverage, total acquisition time=9:34 min) [1] was acquired using a 3T MR scanner (GE Healthcare, Milwaukee, WI) with an 8-channel phased array head coil. Lactate SNR was normalized (nLac) by median SNR of NAA in normal appearing white matter (NAWM) for each exam [2]. Lactate appearing in necrotic region, resection cavity or cerebrospinal fluid were excluded. Patients were classified into 3 groups based on radiologist's report: those who *progressed* at any time point, those who were *non-progressors*, and *undefined* who only had exams less than 2 months from preRT.

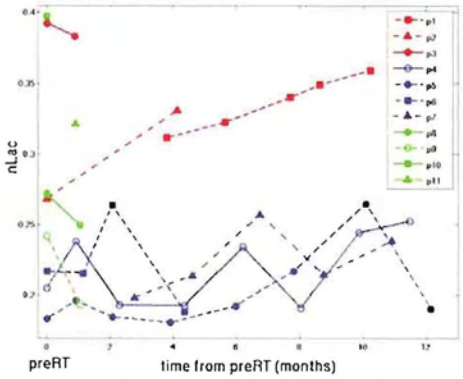

Results: Three patients showed tumor progression (red), four were non-progressors (blue), and four were undefined (green in Figure 1). Patients 1 and 2 showed a consistent increase in the level of nLac. nLac was significantly different across all exams between progressing and non-progressing patients (P=0.00004). The 75th percentile of nLac was significantly different between progressing and non-progressing patients at the preRT exam (P=0.037).

Discussion/Conclusion: In two of the three progressing patients (patient 1 and 2), the location of tumor recurrence at the time of progression coincided with the regions of lactate appearance at earlier exams, which interestingly, possessed no indication of progression by other radiological parameters in T1, T2 weighted images and MRSI (Figure 2,3). T1 enhancement (e) and T2 hyperintensity (f) as well as high Cho-to-NAA ratio (Cho/NAA) in summed spectra (blue voxels in g) indicate tumor progression, which overlaps with the region of lactate at preRT (Figure 2) or earlier exam (Figure 3) shown in the subtracted spectra (yellow voxels in d). The fact that both of these patients showed no radiographic signs of progression, but consistently had lactate at the site of subsequent progression suggests that monitoring of lactate during treatment with radiation/chemo may assist in characterizing tumor tissue and predicting outcome.

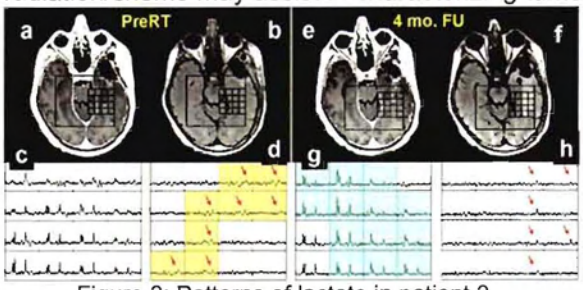

Figure 2: Patterns of lactate in patient 2

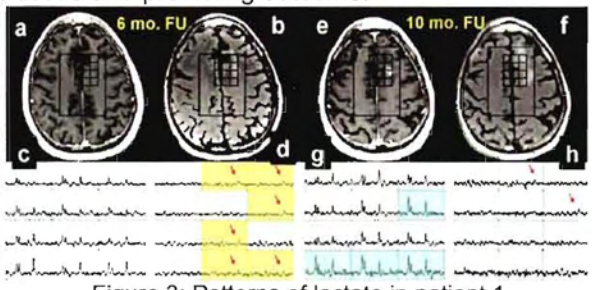

Figure 3: Patterns of lactate in patient 1

References: [1] Park I, et al., *Proc. ISMRM, 15th Annual Meeting, Berlin*, 2007. p 775. [2] Nelson SJ, et al., *Magn Reson Med*.2001;46: 228-239.

Fundings: UC Discovery grant ITL-BIO04-10148 and NIH grant R01CA059880.

In Vivo Hyperpolarized Carbon-13 Localized Spectroscopic Imaging of Mouse Liver

Simon Hu[1,2], Peder Larson[1], Matthew L. Zierhut[1,2], Robert Bok[1], Jason Crane[1], Mark Van Criekinge[1], Sarah Nelson[1,2], John Kurhanewicz[1,2], and Daniel B. Vigneron[1,2]
[1] Dept. of Radiology, UCSF, San Francisco CA. [2] UCSF & UCB Joint Graduate Group in Bioengineering

Introduction

In vivo ^{13}C nuclear magnetic resonance (NMR) spectroscopy has traditionally been limited by low sensitivity. However, recent technological advances have enabled greater than 50,000-fold enhancement of liquid state polarization of metabolically active ^{13}C substrates [1], allowing for rapid assessment of carbon metabolism in vivo. This technology holds great clinical potential, with pre-clinical studies in a mouse model of prostate cancer already demonstrating the ability to monitor disease state [2]. Many other possible applications exist, and the purpose of the present study was to apply hyperpolarized ^{13}C spectroscopy to the investigation of liver metabolism. In this project, we applied dynamic spectroscopy and localized spectroscopic imaging of healthy mouse liver using various data acquisition techniques that we have developed, demonstrating feasibility for future small animal pre-clinical studies.

Methods

^{13}C-1-pyruvate was hyperpolarized using an Oxford Instruments HyperSense^{TM} system (~25% polarization with addition of gadolinium). ~300 µL of 80mM hyperpolarized pyruvate were injected through a mouse tail vein catheter over a 12s duration. All experiments were performed on a GE 3T system using custom dual-tuned $^{1}H/^{13}C$ RF coils. All pulse sequences used a double spin-echo design with adiabatic refocusing pulses [3]. For multi-slice dynamic acquisitions, a flyback echo-planar trajectory was employed during the readout to achieve 8.76 mm resolution in the S/I direction and 3s time resolution. For single slice 2D localized dynamic acquisitions, we used multiband spectral-spatial pulses [4] for the excitation (2.5° flip for pyruvate and 15° flip for lactate and alanine), 8 phase encodes in y, and flyback readout in x to achieve 5 mm x 5 mm x 10 mm x/y/z resolution and 5s temporal resolution. For 3D localized spectroscopic imaging acquisitions [2,5], acquisition parameters were: TE = 140 ms, TR = 215 ms, variable flip angle, centric phase encoding order, 5.4 mm S/I resolution, 4cm x 4xm in plane FOV, and a 16x16 phase encoding matrix. We used an accelerated imaging technique, compressed sensing, to achieve the 16x16 phase encoding (in plane resolution of 2.5 mm x 2.5 mm), which is a factor of 4 enhancement in resolution compared with the 8x8 encoding matrix without acceleration. The compressed sensing scheme we used, which has not been previously reported, is an extension mentioned in [5] in which we added y-gradient blips to achieve an additional factor of 2 increase in acceleration.

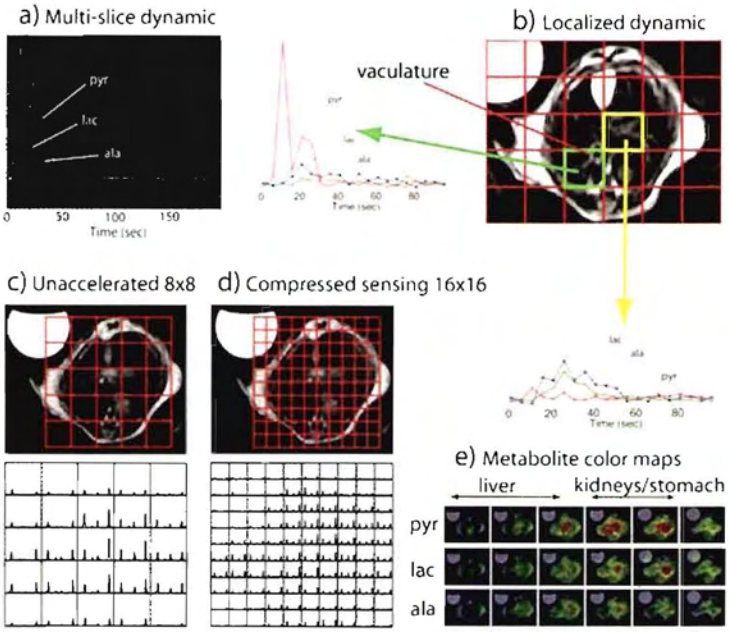

Figure 1: Summary of mouse liver imaging studies. a) Liver slice from multi-slice dynamic b) 2D localized dynamic with two voxels highlighted – a vasculature voxel and a liver tissue voxel c) Slice from unaccelerated 3D localized acquisition d) Enhanced resolution version of 3D localized acquisition using compressed sensing e) Metabolite color maps of pyruvate, lactate, and alanine generated from data in d)

Results/Discussion

Figure 1 summarizes the mouse liver imaging studies we performed. Figure 1a shows a liver slice from a multi-slice dynamic acquisition. We observed a double peak pattern in the pyruvate dynamic curve, which was previously reported for rats [6]. Using a 2D localized sequence, we acquired dynamic curves from 5mm x 5mm in plane voxels (Figure 1b) from the liver of a different mouse. For the first time, multiple voxel dynamics from an axial liver slice were obtained. Figure 1b shows a time course of events: an initial high influx of pyruvate in the voxel containing what appears to be the inferior vena cava (and presumably other vasculature, green voxel), the subsequent appearance of lactate and alanine elsewhere in the liver (yellow voxel, representative liver tissue voxel), a resurgence of pyruvate in the vena cava voxel (green voxel), and finally the peaking of lactate and alanine elsewhere in the liver (yellow voxel). The 2D localized data suggest a possible recirculation effect that could explain the double peak in pyruvate slice dynamic curves. More investigation is needed. Figures 1c and 1d show liver slices from 3D localized acquisitions, highlighting the improvement in resolution achieved with the new compressed sensing acquisition. For example, the outline of the mouse body is better delineated with the 16x16 acquisition. Figure 1e shows a few metabolite color maps generated from the 3D acquisition in figure 1d. The maps show that pyruvate was concentrated in the kidneys and the vasculature region in the center of the slices, lactate was concentrated in the kidneys, and alanine was localized to the liver and stomach.

Conclusion

We showed for the first time multi-slice dynamic, axial slice 2D localized dynamic, and compressed sensing 3D localized hyperpolarized spectroscopic imaging of mouse liver. The characterization of healthy metabolism will serve as a basis of comparison for future pre-clinical studies involving small animal models of liver disease.

References

1. Ardenkjaer-Larsen et al. Proc. Natl. Acad. Sci. USA, 2003. 100:10158-10163.
2. Chen et al. Magn. Reson. Med. 2007. 58:1099-1106.
3. Cunningham et al. J. Magn. Reson. 2007. 187:357-362.
4. Larson et al. Manuscript to be submitted to J. Magn. Reson.
5. Hu et al. J. Magn. Reson. 2008. In Press and Online. doi:10.1016/j.jmr.2008.03.003

Probe based multiphoton microscopy using a MEMS mirror and double-clad photonic crystal fiber

Woonggyu Jung[1,2], Suo Tang[3], Daniel T. McCormick[4],Tiquiang Xie[1], Yeh-Chan Ahn[1], Jianping Su[1,2], Ivan V. Tomov[1], Tatiana B. Krasieva[1], Bruce J Tromberg[1,2], Zhongping Chen[1,2]

[1]*Beckman Laser Institute, University of California, Irvine, USA*

[2]*Department of Biomedical Engineering, University of California, Irvine, USA*

[3]*Department of Electrical and Computer Engineering, University of British Columbia, Canada*

[4]*Advanced MEMS, Berkeley*

A factor that limits the use of multiphoton microscopy (MPM) in clinical and pre-clinical studies is the lack of a compact and flexible probe. In the design and fabrication of such a probe, there are key challenges; (1) a compact scanning mechanism, (2) efficient delivery of an ultrashort pulse, (3) collection of fluorescence signals, (4) optimal micro optics design, (5) integration and packaging. In our study, we merge the benefits of the MEMS scanning mirror and a double-clad photonic crystal fiber (DCPCF) to realize a completed probe. The schematic and photos of the developed MPM probe are presented in Fig. 1.

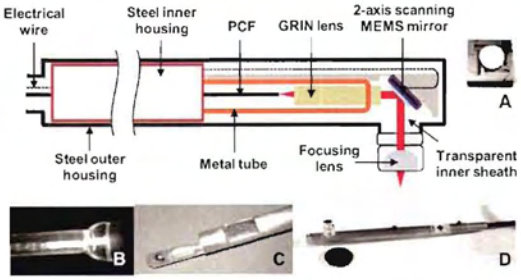

Fig. 1. Schematic and photographs of the MPM probe. (A) Photograph and schematic of two-axis MEMS mirror. (B) Photograph of GRIN lens assembled with DCPCF. (C) MEMS mirror and pigtailed GRIN lens were mounted to custom-made packaging. Photograph depicts the inner portion of the probe prior to integration with the outer housing. (D) Photograph of completed probe. Submarine shaped probe compared for size to a U.S. quarter coin.

Our probe is comprised of a 2-axis scanning MEMS mirror, DCPCF, a gradient index (GRIN) lens and an aspheric lens mounted in aluminum housing. The MEMS device employed in this study had a 2 mm diameter mirror and exhibited x- and y-axis resonant frequencies of 1.26 kHz and 780 Hz, respectively. The scanning angle of each axis was 14° (optical). Fig. 1A presents an image of the diced MEMS mirror. The DCPCF that used in this work has a core diameter of 16 μm and an inner cladding with a diameter of 163 μm. The outer diameter and length of probe was 1 cm and 14 cm, respectively. The diameter of the lens mount was 7 mm and the length was varied from 6 mm to 1.5 cm. The developed probe was integrated into an MPM system and used to image fluorescent beads, paper and biological specimen as shown in Fig. 2.

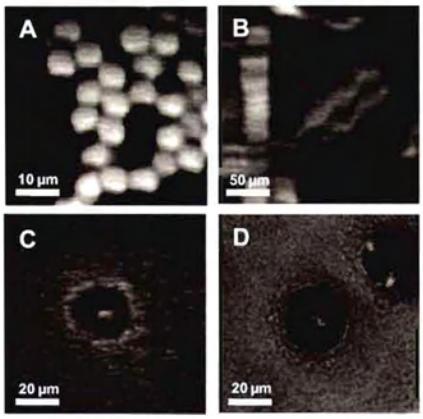

Fig. 3. *In-vitro* MPM images using the compact probe. The excitation power at the sample was 15 mW. (A) Image of 6 μm fluorescent beads. (B) Image of paper. Each fiber is clearly visualized. (C) Image of chondrocyte in a articular cartilage. (D) Image of condrocytes by commercial MPM system. The imaging parameters of the commercial MPM were matched with the same values as our developed system: optical power at the sample, wavelength, NA of objective lens, scanning rate.

In summary, a portable MPM probe using a MEMS mirror and DCPCF was designed and constructed. It provides many advantages, such as size reduction, rapid and precise scanning, efficient short pulses delivery, and high collection rate signals. A future version of the current device could function as an endoscopic tool by means of optimal micro optics and further reduction in packaging size. Such a compact probe may greatly expand the applications of MPM, and is a promising device for high resolution diagnostic imaging.

Digital Noise Reduction for High-throughput On Chip Cell Characterization

Sungkyu Seo[1,*], Ting-Wei Su[1,*], Anthony Erlinger[1], and Aydogan Ozcan[1,2,†]
[1] Electrical Engineering Department, University of California, Los Angeles, CA 90095
[2] Biomedical Engineering IDP, University of California, Los Angeles, CA 90095
*Equal contribution; †Correspondence to: Aydogan Ozcan
ozcan@ucla.edu; http://www.innovate.ee.ucla.edu

We recently illustrated that without using any lenses, microscope objectives or any mechanical scanning, it is possible to rapidly characterize an ultra-large volume of a ***heterogeneous*** cell solution (e.g., ~5 ml) by recording the diffraction signature of each cell onto a opto-electronic sensor array (see Fig. 1). We refer to this new high-throughput cell characterization scheme as multi-color LUCAS (Lensless, Ultra wide-field Cell monitoring Array platform based on Shadow imaging). Here we experimentally illustrate that to improve the automated cell characterization accuracy of multi-color LUCAS images, digital noise reduction in the raw image can be effectively utilized. In LUCAS platform, there are several noise sources such as potential dust or unwanted micro-particles on the sensor surface or within the sample volume; dead pixels in the sensor array; or detector noise (e.g., read-out noise, etc). All of these noise terms degrade the quality of the raw LUCAS image, which then translates itself to an increased error rate for automated cell counting results as highlighted in Fig. 2(a). To address this issue, we implemented several image improvement methods, i.e. background image subtraction, and use of digital noise reduction filters to minimize the influence of these noise artifacts on the performance of the multi-color LUCAS platform. Here, we evaluate the quantitative performance of these digital noise reduction approaches for rapid on chip characterization of a heterogeneous cell solution of ~5 ml.

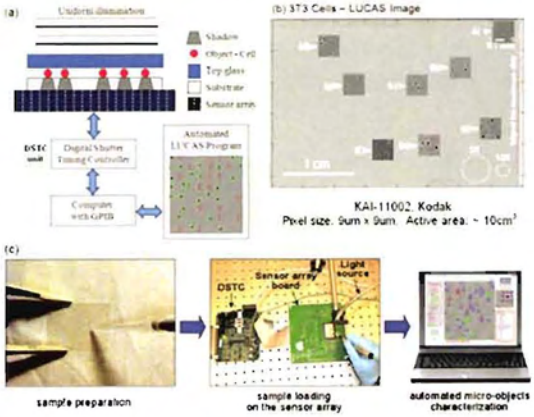

Figure 1. (a) Experimental multi-color LUCAS set-up illustrating the effect of diffraction on the cell shadow; (b) Single frame LUCAS image for 3T3 cells that is captured using the set-up of (a) over an ultra-wide field of view of ~10 cm^2. The insets show the zoomed images of various points on the LUCAS image illustrating the diffraction signatures of individual 3T3 cells. The same figure with white dashed circles also shows the field-of-view of 10X and 5X objective-lenses. This figure demonstrates that LUCAS can monitor a field-of-view that is ~2 orders of magnitude wider than a regular optical microscope. (c) Simplified illustration of LUCAS multi-color imaging procedures.

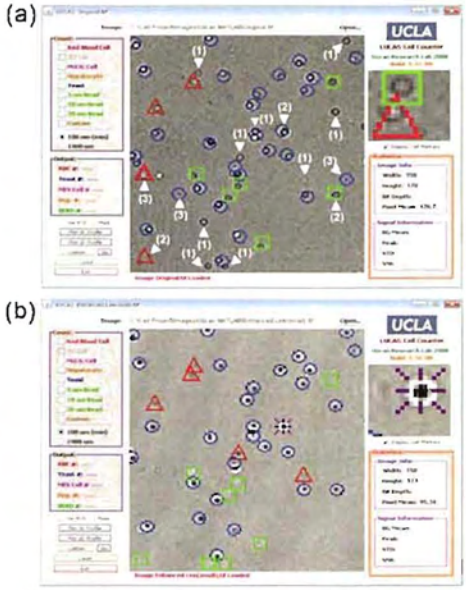

Figure 2. Multi-color LUCAS characterization results for a heterogeneous solution imaged at a height of 1068 μm and λ=300 nm. (a) Red triangles, blue circles and green squares mark the locations of RBCs, yeast cells and micro-beads, respectively, which are automatically calculated using the decision algorithm applied to the ***raw*** LUCAS image of this heterogeneous mixture. We also marked the errors made in the calculated results with white triangles showing the error location and its type. (b) For the same region of interest, the same "decision algorithm" can yield a count/characterization accuracy of **100%** by utilizing a digital filter (e.g., Enhanced Lee filter) that enhances the signal-to-noise ratio and the image quality of the LUCAS signatures.

Development of an implantable, wireless vital signs sensor suite

Robert Tan[1], Timothy McClure[2], Jacob Schmidt[1], Peter Schulam[2,3]

[1]University of California, Los Angles Department of Bioengineering, [2]University of California, Los Angeles Department of Urology, [3]Center for Advanced Surgical and Interventional Technology

Currently, continuous patient monitoring requires tethering of the patient to large bulky sensors in a hospital setting. These existing sensors obtain physiological data in an artificial and static environment; one cannot analyze how the patient's lifestyle and normal environment affects physiological parameters. We are developing a wireless, fully implantable sensor system capable of detecting pressure, temperature, blood oxygen tension, and heart pulse rate that actively and continuously records and transmits data in real time. While implantable sensors have been fabricated before, they have typically been passive devices and limited to sensing one quantity, and to our knowledge, this work represents the first time such an idea has been undertaken.

We are developing a wireless, fully implantable sensor system capable of detecting pressure, temperature, blood oxygen tension, and heart pulse rate that actively and continuously records and transmits data in real time. This minimally-invasive implantable system consists of three components: the sub-mm sensor suite; the signal processing unit, battery, and wireless transmitter; and an external PDA that receives and logs the data. Currently, we have developed a piezoresistive pressure sensor based on this platform. Briefly, a MEMS pressure sensing chip is affixed and wirebonded onto a ceramic board, which is wrapped in polyethylene and covered with silicone. Wires threaded through a 7.5F catheter are attached to the board and to a central processing unit, which is also attached to a 433 MHz wireless transmitter and a lithium-polymer battery.

Preliminary *in vitro* data for the pressure sensor demonstrate its ability to measure pressure within physiological ranges of 0-1.5 PSI (0-105.5 cmH_2O) with a resolution of 0.02 PSI (1.4 cmH_2O). Thermal drift was minimized by limiting the device operation to 30 μs intervals every second, reducing joule heating by three orders of magnitude and increasing the operational lifetime to 96 hours. Silicone, a porous polymer, enabled water vapor to diffuse through the device packaging and condense onto electrical components, causing malfunction. Polyethylene was found to be a more suitable barrier against water vapor. *In vivo* tests (n=3) of an ambulatory porcine model resulted in urinary pressure data that included a possible urination event. Data transmission was demonstrated up to 20 feet away; however, the tests also revealed shortcomings in the packaging design.

This work represents the first step in the development of a long term, implantable real-time vital signs monitor that has large implications for the medical, military, and athletic communities.

This work was funded by the United States Army Telemedicine and Advanced Technology Research Center (TATRC).

Lin, C.K., Jea, D., Dabiri, F., Massey, T., Tan, R., Sarrafzadeh, M., Srivastava, M.B., Schulam, P.G., Schmidt, J., Montemagno, C., "The Development of an In-vivo Active Pressure Monitoring System," 4th International Workshop on Wearable and Implantable Body Sensor Networks , March 2007.

Shrinky-Dink Gradient Generator for Single-Cell Chemotactic Quantification

Diep Nguyen[1], Jon Pegan[2], Bing Xia[1], Anthony Grimes[2], Jennifer O. Manilay[3], Michelle Khine[1, 2]

[1]Graduate Group in Biological Engineering & Small-scale Technologies, [2]School of Engineering, [3]School of Natural Sciences, University of California, Merced

Abstract:

The study of cellular migration in response to gradients of chemical-cues can provide insight into many disease mechanisms such cancer metastasis and immunological responses. The application of microfluidic devices allows for investigation on the effects of the microenvironment on migratory patterns. Here we report a novel microfabrication method to easily create gradient generators utilizing polystyrene molds for chemotaxis studies. Using ink-jet printing of Shrinky-Dinks, which are essentially pre-stressed polystyrene sheets, various patterns of gradient generators can be quickly produced. Through heat-induced shrinking of these patterns, high-aspect micromolds are generated. To produce the gradient generators, polydimethylsiloxane (PDMS) can then be molded onto the microfabricated patterns. Chemotaxis experiments are conducted using neutrophils differentiated from human promyelocytic leukemia (HL60) cell line under generated gradients of interleukin-8 (IL-8). Single-cell trafficking of cell migration was achieved and parameters can be categorized under various flowrates and IL-8 concentrations based on velocity, distance traversed and total displacement along a defined Cartesian coordinate. To quantitatively correlate the migratory behavior with the number of IL-8 receptors expressed on the cell membrane, IL-8 receptors will be stained with corresponding antibodies and imaged with fluorescence microscopy. In summary, we have developed an ultra-rapid process to create gradient generators for chemotaxis assays, obviating the need for photolithography altogether. Finally, we demonstrate the effectiveness of this approach by tracking cells under various chemotactic cues at the single-cell level.

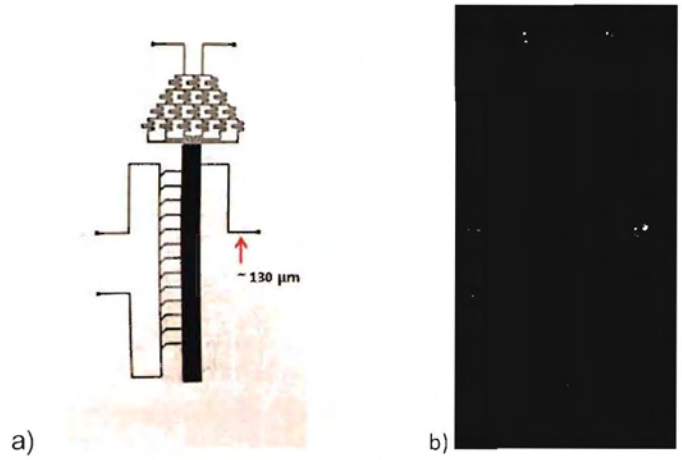

Fig. 1. Microfabricated fabricated devices: a) Shrinky-Dink Mold, b) PDMS gradient generator

DNA Assembly and Patterning of Functional Nanosystems

Faculty (PI): Mihri Ozkan[1], Cengiz Ozkan[2]
Researchers: Hayri Engin Akin[1], Maziar Ghazinejad[2], Huiqing Ma[3], Rong Li[4]
University: Electrical Engineering[1], Mechanical Engineering[2], Bioengineering[3], Biochemistry[4], UCR

To accomplish 100% selectivity during self- and directed- assembly of circuit components using nucleic acids, engineered DNA sequences are designed, tested for selectivity and then attached to the circuit components such as CNTs and NWs to provide desired integration and assembly of circuits on Si-CMOS. Showing us base specific hybridization of DNA can provide error free desired assembly and integration of circuits. Complimentary hybridization of short oligos as a lock and key patterning mechanism for integration of nanofunctional components on Si is implemented. Selective hybridization of oligos as lock and key is demonstrated as a proof of concept for controlled, high throughput assembly of nanostructures. Biotinylated lock oligos with 100 nM concentration are addressed on to the Si microarray platform through the application of current on the pads of the microarray. Key oligos with 100 nM are sent with a fluorophore at their end. Fluorophore made them visible under the microscope. After hybridization, thermal, electrical and washing stringency conditions are applied to eliminate the undesired mismatch signals on the pads. The signals from the matching lock and key segments to the mismatching ones are compared and 800 times selectivity is obtained. Engineered oligo sequences showed us 100% specificity. In addition, SWNT-DNA-SWNT and SWNT-PNA-SWNT nanoarchitectures have been synthesized in solution via the EDC coupling method. Electrical measurements (I-V characterization) of the nanoarchitectures demonstrate negative differential resistance (NDR) with the presence of SWNT-ssDNA and SWNT-ssPNA interfaces. I-V behavior under different temperatures shows that conductivity of the nanostructures varies with different temperatures. In addition, field effect transistors (FET) were fabricated using the nanoarchitectures where gate voltage was applied on the back of the Si/SiO2 substrate. Measurements of drain current versus gate voltage shows that SWNT-ssPNA-SWNT conjugates behave as p-type semiconductors.

Microfabricated Cylindrical Wells Facilitate Single-Molecule Enzymology of Bovine α-Chymotrypsin.

Angela Y. Chen[1], Ashish S. Jani[2], Lifeng Zheng[2], Peter J. Burke[1, 2], and James P. Brody[1].
Department of Biomedical Engineering[1] University of California, Irvine
Department of Electrical Engineering and Computer Science[2] University of California, Irvine

While ensemble-averaged kinetics masks the dynamics of individual enzymes, single-molecule studies have the capacity to delineate each enzyme's activities and substates in real time. We isolated our model enzyme, α-chymotrypsin, into single molecules by using PDMS wells. The wells are designed 2μm in diameter and 1.35μm in height, forming an array with a step size of 2μm. Not only do the wells isolate individual enzymes, but they also allow the simultaneous observation of a large number of enzymes, each enclosed in a single well. We used a concentration of 0.04 nM of α-chymotrypsin to ensure that each 2μm chamber enclosed less than one molecule of enzyme on average. By performing a protease assay with casein conjugated to BODIPY Texas Red as the substrate and α-chymotrypsin as the enzyme, we captured the fluorescence of each 2μm well with a CCD camera, recording an image every 5 minutes after 50 minutes of incubation over a total duration of 2 hours. We found that each α-chymotrypsin molecule has unique activity, and the heterogeneity of enzymes can be seen in the diverse trajectories of intensity recorded over time. In addition to the single-molecule study, we performed an assay for the ensemble study. By using 96-well microplates in the fluorometer, we determined α-chymotrypsin's turn-over rate to be approximately 1,580 substrate molecules per minute. We conclude that the behavior of individual enzymes may vary from the ensemble-averaged trend, and microfabricated wells can be a useful tool for single-molecule studies.

Immunological synapse formation in B cells

Philippos K. Tsourkas[*], Subhadip Raychaudhuri[*†‡§]
[*]*Dept. of Biomedical Engineering,* [†]*Biophysics Graduate Group,*
[‡]*Graduate Group in Immunology,* [§]*Graduate Group in Applied Mathematics*
University of California, Davis
One Shields Avenue, Davis, CA 95616, USA

[§]Address correspondence to: tsourkpk@yahoo.com

Recent experimental studies have shown that during the interaction between a B cell and an antigen-presenting cell (APC), surface-bound species segregate into a concentric pattern known as the "immunological synapse". The mature B cell synapse is characterized by a central cluster of B cell receptor/antigen (BCR/Ag) complexes surrounded by a ring of adhesive LFA-1/ICAM-1 complexes. In our work, we have used a computational approach to try to understand the formation mechanism of the immunological synapse in B cells, which is the subject of current debate. We use a Monte Carlo approach that simulates individual reaction and diffusion events on cell surfaces in a probabilistic manner with a clearly defined mapping between our model's probabilistic parameters and their physical equivalents. Our model incorporates the bivalent nature of the BCR as well as changes in membrane shape due to receptor-ligand binding. Our results indicate that cytoskeletally-driven, convective motion of BCR/Ag molecules towards the center of the contact zone is a potential mechanism of immunological synapse formation in B cells. Our modeling results also show that strong biased diffusion of free BCR and integrin molecules has a negative effect on synapse formation by excluding BCR/Ag complexes from the center of the contact zone. Comparison of our model's results to those of experiments shows that our model produces synapses for realistic length, time, and affinity scales. We also show how the diffusion trajectories of individual BCR and antigen molecules can reveal the presence of any bias in diffusion. Thus, our results can guide further single molecule tracking experiments to elucidate the synapse formation mechanism in B cells, and potentially in other immune cells.

Exploration of SUMO-SENP2 interactions using a high-throughput computational protocol.

Chris A. Kieslich, Jiayu Liao, Dimitrios Morikis
Department of Bioengineering
University of California, Riverside

Sumoylation of cellular proteins by the ubiquitin-like protein, SUMO, has been found to be one of the essential regulation mechanisms in signal transduction and genome integrity. Conjugation by SUMO first requires the maturation of the precursor through the cleaving of a C-terminal peptide. Following SUMO conjugation the SUMO peptide can also be removed from its substrate in vivo. SENP2, an endopeptidase, is responsible for both maturation of SUMO-1 into its conjugatable form, and the deconjugation of SUMO-1 containing species, and therefore plays significant role in the regulation of SUMO-1 sumoylation.

In this study, a high-throughput computational protocol[1] was used to elucidate possible interactions of interest in the SUMO-SENP2 complex. The protocol involves: (i) performing a computational Alanine scan, including only ionizable amino acids, (ii) calculation of electrostatic potentials according to the Poisson-Boltzmann equation, (iii) generation of images of spatial distributions of electrostatic potentials, (iv) calculation of electrostatic similarity indices (ESI), using the calculated spatial distributions of electrostatic potentials, and (v) clustering of ESIs. When calculating the free energies of association the contributions of solvation, nonpolar, and Coulombic affects were separated. Finally, the generated clusters were ranked according to calculated free energies of association. A total of 94 Alanine mutants were created and evaluated based on an X-ray structure of the complex formed between the catalytic domain of SENP2 and SUMO-1.[2]

The data depict important interactions for both SUMO-SENP2 binding and the stability of the individual components of the complex. Among the interactions of interest are three intra-molecular and two inter-molecular salt bridges which may be vital to SUMO-SENP2 binding and stability. The produced predictions provide physichocemical insight into the mechanism of SUMO-SENP2 binding and will be used to guide mutagenesis experiments, in hope of understanding binding specificity between SENP2 and SUMO-1.

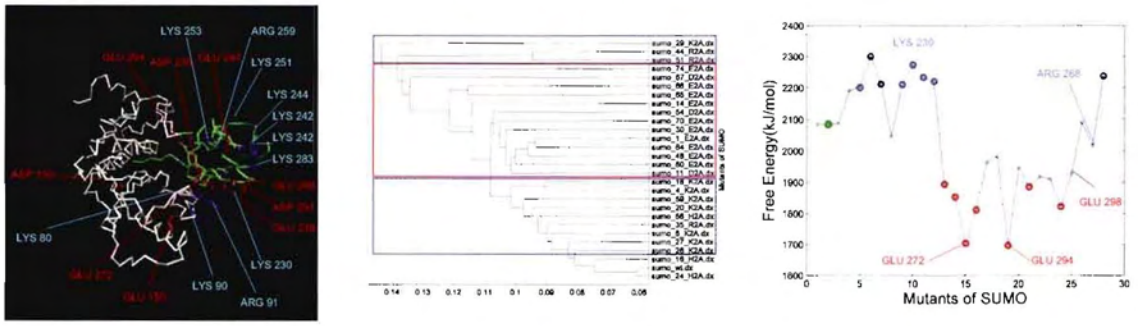

(A) C-alpha trace of the X-ray structure of SENP2 (white) and SUMO-1 (green) complex. The side chains of residues with predicted significant free energy deviations with respect to the parent complex are labeled (B) ESI clustering for SUMO-1 mutants. (C) Free energies of association for SUMO-1 mutants ordered according ESI clustering (middle). The labeling color code is blue for positive residues and red for negative residues.

[1]Yang J, Gunopulos D, Morikis D (2007) In Preparation.
[2]Reverter D, Lima C (2004) Structure 12:1519-1531.

Bioengineering of polymeric drug carriers for cancer therapeutics using computational modeling

Lili X. Peng [1], Robert Swift [2], Anthony Ivetac [2], Sang Van [3], J. Andrew McCammon [2], Lei Yu [3], Stephen B. Howell [4], and David A. Gough [1]

[1] *Department of Bioengineering, University of California, San Diego, La Jolla, CA 92093-0412,* [2] *Department of Chemistry and Biochemistry, University of California, San Diego, La Jolla, CA 92093-0365,* [3] *Nitto Denko Technical Corporation, Oceanside, CA, 92058,* [4] *UCSD Moores Cancer Center, University of California, San Diego, La Jolla, CA 92093-0819*

Polymeric nanoparticles are of great interest as drug carriers due to their potential for simultaneously targeting tumors and limiting drug exposure to normal tissues. The classical method of drug carrier design invokes trial-and-error testing of chemical substances on animals and subsequently matching of effects to treatments. This procedure can be time-consuming and expensive. In our study, we are designing a nanoparticle consisting of a cancer drug, Paclitaxel (PTX), covalently bound to a biopolymer, poly-L-glutamyl-glutamine (pGGA). We use an *ab initio* approach involving computational modeling spanning the micro-to-mesoscale regimes as a novel alternative. It has been established that the cellular uptake of nanoparticles and depends on physicochemical properties such as size and shape. Non-spherical, disc-like, and cylindrical-shaped particles have been shown to outperform their spherical counterparts while crossing transport barriers in drug delivery. To construct these non-spherical geometries, coarse-grained models of PTX-pGGA were developed by varying the hydrophobic:hydrophilic (PTX:pGGA) mass ratio and covalent attachment sites of PTX on pGGA. These systems were then run for 200ns using the GROMACS and dissipative particle dynamics simulation packages to observe self-assembly of PTX-pGGA into specific geometries. The plan is to demonstrate molecular modeling as a novel tool that allows us to engineer a successful intravenous cancer therapeutic. With this model we expect to suggest optimal physicochemical properties of PTX-pGGA for synthesis and testing.

Integrative Experimental and Computational Studies of Tumor Microvasculature

Nzola De Magalhães, M.S.[1], John Lowengrub, Ph.D [1,2]
[1]Department of Biomedical Engineering, University of California, Irvine
[2]Department of Mathematics, University of California, Irvine

Angiogenesis remains the most important mechanism exploited by tumors to secure their survival by serving as a means for nutrient acquisition, and as a vehicle for invasion and repopulation. Because of this dependency, angiogenesis has been a main target of study for the development of anti-cancer therapies. Tumor induced angiogenesis is a very complex biological process, involving multiple pathways and many signaling molecules that can interact cooperatively. Due to the variability of molecules and their cooperative function during angiogenesis, experimental investigations of these relationships can be limited. As a result, scientists have integrated experimental investigations with computational platforms to allow faster, quantitative, objective, and more automated analysis of biological processes. In contrast to experimental platforms, computational models offer the scientist the ability to perform quantitative investigations of multiple biological parameters simultaneously allowing the assessment of relationships and correlations between these parameters. In addition to their automated and quantitative investigation capability of tumor dynamics, computational models can be used to predict tumor behavior and response to therapy. The predictive capability of tumor simulators can have future implications in the development of noninvasive cancer diagnostic tools.

The objective of this project is to integrate a three dimensional in-vivo tumor biological model with a multi-scale virtual cancer simulator to investigate and predict quantitatively the dependency of tumor-induced angiogenesis on the spatial-temporal distribution of VEGF and HIF-1alpha, and tumor cell population in three-dimensional tumors. To meet the objective, the project will be conducted in two stages: experimental, computational. In the experimental stage, a three-dimensional in-vivo tumor biological model will be developed using human tumor derived spheroids and a shell-less chicken chorioallantoic membrane (CAM). The biological model will be used to induce tumor growth and angiogenesis, and to generate experimental parameter values. In the computational stage, the experimental parameters will be integrated into the pre-existing computational model to simulate tumorinduced angiogenesis. The computation model will then be calibrated and optimized to correlate the simulation results with in-vivo observations.

Serum-Free Derivation of Endothelial Cells from Embryonic Stem Cells

Alicia A. Blancas[1] and Kara E. McCloskey[1,2*]

[1]Graduate Program in Quantitative and Systems Biology
University of California, Merced

[2]School of Engineering
University of California, Merced

Vascular progenitor cells derived from stem cells could potentially lead to a variety of clinically relevant applications including cell-based therapies and tissue engineering. Previously, our laboratory developed methods for isolating purified proliferating populations of vascular endothelial cells (EC) from mouse embryonic stem cells (ESC) using Flk-1 positive sorted cells, VEGF supplementation, and a rigorous manual selection technique required for endothelial cell purification and expansion, exhibiting approximately 25 population doublings.

These cell culturing conditions, however; required high levels of fetal bovine serum (FBS). Since FBS composition can vary significantly from batch-to-batch, the reproducibility of some aspects of these experiments has been somewhat unreliable. Attempts for reproducibility of serum cultures leads to tiresome batch lot testing. Testing must then be repeated when the desired lot is exhausted. Development of a serum-free induction system allows more control over the stem cell microenvironment.

Serum-free maintenance of mouse ESC has been previously established, but efforts to develop serum-free cultures for vascular differentiation have been more difficult. Our lab is currently developing an induction medium in which Knockout Serum Replacement, VEGF, and BMP-4 are used in lieu of traditional FBS. Results indicate that it is possible to generate comparable percentages (30%) of Flk-1+ vascular progenitors without FBS supplementation, but the serum-free cultures proliferate at a rate 3X slower than cultures with FBS.

We have also investigated the final expansion medium for the Flk-1 positive cells to develop into mature endothelial cells. Preliminary results indicate the presence of VE-cadherin+ and PECAM-1+ cells from cells cultured post-Flk-1+ enrichment in a chemically defined EC medium. These studies allow the full derivation process of mature endothelial cells from embryonic stem cells under serum free conditions.

ACCELERATING ANGIOGENESIS IN SCAFFOLD BY DELIVERY OF VASCULAR ENDOTHELIAL GROWTH FACTOR

[1]Singh S, [1,2]Wu BM, [1,3]Dunn JC
Dept. of [1]Bioengineering, [2]Material Science and Engineering and [3]Surgery,
UCLA, Los Angeles, CA.

INTRODUCTION: The purpose of this research is to expedite blood vessel development in the implanted scaffolds. In the absence of blood vessels, the survival of cells in tissue engineered scaffolds is poor. Our specific objective is to accelerate angiogenesis in three-dimensional poly(ε-caprolactone) (PCL) scaffold by the delivery of vascular angiogenic growth factor (rhVEGF-165). It is mostly assumed that the *in-vivo* response is attributable to the release of soluble growth factors from the scaffold. As such, scaffolds are designed to modulate release kinetics of growth factors in order to improve their efficacy. However, biological contribution of scaffold-bound VEGF is largely unexplored. We intend to test our hypothesis that VEGF which is retained on the surface of heparin-modified scaffold can recruit new blood vessels inside the scaffold. Heparin mediates the interaction of VEGF-165 with extra-cellular matrix. We anticipate that heparin can bind VEGF to the construct while preserving its bioactivity. Our hypothesis is based on the studies that demonstrate matrix-bound VEGF to be more effective than soluble VEGF in supporting the vessel growth in tumor development.

METHODS: Porous PCL scaffolds were prepared by solvent casting/particulate leaching technique. The surface of the scaffolds was modified using collagen type-I (col-PCL) or heparin (hep-PCL). Neutralized collagen-I solution was coated on pre-fabricated scaffolds. On other scaffolds, heparin was cross-linked on surface using carbodiimide and hydroxysuccinimide. For *in vitro* release studies, radiolabeled VEGF-165 was absorbed on the scaffold and immersed in phosphate-buffer saline (PBS) or fetal bovine serum (FBS). To mimic physiological release kinetics, scaffolds were seeded with smooth muscle cells and incubated in serum-containing media. Biological activity of VEGF released from scaffold was determined by endothelial cell proliferation assay and chlorioallantoic membrane assay. *In vivo* studies involved subcutaneously implantation of scaffold in the back of C57BL/6 mice for 7 days. Some scaffolds were pre-washed in PBS before implantation to get rid of freely-soluble growth factor. To identify perfusable vessels, endothelium-binding lectin was injected intravenously before harvesting the scaffold. The density and area of blood vessels was quantified by immunohistology. The vessels were identified by endothelial cell marker CD-31 whereas mature blood vessels were identified by α-smooth muscle actin which is expressed in both pericytes and smooth muscle cells.

RESULTS: Hep-PCL scaffold shows diminished burst release and higher retention of VEGF than non-modified and col-PCL scaffolds. *In-vitro* assays proves that VEGF maintains its bioactivity upon release from the scaffolds. Implantation of scaffold indicates a VEGF dose-dependent increase in average vessel density inside the scaffolds. Most importantly, pre-washing scaffolds before implantation exhibits improved *in vivo* response towards lower doses of VEGF. These results suggests that both the released and the scaffold-bound fraction of VEGF are biologically active.

DISCUSSION: These studies will contribute to defining the scaffold design requirements for efficient delivery of VEGF. Future studies can utilize heparin-modified scaffolds to create versatile and stable gradient of VEGF.

THERMAL MODELING AND EXPERIMENTAL VALIDATION OF HAIR AND SKIN TISSUE HEATED BY INTENSE PULSED LIGHT

Feng Sun, Alex Chaney and Guillermo Aguilar

Mechanical Engineering Department, University of California, Riverside, CA

Background and Objective: Intense Pulsed Light (IPL), emitting high-intensity polychromatic light in a broad wavelength spectrum (515-1200 nm), has been extensively applied in dermatologic practice, e.g. epilation treatment for hypertrichosis. The present study aims to develop and validate a numerical heat diffusion and damage assessment model to predict light-tissue interactions, heat generation, temperature distribution and tissue damage during epilation using IPL.

Study Design/Materials and Methods: A Monte Carlo algorithm is used to describe light-tissue interactions and compute the heat generation that is subsequently introduced into an explicit finite difference scheme to calculate the temperature variations within the modeled human skin. The numerical model is experimentally validated *in vitro* using a multi-layer agar gel as the tissue phantom. A systematic parametric study is performed to investigate the effects of various parameters on the temperature of the hair shaft and the epidermal-dermal junction.

Results: Numerical results agree well with the experimental measurement of temperature variation in the tissue phantom during IPL heating and the cooling process that follows. The results indicate that immediately after IPL pulses, the temperature gradient concentrates on the upper part (0.5 mm) of the modeled hair shaft with a total length of 3 mm. Parametric studies reveal that average hair shaft temperatures increase linearly with IPL fluence, but decrease with elongated IPL pulse duration. The heat transfer coefficient of the convective surface cooling (10 ~ 1000 W/m_2-K) shows minimal effect on the average hair shaft temperature. Thermal damage is highly dependent on IPL fluence and absorption coefficient of modeled tissue.

Conclusions: An optical-thermal-damage model is developed and validated for hair and skin tissue heating during IPL therapies.

Collagen matrices: assessment of local stiffness by fluctuation spectroscopy

Kandice Tanner and Enrico Gratton
Laboratory for Fluorescence Dynamics, Department of Biomedical Engineering, University of California, Irvine.

We studied the migration of individual tumor cells, derived from the human glioma cell line ACBT that were implanted into a 3D gel matrix of collagen type I. Depending on the density of the matrix, cells can migrate in this 3D tissue model. The properties of the matrix are crucial for the migration of the cells. The cells and the collagen fiber network where imaged using a confocal microscope in the reflection mode so that the sample could be observed for a long period of time without bleaching. We developed a method based on image correlation spectroscopy and on local measurement of thermal fluctuations to determine the average size and the local stiffness of the collagen fibers. Intensity fluctuations were generated by the flickering of the reflections from the fibers. The reflected intensity from a single point in the fiber fluctuates due to fiber position fluctuations. We found a correlation between the fiber diameter and the fluctuation spectrum. Using continuous acquisition for several hours we determined the displacement of the fibers close to the cell as the cell forces its way in the 3D network during the migration process. We also observed changes in the fluctuation spectrum at specific locations probably due to the formation of cellular adhesions

Cell response to micro-topographical cues in 2D and 3D systems

Perla Ayala[1], Rahul G. Thakar[2], and Tejal A. Desai[1, 2, 3]
1. UCSF/UCB Joint Graduate Group in Bioengineering
2. Department of Physiology, UCSF
3. Department of Bioengineering and Therapeutic Sciences, UCSF

Chemical signals modulate cell migration, proliferation, differentiation, and death. Similarly, physical signals, and mechanical stresses can be converted into intracellular responses that regulate cell behavior and fate. The design and development of novel platforms for regenerative therapies requires an understanding of how physical and mechanical cues affect cell behavior. One method to study this interaction is the incorporation of microtopography into the therapy. Microtopography allows for the controlled manipulation of the cellular microenvironment and has far reaching effects on the system. For example, microtopgraphical cues discourage cellular proliferation compared to a flat, bare surface. To have a better understanding on the mode of regulation that microtopography provides to the cells we created restricted micro-scale environments. We evaluated various possibilities including the presence of mechanical gradients, chemical factors, and local geometric changes, which affect the interaction of the cell with the surrounding microtopography. Studies in 2D evaluated the impact of the microrods, chemistry, shape, and rigidity on cell behavior. It was observed that cells interacted with the microtopography in an organized manner even if surfaces had not been previously functionalized with ECM molecules. In addition, microtopography facilitated cytoskeletal alignment and allowed for cell organization and a more contractile phenotype compared to cells on a flat surface.

To make this *in vitro*, two-dimensional phenomenon into a viable regenerative platform, a system must be devised to create microtographical cues that include the third dimension. We have developed a three-dimensional system utilizing microtopography in the form of microrods suspended in matrigel. We have observed NIH 3T3 fibroblasts cultured with these microrods form a three-dimensional cell culture that significantly inhibits ($P<0.05$) the proliferation of the fibroblasts as compared to a three-dimensional matrigel culture without microrods. Fibroblast proliferation in 3D matrigel matrices was affected by both hydrophobic SU-8 photoresist and by hydrophilic polyethylene glycol dimethacrylate (PEG-DMA) microrods, two materials with different chemical and mechanical properties. These observations indicate that the decrease in fibroblast proliferation could be associated with a geometric and/or mechanical signal regulating mechanotransduction.

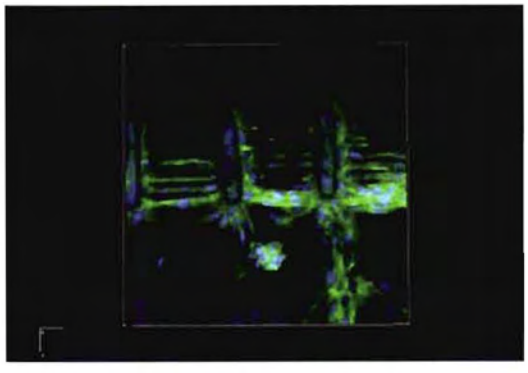

Figure 1. PEGDMA microrods on a silicon surface promote cell alignment and contractile phenotype.

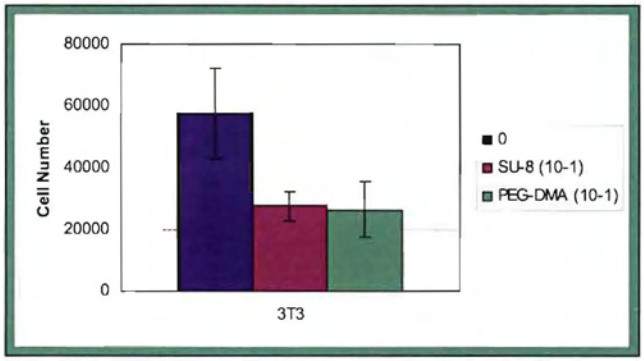

Figure 2. SU-8 and PEGDMA microrods inhibit fibroblast proliferation in a 3D matrigel matrix.

The role of alpha-helix formation in the self-assembly of protein-analogous micelles

Mark Kastantin and Matthew Tirrell

Department of Chemical Engineering
University of California, Santa Barbara

Alpha-helical structure in a peptide chain has been shown to affect the geometry of self-assembled systems containing these molecules.[1-3] In a related phenomenon, incorporation of a polypeptide into a self-assembled system has been shown to affect the helix-coil transition relative to the free polypeptide.[4] This work presents a quantitative model of the interaction between self-assembly and the helix-coil transition in micelles formed from hydrophobic hydrocarbon tails and water-soluble polypeptides. Such structures are termed protein-analogous micelles and can exist in spherical, cylindrical, or flat geometries as dictated by thermodynamic considerations.

This work shows that alpha-helix formation is stabilized by the micellization process while the amount of stabilization increases with the strength of attraction between hydrophobic tails. Helix formation drives the micelle to form structures with less curvature than would be expected if the polypeptide existed in a random-coil state. A transition in protein-analogous micelles is expected from spherical to cylindrical micelles as helical content of the polypeptide headgroup increases. This prediction is verified experimentally for a protein-analogous micelle in which helical content is controlled using pH. These results aid the design of protein-analogous micelles in which a target shape is desired.

1. Nakajima, A., T. Hayashi, et al. (1968). "Phase equilibria of rodlike molecules in binary solvent systems." Biopolymers **6**(7): 973-982.
2. Gebhardt, K. E., S. Ahn, et al. (2007). "Rod-sphere transition in polybutadiene-poly(L-lysine) block copolymer assemblies." Langmuir **23**(5): 2851-2856.
3. Lin, J. P., G. Q. Zhu, et al. (2008). "Aggregate structure change induced by intramolecular helix-coil transition." Polymer **49**(5): 1132-1136.
4. Bitton, R., J. Schmidt, et al. (2005). "Self-assembly of model DNA-binding peptide amphiphiles." Langmuir **21**(25): 11888-11895.

Fluorescence Biosensing for an Anticoagulant Drug, Warfarin

Jacob M Vasquez[2], Andrew Vu[1], Jerome Schultz[1], Valentine Vullev[1]
University of California, Riverside [1]Department of Bioengineering, [2]Department of Biochemistry and Molecular Biology

---

Warfarin is the most common agent used for control and prevention of venous as well as arterial thromboembolism (Blood Clots). Warfarins anticoagulant activity is evident at therapeutic doses as minuscule as 2-10mg for a 100kg person. The mode of action for warfarin arises through the antagonism of Vitamin K, which leads to the formation of non-functional prothrombin blood clotting factors. The actual effects of the warfarin can be estimated by measuring the blood clotting rate called prothrombin clotting time. In a drug as powerful as warfarin which has a very narrow therapeutic index, a more exact quantification technique would be useful. Warfarin forms inclusion complexes with a family of cyclic oligosaccharides, cyclodextrins (CD). The formation of these complexes results in enhancement of the fluorescence of warfarin that we use as a handle for warfarin quantification in biological liquids. To further increase the specificity of the method and to shift the excitation and detection of the fluorescence sensing to the visible region of the spectrum, we utilize auxiliary redox chromophores (AC) that manifest different rates of photoinduced electron transfer with warfarin. The detection and identification of warfarin can be extracted from extent of quenching of the AC emission in the visible region. We characterized the photophysical properties of warfarin in solvents with varying polarity and viscosity. The fluorescence quantum yield of warfarin correlated: (1) strongly with the solvent viscosity and (2) weakly with the solvent polarity. This finding indicated that it is the change of the viscosity, rather than polarity, of the microenvironment that causes the fluorescence enhancement of warfarin upon binding to CD. Fluorescence titration, utilizing the observed emission enhancement, allowed us to determine the binding constant of warfarin to CD with different sizes (α, β and γ) and determine the effective viscosity in the cavity of the inclusion complex. Stern-Volmer analysis of fluorescence quenching allowed us to determine the propensity of warfarin to undergo photoinduced charge transfer with different ACs. We believe that our method can be readily adopted for biosensing and quantification of a broad range of compounds with medical importance.

Nucleic acid lipid films with programmable mechanical, biodegradable and drug release properties as drug delivery vehicles towards human breast cancer cells

Surekha Gajria[1,3], Thorsten Neumann[1,3], Wirasak Smitthipong[1,2], Matthew Tirrell[1,2] and Luc Jaeger[1,3]
[1]Materials Research Laboratory, [2]College of Engineering, [3]Department of Chemistry and Biochemistry; University of California, Santa Barbara, CA 93106, USA

Please submit all queries by email to tirrell@engineering.ucsb.edu and by phone to (805) 893-5302

Negatively charged nucleic acids strands (DNA & RNA) self-assemble with cationic lipids like DDAB to form water-insoluble complexes. These complexes form self-standing films if they are cast on solid surfaces from an organic solvent such as isopropanol. We are now focusing on developing the biocompatibility and biodegradability of these films as well as their mechanical properties for drug delivery. We used drugs that can intercalate into the nucleic acid (NA) double strands, such as daunorubicin, which is commonly used in breast cancer therapy. These drugs could be released by local enzyme degradation of the N-lipid scaffold within the body while the remaining film components can be easily degraded to monomer units. The concentration and time rate of local treatment can be varied by the NA composition of the material. Additionally these NA-based materials can easily be generated and could be produced on a large scale. We have seen that these complexes when blended with the neutral biocompatible polymer PEG (polyethylene glycol) can show mediated toxicity to human breast cancer cells rather than normal human breast epithelial cells.

Engineering Transferrin Mutants to Enhance Targeted Drug Delivery

Dennis J. Yoon[1], David S. H. Chu[1], Christopher W. Ng[1], Edward A. Pham[1], Anne B. Mason[2], David Hudson[3], Valerie C. Smith[3], Ross T. A. MacGillivray[3], and Daniel T. Kamei[1]

[1]Department of Bioengineering, University of California, Los Angeles, CA 90095
[2]Department of Biochemistry, University of Vermont College of Medicine, Burlington, VT 05405
[3]Department of Biochemistry and Molecular Biology, University of British Columbia, Vancouver, BC V6T 1Z3, Canada

The serum iron transport protein transferrin (Tf) has been investigated as a potential drug carrier to allow specific targeting of cancer therapeutics to cancer cells, since the transferrin receptor (TfR) is overexpressed in a broad range of cancers. Specific targeting of drugs to cancer cells may help alleviate nonspecific toxicity associated with chemotherapy and radiation treatments. The use of Tf conjugates for cancer therapy is currently being assessed in clinical trials.

Upon binding to TfR, Tf is endocytosed, where it can then deliver its payload. Unfortunately, Tf is recycled rapidly to the cell surface, significantly reducing the time Tf has to deliver its drug. Therefore, we previously developed a mathematical model that identified the inhibition of intracellular iron release as a design criterion for increasing the cellular association of Tf with cells (1). We then generated a Tf variant with a slower iron release rate by replacing the synergistic anion of Tf, carbonate, with oxalate. This Tf variant was then shown to exhibit a 51% increase in cellular association, in turn, leading to a considerable increase in HeLa cell killing efficiency when conjugated to DT.

To determine if an even greater cell killing efficiency could be achieved, we have generated three recombinant Tf mutants with site-directed mutagenesis, exhibiting slower iron release rates compared to native Tf. We have radioactively labeled the native Tf and the mutants with iodine-125 and performed cellular trafficking experiments to demonstrate enhancements in cellular association. The native Tf and our three Tf mutants were incubated with HeLa cells at a 1 nM concentration for up to 2 h, and the amount of internalized Tf was monitored as a function of time. One such trafficking experiment shows that the HeLa cells internalized significantly greater amounts of a representative Tf mutant over their native Tf counterpart (Fig. 1). Comparing the AUC values of the two curves, we obtain a value of 1.6×10^7 (#·min)/cell for native Tf and a value of 3.6×10^7 (#·min)/cell for the mutant. This translates to an AUC increase of 129%.

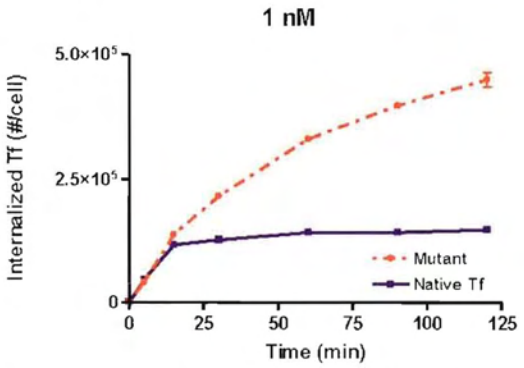

Fig. 1 Internalized Tf/cell for native Tf and mutant at a concentration of 1 nM over a 2 hour period. Error bars represent the standard deviation from an average of three measurements.

Moreover, surface plasmon resonance measurements were performed to demonstrate that these enhancements could be primarily attributed to differences in iron release rates rather than alterations in binding affinity of Tf for TfR due to the mutations. The drug carrier efficacy of these mutants is currently under investigation.

REFERENCES

1. BJ Lao, WP Tsai, F Mashayekhi, EA Pham, AB Mason, DT Kamei. *J Control Release* **117** (2007) 403-412.

Development of FRET-based high-throughput screening to discover SUMO E3 ligase inhibitors

Yang Song, Xiulin Shen, Jiayu Liao

Department of Bioengineering at University of California, Riverside

Covalent modifications of proteins are general mechanisms to alter protein functions in most cells, especially in eukaryotic cells. SUMO (Small Ubiquitin-like MOdifer) is a well-known protein family which with the assistance of SUMO E3 ligases modifies many proteins involved in diverse cellular processes. However, the investigations of SUMOylation in different cellular processes are limited by the difficulties in determining the interaction between the E3 ligase and the substrates as well as the lethality of gene knockout studies given the importance roles of SUMO in *vivo*. Using fluorescent protein variants we are developing high-throughput FRET-based screening methods to discover small chemical inhibitors of SUMO E3 ligase, which will serve as unique tools for the functional studies of SUMOylation.

Technological Advances in Biomimetic Membrane Platforms

Jason L. Poulos[1], Tea-Joon Jeon[1,2], Jacob J. Schmidt[1,3]

[1]Department of Bioengineering, [2]Department of Chemical and Biomolecular Engineering, and [3]California Nanosystems Institute, University of California, Los Angeles, CA

Membrane channel proteins are major targets of drug discovery and screening and recent work has also shown their potential as single molecule sensors. Conventional freestanding membranes housing these proteins can be problematic to form and are extremely fragile, limiting any technology using these membranes. We have developed a number of technologies for membrane formation and stabilization including hydrogel encapsulation/conjugation, freezing of membrane precursors, and high throughput automation using inverted phases. With these techniques, we have created membranes that can withstand severe perturbation, support long-term continuous measurements, can be shipped, and are compatible with high throughput robotic systems for drug discovery.

Non-invasive fluorescence imaging of PMN infiltration and vascular permeability during cutaneous inflammation in vivo

Min-Ho Kim[1], Fitz-Roy E. Curry[2] ,and Scott I. Simon[1]

[1]University of California, Davis, Biomedical Engineering, Davis, CA ; [2]University of California, Davis, Physiology, Davis, CA

Introduction. The influx of neutrophils (PMNs) and vascular leakage are two key phenomena in early inflammatory events in response to tissue injury. Quantitative measurement of PMN infiltration and vascular permeability in tissue are typically performed on histological sections of tissue samples. However, these approach require the sacrifice of animals at each time point and neither they provide high temporal and spatial resolution of dynamic changes in PMN infiltration and vascular permeability. The objective of this study was to develop a real time non-invasive fluorescence imaging technique to simultaneously detect the kinetics of vascular permeability and PMN infiltration in a full thickness skin wound of mice in vivo.

Methods. Fluorescence imaging of PMN influx was achieved using a transgenic mouse model, in which enhanced green fluorescent protein (EGFP) was knocked into the lysozyme gene resulting in preferential labeling of mature PMNs. We employed an experimental model of skin wound healing using EGFP-lysozyme-mice in conjunction with whole-body small animal fluorescence imaging system (Xenogen 100, Xenogen Inc.). The non-invasive imaging of plasma protein leakage was achieved by tail-vein injection of fluorescence conjugated albumin as a tracer for molecular diffusion across the endothelium as evaluated by quantifying time-dependent change in fluorescence intensity within a wound.

Results. Both in vivo and in vitro titration data validated that GFP fluorescence intensity directly correlates with the number of EGFP-PMNs within a wound. The fluorescence intensity of albumin measured within the wound bed was also linearly correlated with the concentration injected into the tail-vein. PMN influx after wounding increased linearly and reached a maximum value at day 1 and plateaued at day 3, before precipitously dropping by day 5. Between 1 and 24 hours of skin wounding, basal vascular permeability increased by 3-fold and at a more rapidly than the rate of neutrophil infiltration. Both temporal and spatial mapping of EGFP-PMN recruitment and fluorescently labeled albumin influx within the wound bed revealed a decoupling between these two processes. Additionally, systemic depletion of neutrophils by pretreatment with antibody Gr-1 did not result in significant decrease in vascular permeability at 24 hour post-wounding. Taken together, these results indicate that vascular permeability does not correlate with the kinetics of EGFP-PMN recruitment and those two processes are decoupled during cutaneous wounding.

Discussion. A fluorescence-based imaging approach combined with genetic labeling of neutrophils was developed and shown to be a sensitive and convenient tool for non-invasive quantification of inflammation and for the kinetics of neutrophil infiltration into the wounded skin over extended durations without need for animal sacrifice. Using this whole animal fluorescence imaging, we demonstrated that in response to tissue injury, the endothelium maintains a tight junctional barrier to protein leakage that is independent of PMN infiltration. This result supports the notion that endothelim has an ability to tightly regulate molecular diffusion in response to tissue injury, despite massive influx of PMNs.

Self-Assembled Nanostructures for Cancer Therapy

Matthew Black[a], Mark Kastantin[a], Priya Karmali[b], Venkata Ramana[b], Erkki Ruoslahti[b], Matthew Tirrell[a]

(*a*)Department of Chemical Engineering, University of California Santa Barbara
*(b)*Burnham Institute for Medical Research at the University of California Santa Barbara

Peptide amphiphiles (Figure 1a) consist of a hydrophilic peptide head group conjugated to a hydrophobic alkyl tail. The amphiphilic nature of the molecules drives self assembly into micelles or vesicles. Mixing different molecules under appropriate conditions can bring multiple functionalities into the same structure without the need for complex chemistries. The goal of this work is to bring tumor targeting peptides, therapeutic peptides, cell penetrating peptides, and conventional chemotherapeutic agents into the same nanostructure for cancer therapy.

Utilizing targeting peptides can allow for lower doses of therapeutic agent and can avoid the systemic toxicity and side effects associated with many anticancer agents. Two targeting peptides, CREKA (Figure 1b) and CGNKRTRGC (Lyp-1), are able to bring micelles specifically to tumors *in vivo.* Very little uptake of the micelles is seen in the liver, spleen, or other organs in the mice. A 20 amino acid peptide derived from the BH3 domain of the pro-apoptotic BID protein was chosen as a therapeutic peptide. Self assembly of the BID BH3 domain peptide amphiphile into micelles stabilizes the alpha helical secondary structure of the peptide. We are currently working to show that this induces apoptosis in cancer cells *in vitro*. The hydrophobic anti-cancer drug paclitaxel was incorporated in the hydrophobic core of distearoyl-PEG micelles. The paclitaxel retains its activity in the micelles and had a similar IC_{50} as paclitaxel delivered in 10% DMSO. Future work aims at combining these components into a single nanostructure (Figure 1c) to create a safe and effective cancer therapeutic.

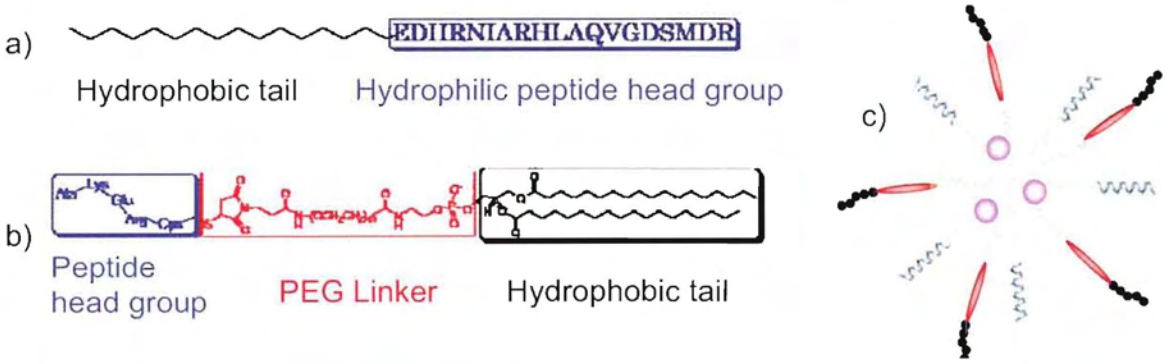

Figure 1 a) BID BH3 domain peptide amphiphile used in this work. b) CREKA targeting peptide attached to PEG linker and distearoyl tail. c) Multifunctional micelle with targeting peptide, therapeutic peptide, and hydrophobic drug in a single nanostructure.

Molecular Engineering of Polyarginine-Polyleucine Block Copolypeptides for Drug Delivery

Victor Z. Sun, Zhibo Li, Xun Gong, Timothy J. Deming, Daniel T. Kamei
Department of Bioengineering, University of California, Los Angeles, CA 90095

Many different drug carriers have been used to enhance the efficacy of drugs. For example, encapsulation of drugs into liposomes can help minimize their enzymatic or proteolytic degradation. Use of micelle carriers can assist the delivery of hydrophobic drugs by increasing their solubility in blood. Pegylation, on the other hand, can increase the half-lives of drugs by helping them avoid inactivation by the immune system and clearance by the kidneys.

Our focus has been on investigating amino acid based materials for drug delivery. Specifically, we previously engineered an arginine-leucine ($R_{60}L_{20}$) block copolypeptide that was able to form vesicles that could transport dye-labeled dextran *in vitro* into both epithelial and endothelial cells without being toxic. These vesicles were also shown to be stable in serum-free media, be processed to different sizes, and be prepared in large quantities[1].

We have recently been using transport inhibitors to elucidate how the $R_{60}L_{20}$ vesicles gain entry into the cell. Moreover, we have also been conducting immunofluorescence experiments to identify the trafficking pathway of the vesicles inside the cell. With the data we are collecting, we plan to engineer the next generation of these polypeptides that are more effective in delivering drugs.

To study the endocytosis pathway utilized by the $R_{60}L_{20}$ vesicles, we used transport inhibitors to block certain pathways. Specifically, we blocked macropinocytosis with cytochalasin D, caveolae-dependent endocytosis using nystatin, and clathrin-coated pit endocytosis using phenylarsine oxide. In these experiments, after the addition of the inhibitors, the cells were incubated with FITC labeled $R_{60}L_{20}$ vesicles and imaged with confocal microscopy. Cytochalasin D had a significant affect on the cellular uptake of the vesicles (Figure 1), suggesting that macropinocytosis plays a role in their endocytosis.

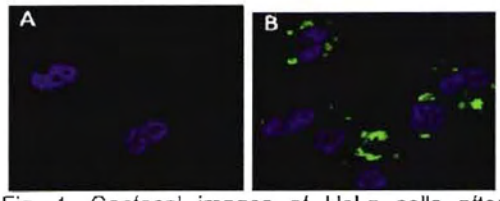

Fig. 1. Confocal images of HeLa cells after incubation with 100 nm diameter FITC-labeled $R_{60}L_{20}$ polypeptide vesicles in the (a) presence or (b) absence of the transport inhibitor cytochalasin D

To investigate the fate of the $R_{60}L_{20}$ polypeptide vesicles inside the cell, we have been loading the cells with FITC labeled $R_{60}L_{20}$ vesicles and staining the early endosome and lysosome using immunofluorescence. Results from these confocal studies should allow us to map out the trafficking pathway of these vesicles, which will be useful in assessing their drug delivery capabilities.

REFERENCES

1. Holowka EP, Sun VZ, Kamei DT, and Deming TJ, "Polyarginine segments in block copolypeptides drive both vesicular assembly and intracellular delivery." *Nature Materials* **6** (2007) 52-57.

Design and characterization of peptide amphiphile-based immunotherapeutics: Amyloid-β peptides and Alzheimer's disease

Amanda Trent, Dimitris Missirils, Matthew Tirrell

Materials Research Laboratory, University of California, Santa Barbara

Peptides play a critical role in determining the magnitude and specificity of cellular and humoral immunity. For this reason, peptide-based antigens capable of stimulating a specific and efficient immune response have long been sought to treat or prevent infectious diseases and other chronic ailments such as cancer. However, strategies for developing peptide-based immunotherapy face significant hurdles, including achieving potent immunogenicity, minimizing toxicity, and overcoming delivery challenges.

One possible alternative for satisfying these requirements is the design of peptide amphiphiles (PA), in which peptide antigens acylated with hydrophobic carbon tails can self-assemble into supra-molecular aggregates. The general properties of PA aggregates, including the multivalent presentation of antigen, the flexibility to control formation of various micellar and vesicular structures for delivery purposes, and the fact that peptide secondary structure is induced upon assembly, make PAs attractive for immunotherapeutic drug design. Moreover, the potential of hydrophobic tails to act as adjuvants may render the use of common toxic adjuvants dispensable.

We propose using amyloid-β peptides (involved in Alzheimer's Disease pathology) as model antigens to demonstrate the proof-of-principle concept of PA-based vaccines. Data revealing aggregate size, shape, composition, and peptide conformation will be presented. Subsequent to this basic physical characterization, in vitro assays as well as animal studies will then be used to determine the strength and specificity of the elicited immune response of the amyloid- β constructs.

LIPID-STABILIZED MICROBUBBLES FOR BIOMEDICAL IMAGING AND TARGETED DRUG DELIVERY

Kanaka Hettiarachchi[1], Paul A. Dayton[3], and Abraham P. Lee[1,2]
[1]*Department of Biomedical Engineering, University of California, Irvine, USA*
[2]*Department of Mechanical and Aerospace Engineering, University of California, Irvine, USA*
[3]*Joint Department of Biomedical Engineering, University of North Carolina – North Carolina State University, USA*

The precision engineering of micrometer-sized lipid-stabilized microbubble drug delivery vehicles using digital "droplet-based" microfluidics technology is reported. These vehicles have a drug carrying capacity greater than a microbubble, acoustic activity greater than that of a liposome, controlled drug loading, and a monodisperse size distribution with consistent stability. The encapsulation of an extra oil layer between the outer lipid shell and inner bubble gaseous core allows the transport of highly hydrophobic drugs such as Paclitaxel at high concentrations. Photolithography techniques are applied to fabricate novel PDMS-based microfluidic devices that feature a combined triple hydrodynamic flow-focusing region and expanding nozzle geometry with a narrow orifice. Spherical vehicles are formed through flow-focusing by the self-assembly of phospholipids to a lipid membrane around the gas core and oil layer, followed by a forced shape transformation at the orifice. Following a tightly controlled recipe of shell materials, geometrical conditions, pressure differences from flow parameters, and surrounding medium composition allows for the formation of monodisperse stabilized vehicles with consistent drug loading. Additionally, we demonstrate that we can functionalize these vehicles for cell-specific targeting, create hybrid vehicles for multimodal imaging, and locally deliver chemotherapeutics.

Title:

Quantified Deep Tendon Reflex Device for Evaluating Response and Latency Using an Artificial Reflex Device

R. C. LEMOYNE[1], C. COROIAN[2], T. MASTROIANNI[3], W. S. GRUNDFEST[1];
[1]Biomed. Engin. IDP, [2]David Geffen Sch. of Med., UCLA, Los Angeles, CA; [3]Cognition Engin., Pittsburgh, PA

Abstract:
A traditional method used in neurological examination is the testing and evaluation of the deep tendon reflexes. Two essential parameters for a deep tendon reflex evaluation are response and latency. Reflex response and latency may provide insight as to the status and severity of upper motor neuron syndrome and peripheral neuropathy. Response can be quantified by ordinal scales, such as the NINDS Myotatic Reflex Scale. However the accuracy of ordinal scales used to quantify reflex response is an issue of controversy. Most notable is the ordinal scale reflex response evaluation methods lacks temporal data. Latency can be accessed by an electrodiagnostic examination, but an electrodiagnostic examination requires specialized and expensive resources. A device which quantifies deep tendon reflex response and latency by incorporating tandem wireless 3D MEMS accelerometers has been developed. The device utilizes quantified input from a potential energy derived swing arm. The response is measured by a wireless 3D MEMS accelerometer mounted to the lower leg. The latency is derived from the temporal disparity between the acceleration waveforms of the swing arm mounted wireless 3D MEMS accelerometer and lower leg mounted wireless 3D MEMS accelerometer. The device is tested and evaluated using an artificial reflex device, which mechanically simulates reflex response and latency. Initial test and evaluation demonstrates high degree of precision for reproducibility. Initial evaluation in human subjects confirms the feasibility and reproducibility of using this device to access deep tendon reflexes.

Influence of Crack Propagation Orientation on R-curve Fracture Mechanics of Equine Cortical Bone

J. A. Creel[a], S. M. Stover[a,d], R. B. Martin[a,c], S. J. Hazelwood[a,b], J. C. Gibeling[a]
[a] Biomedical Engineering Graduate Group, UC Davis
[b] Biomedical and General Engineering, Cal Poly SLO
[c] Orthopaedic Research Laboratories, School of Medicine, UC Davis
[d] J.D. Wheat Veterinary Orthopedic Research Laboratory, School of Veterinary Medicine, UC Davis

Objectives for this research were to experimentally determine if bone exhibited R-curve fracture behavior in multiple crack propagation orientations for specimens from the lateral and dorsal regions of equine third metacarpal cortical bone, and to investigate potential relationships of R-curve behavior with fractography and histologic findings. In the first set of experiments R-curves were examined for specimens in which cracks propagated in three different orientations with respect to the long axis of the bone: transverse, radial and longitudinal. In the second set of experiments fractured specimens were examined using SEM imaging, histologic techniques, and surface topography mapping. All three orientations exhibited R-curve behavior, justifying a departure from traditional linear elastic fracture mechanics in order to fully characterize the fracture behavior of bone. The transverse specimens were found to have significantly higher maximum fracture toughness values, K_{max}, than either of the other two orientations (Figure 1). For the transverse specimens the lateral region was found to have a significantly higher K_{max} than the dorsal region; this was not the case for the other two orientations. The crack length associated with the maximum toughness value, a_{max}, was found to be significantly longer in the longitudinal and radial orientations when compared with the transverse orientation. The dorsal region had more osteons with either alternating hooped and longitudinally oriented collagen fibers or solely hooped collagen fibers than the lateral region. But the hypothesis that these, and osteons where the outer layer of collagen fiber is hooped and the inner layers are longitudinally oriented, would resist pullout, thus increasing fracture toughness, was not supported. The dorsal region had more osteons with larger diameters than the lateral region. These larger osteons provided more cement line length that could serve to initiate crack propagation and correspond to lower K_{max} values for the dorsal region. For both the radial and longitudinal orientations the crack was significantly more likely to penetrate osteons with predominantly longitudinally oriented collagen fibers than other osteons with other collagen fiber orientations.

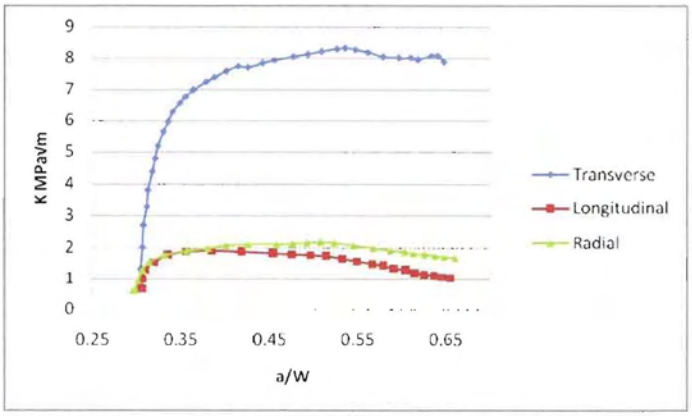

Figure 1: Example R-curves for each orientation

Engineering 3D Microarchitectures for Cell Co-Culture Studies

A gradient generating microfluidic platform with patterned 3D hydrogels

Carlos Huang,[1] Hyeryung Seon,[2] Jente Lu,[1] Andrew Putnam,[1,2] and Noo Li Jeon[1]
Department of Biomedical Engineering[1],
Department of Chemical Engineering and Materials Science[2],
University of California, Irvine

Metastasis of cancer cells involves a complex series of events which are not completely understood. The migration and invasion of cancer cells have been studied extensively in 2D culture systems as well as in transwell Boyden chambers. These systems, however, do not allow real time observation of cells in a 3D environment. To better understand the metastatic process, we have developed and employed microfluidic devices to simulate the 3D *in vivo* environment. Microfluidic devices allow us to study the diffusion of soluble factors in a controlled fashion and pattern structures to observe cell migration via chemotaxis in a 3D extracellular matrix. In this study, we present the development and characterization of our microfluidic device along with preliminary studies using a metastatic breast cancer cell line (MDA-MB-231) and mouse leukaemic monocyte macrophages (RAW). Our device contains an array of posts designed to entrap hydrogels in specific microchannels. Cells can be easily suspended within the device by injecting them with gel precursor solutions that polymerize in situ. Two large reservoirs, attached to channels adjacent to the hydrogels, provide media and nutrients to our system. In addition, by juxtaposing gel channels, we have engineered microenvironments of specific widths to study cell-cell as well as cell-matrix interactions. In this study, MDA-MB-231 cells suspended in type I collagen gels were cultured with RAW cells suspended in Matrigel in adjacent channels. Heterotypic cell interactions were observed via fluorescence microscopy for up to one week, with notable invasion of the macrophages into the channels loaded with tumor cells. These studies provide a foundation for future co-culture systems for real-time observation of cell-cell and cell-matrix interactions within a 3D environment.

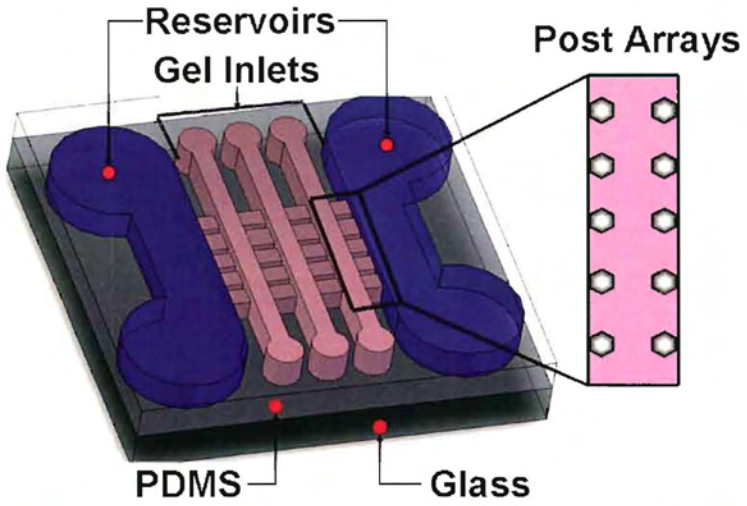

3D-Shrinky-Dink Vortex Micromixer for Efficient Mixing

Chi-Shuo Chen, Maureen Long, Anthony Grimes, Michelle Khine
School of Engineering, University of California, Merced

The ability to mix macromolecular solutions is fundamentally important for biochemical reactions, chemical synthesis, and biological processes. Rapid mixing is critical, for example, in biochemical detection involving hybridization analyses or immunoassays. However, to achieve a high mixing efficiency in micro-scale devices, complex designs and/or active components are typically required. Because molecular diffusion governs mixing at these small scales, the lengths required for effective passive mixers are often prohibitive and hence negate many of the benefits of miniaturization. Moreover, rapid mixing is generally challenging.

In our present study, we show that enhanced micromixing can be achieved in a topologically simple and easily fabricated 3D microvortex. We previously presented a novel approach for the ultra-rapid direct patterning of complex three-dimensional polystyrene microfluidic chip. In order for these chips to be useful, we characterize our mixing efficiency of both solutions and suspensions. For each mixer, we simultaneously flowed two aqueous fluids of different concentrations of blue dye diluted with water. We quantified the absorption optical density of the solutions at the connection channel by photometric microplate absorbance reader (Multiskan EX, Thermo Electron.) in our preliminary experiments, we successfully enhanced mixing efficiency using the vortex mixer. These results demonstrate that our new design significantly improves the mixing efficiency over conventional 2-D micromixers. Also, compared to mixing efficiency fluctuation in the serpentine mixer, the mixing efficiency of 3-D microvortex is more stable at different flow rates.

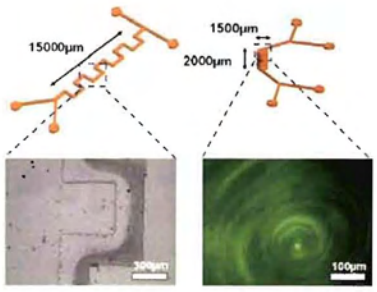

***Figure1**. Schematic diagram of 15000 μm length serpentine channels and 1500 μm microvortex. (Left) Optical micrograph showing a top view of a dye stream in a channel. (Right).*

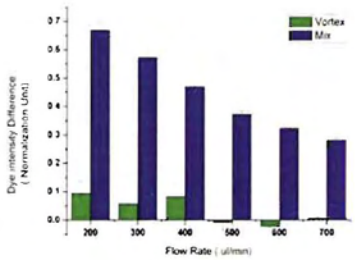

***Figure2**. Difference in dye intensity of outlets from the planar (blue) versus 3D (green) chips at different flow rates.*

PET Image Reconstruction with Shape Prior Using Multiphase Level Set Method

Jinxiu Cheng-Liao and Jinyi Qi,

Department of Biomedical Engineering, University of California - Davis

Combined positron emission tomography (PET) / computed tomography (CT) systems improve the ability to distinguish pathology from normal uptake and to precisely localize abnormal loci by acquiring both anatomical and functional images during one scan. The co-registered CT image is often used for attenuation correction in PET reconstruction. The anatomical boundary information in CT image can also be used to improve the quality of PET images.

Here we propose a novel approach to maximum *a posteriori* (MAP) reconstruction of PET images with CT-based prior information. The image prior models both the smoothness of PET images and the similarity between functional boundaries in PET and anatomical boundaries in CT. Minimal smoothing is applied across functional boundaries to preserve sharp edges. Level set functions are use to describe the anatomical boundaries from CT and to track the evolution of the functional boundaries in PET. The proposed method does not assume an exact match between PET and CT boundaries, but rather maximizes the similarity between the two boundaries, while allowing different region definition in the PET image to accommodate possible signal and position mismatch between the two images. This is an important feature as mismatches between anatomical and functional boundaries have been observed in clinical images that could be caused either by inherent difference in the contrast mechanisms or subject motion.

We conducted computer simulations to evaluate the performance of the proposed method. A digital phantom is built based on a PET/CT scan of a mouse. The CT image is manually segmented to obtain the anatomical boundaries. Compared with the other methods, our method produced smooth images with sharp functional boundaries. The proposed method also improves image quantification with region of interest (ROI) studies.

Acknowledgment: This work is supported by NIH under grant no. R01EB000194.

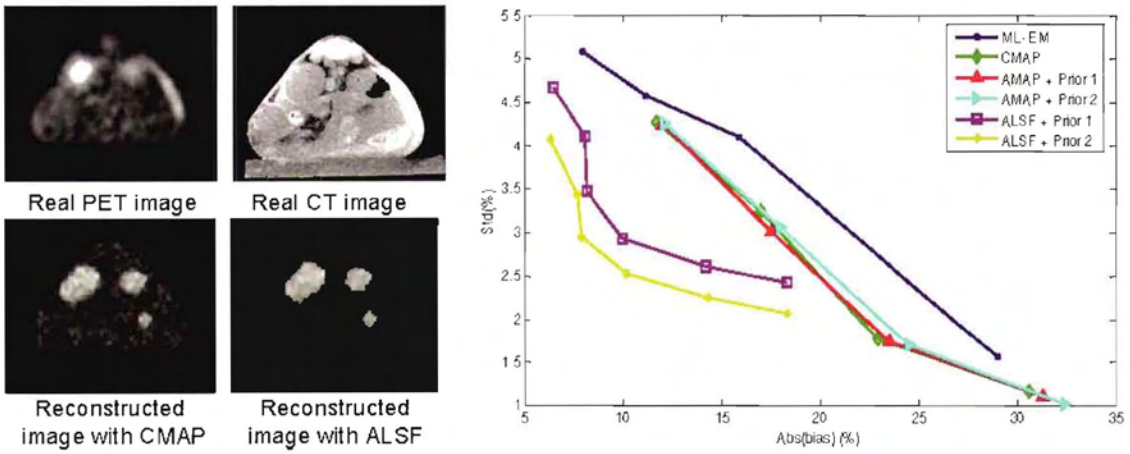

Fig.1 Left: transverse slice of the PET/CT image of a mouse (top row) and the reconstructed PET image with CMAP and ALSF(bottom row). A hot spot is added to simulate a tumor (lower right in the PET phantom images). Prior 1 and prior 2 simulate different types of boundary mismatch. Right: bias-variance curves of different reconstruction algorithm for quantifying the tumor uptake. "CMAP" refer to the conventional MAP without using anatomical information. "AMAP" refer to the MAP that does not smooth across an anatomical boundary. "ALSF" refer to our method.

Improving the spatial resolution and sensitivity of small animal PET scanners

Sara St. James[1], Yongfeng Yang[1], Yibao Wu[1], Richard Farrell[2], Purushottam Dokhale[2], Kanai S. Shah[2], Simon R. Cherry[1]

[1] Department of Biomedical Engineering, University of California-Davis, One Shields Avenue, CA 95616, USA

[2] Radiation Monitoring Devices Inc., Watertown, MA 02172, USA

Improvements to small animal PET scanners may be obtained by improving the spatial resolution, the uniformity of the spatial resolution across the field of view and the sensitivity of small animal PET scanners. Commercially available small animal PET scanners can achieve a spatial resolution of 1.4 mm and sensitivity of up to 10 %. In current small animal PET scanners, the spatial resolution degrades as the object being imaged is moved away from the center of the field of view, due to a parallax error that occurs as the object is moved away from the center of the field of view.

Improvements in sensitivity, spatial resolution and uniformity of spatial resolution across the field of view may be realized by using PET detectors that have smaller pixel elements in the axial and trans-axial directions, longer crystal elements and employ depth of interaction (DOI) encoding to minimize the parallax error. With DOI detectors, the diameter of the ring of the PET scanner may be decreased, minimizing the number of detectors required to achieve the same solid angle coverage as a scanner with a larger ring diameter.

We have developed PET detectors that employ continuous DOI encoding. The scintillation crystals in the detector are read out at both ends of the scintillation crystal using position sensitive avalanche photodiodes (PSAPDs), and the ratio of the signal from the two avalanche photodiodes is proportional to the depth in the crystal where the photon interacted. Detectors based on 13 X 13 arrays of 0.5 X 0.5 X 20 mm^3 scintillation crystals have been characterized. The scintillation crystal used is lutetium oxyorthosilicate (LSO). A photograph of the detectors is shown in Figure 1.

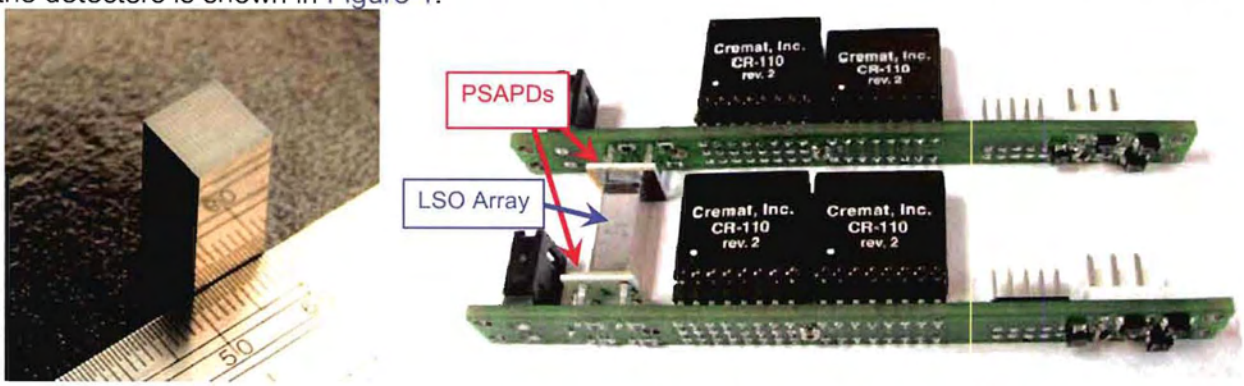

Figure 1: Photographs the array of scintillation crystals used (left) and the LSO array placed with each face coupled to PSAPDs (right).

These detectors have been characterized with respect to the ability to determine in which crystal the photon interaction occurred, the energy resolution and the depth of interaction resolution. A small animal PET scanner based on this detector design would have improved sensitivity and spatial resolution compared to commercially available scanners.

In vivo Water State Measurements in Breast Cancer using Broadband Diffuse Optical Spectroscopic Imaging

So Hyun Chung[1,2], Albert E Cerussi[1], Catherine Klifa[3], Hyeon-Man Baek[4], Ozlem Birgul[4], Gultekin Gulsen[4], Sean I Merritt[5], David Hsiang[6] and Bruce J Tromberg[1,2]

[1]Beckman Laser Institute, University of California, Irvine, 1002 Health Sciences Road, Irvine 92612, CA, USA
[2]Department of Biomedical Engineering, University of California, Irvine, 3120 Natural Sciences II, Irvine, CA 92697-2715, USA
[3]Magnetic Resonance Science Center, Radiology, University of California, San Francisco, 505 Parnassus Avenue, Box 0628, San Francisco, CA 94143-0628, USA
[4]Tu and Yuen Center for Functional Onco Imaging, Department of Radiological Sciences, University of California, Irvine, 108 Irvine Hall, Irvine, CA, 92697-5020, USA
[5]Masimo Corporation, 40 Parker, Irvine, CA 92618, USA
[6]Department of Surgery, Chao Family Comprehensive Cancer Center, Univiersity of California, Irvine, Healthcare, 101 The City Drive South, Orange, CA 92868, USA

Abstract

Structural changes in water molecules are related to physiological, anatomical and pathological properties of tissues. Near infrared (NIR) optical absorption methods are sensitive to water, however detailed characterization of water in thick tissues is difficult to achieve because subtle spectral shifts can be obscured by multiple light scattering. In the NIR, a water absorption peak is observed around 975nm. The precise NIR peak shape and position is highly sensitive to water molecular disposition. We introduce a Bound Water Index (BWI) that quantifies shifts observed in tissue water absorption spectra measured by broadband Diffuse Optical Spectroscopic Imaging (DOSI). DOSI quantitatively measures light absorption and scattering spectra and therefore reveals bound-water spectral shifts. BWI as a water state index was validated by comparing broadband DOSI to Magnetic Resonance Spectroscopy, diffusion-weighted MRI and conductivity in bound water tissue phantoms. Non-invasive DOSI measurements of malignant and normal breast tissues performed in 15 subjects showed a significantly higher fraction of free water in malignant tissues ($p<0.0001$) compared to normal tissues. BWI of breast cancer tissues inversely correlated with Nottingham-Bloom-Richardson histopathology scores. These results highlight broadband DOSI sensitivity to molecular disposition of water, and demonstrate the potential of BWI as a non-invasive *in-vivo* index that correlates with tissue pathology. Spatial variation of water state in breast tissues also has been observed during chemotherapy process in complete, partial and non-responders.

Title: Correlation of non-linear optical signals within collagen bioengineered models

Authors: Yu-Jer Hwang, Julia L. Lyubovitsky

Authors Affiliation: University of California, Riverside

Non-linear optical methods including multi-photon optical microscopy (MPM) that combines second harmonic generation (SHG) and two-photon fluorescence(TPF) signals have been used extensively in conjunction with evaluating structural changes of fibrous extracellular matrix (ECM) protein collagen. Due to a lack of an adequate understanding of how do different molecular and supramolecular state so this structural protein influence optical signals, translating this technology for use in routine studies of tissues and fibrous protein-based materials is problematic and has not been yet accomplished. There is a need for controlled systematic studies on simplified and characterized collagen-prototype systems to map out the optical signals.

Preliminary studies indicated that MPM optical microscopy which uses non-linear spectroscopy to generate image contrast is sensitive to different supramoleculary assembled collagen states; hence we developed a collagen bioengineered model validation tests to systematically evaluate the relationship between the supramolecular assembly of these biologically significant polymers and nonlinear optical signals they generate (1). Because several collagens spontaneously form supramolecular assemblies such as fibrils and fibers under suitable *in-vitro* conditions, we characterized the reconstituted collagen fibrils obtained from rat-tail acid-soluble collagen type I and human recombinant collagens type I and type III under final polymerization conditions: concentration, ionic strength, pH, volume of the gel formed and employment of cross-linking reagents. We followed turbidity at 450 nm during polymerization and used electron microscopy to assess striation within generated fibrils.

References:

(1) A. Zoumi, A. Yeh and B. J. Tromberg, "Imaging cells and extracellular matrix *in-vivo* by using second-harmonic generation and two-photon excited fluorescence, 99, pg. 11014-11019 (2002)

Feedback control of a DNA molecule tethered in a nanopore to repeatedly probe DNA-binding enzymes

Noah A. Wilson, Robin Abu-Shumays, Kate R. Lieberman,

Mark Akeson and William B. Dunbar

Departments of Computer Engineering and Biomolecular Engineering

University of California, Santa Cruz

This work demonstrates feedback voltage control of a single DNA molecule tethered in a biological nanopore. The nanopore device monitors ionic current through a single protein pore inserted in a lipid bilayer. The limiting aperture of the pore is just sufficient (1.5 nm diameter) to accommodate single-stranded DNA.

The tethered DNA is double stranded on each end, with a single stranded segment that traverses the pore. Voltage control is used to regulate the motion of the tethered DNA, for repeated capture and subsequent voltage-promoted dissociation of DNA-binding enzymes above the nanopore. In initial experiments using the Klenow fragment of Escherichia coli DNA polymerase I, control of 8 independent tethered DNA molecules yielded 337 dissociation events in a period of 380 seconds. The resulting distribution of DNA-protein dissociation times can be used to model the free energy profile of dissociation. Moreover, the approach is applicable to numerous enzymes that bind or modify DNA or RNA including exonucleases, kinases, and other polymerases.

Single Molecule Measurements of DNA Immobilized in a Biological Nanopore

Robert F. Purnell[1], Kunal K. Mehta[1], and Jacob J. Schmidt[1,2]
[1]Department of Bioengineering, [2]California Nanosystems Institute, University of California, Los Angeles

There is significant interest in the use of biological and synthetic nanopores for single molecule detection. Biological nanopores, in particular alpha-Hemolysin (αHL), offer the capability of sensing a large variety of single molecules, including polynucleotides at a rapid rate. Recently, researchers have investigated the possibility of using αHL to determine the sequence of a single-stranded DNA (ssDNA) molecule by monitoring the ionic current through αHL as it translocates through the pore. This is particularly attractive for DNA sequencing because it would enable high-throughput analysis of DNA samples, significantly reducing cost. To enable single-molecule DNA sequencing with nanopores one must be able to uniquely identify the bases at a single base resolution within the pore.

In this study, 40-base strands of polyadenine (polyA), polycytosine (polyC), and polythymine (polyT) are terminated with a streptavidin-biotin cap on the 5' end of the strand. In addition to preventing complete translocation, this macromolecule (d = 4 nm) cannot pass into the interior of the pore (d = 2.5 nm). We have found this eliminates all unfavorable interactions between the immobilizing agent and the interior residues of the pore. Using this method significantly decreases multi-state behavior in the current signals. When all strands are analyzed sequentially by the same pore, we observe three distinct blockage currents that correspond to the addition of each of the strands. Here, we report the blockage currents of polyA, polyT, and polyC strands immobilized inside the αHL pore. These results will serve as baseline values for future experiments to measure differences between the nucleotides dynamically as a heteronucleotide strand traverses the pore.

Position and Intensity Estimation of Neurons using Low-Dimensional Generative Models

Chang Won Lee and Zoran Nenadic

Department of Biomedical Engineering, UC Irvine

Neurons communicate by producing transient electrical pulses called action potential (AP). These potentials can be measured intracellularly or extracellularly, which constitutes a major technique in neuroscience research. Although extracellular recording is preferred in most in vivo studies, it is very tiresome and tricky. Multi-sensor recording technology in which four or more sensors are closely placed (< 50 microns) is a promising technique to measure APs extracellularly. This technique yields a better quality of recorded APs which facilitates subsequent processing and analysis of APs. Despite this advantage, experiments with multi-sensor recording technology are still time-consuming and require human supervision. In addition, many essential benefits of multi-sensor recording technology are currently not exploited. In order to utilize full advantages of multi-sensor recording technology, we develop a method to estimate a position and intensity of a neuron based on their APs collected through a multi-sensor microelectrode. Based on volume conductor theory and biophysics of neuronal membrane, the generation of APs can be simplistically described by low-dimensional generative models (e.g. dipoles or monopoles). By applying these models to analyze measured APs, it is possible to make an inference about the actual position and intensity of underlying neurons. Our method has been tested with computer simulations—*in silico*. The estimation of position and intensity of neurons allows us to guide the electrode toward or away from neurons and track changes in measured APs, which are the core activity in neuroscience experiments. Furthermore, this method can be used to identify the types of neurons such as stellate and pyramidal neurons and recommend design specifications for multi-sensor electrodes including number of sensors, sensor arrangement, and a space between sensors.

Induced Fluorescence Enhancement: A Method for Identifying Bacterial Species

Marlon Thomas, Elizabeth Zielins and Valentine I. Vullev*

Department of Bioengineering, University of California, Riverside, CA 92521

Abstract

The virulence and increasing antibiotic resistance of certain bacterial strains creates a need for efficient and timely detection of environmental pathogens. We evaluated the kinetics of the fluorescence enhancement of cationic dyes as an assay for differentiation between bacterial specie. For several benzothiazole cationic dyes, such as 3-3'-diethylthiacyanine, we observed fluorescence enhancement in the presence of vegetative bacteria and bacterial spores. Different bacterial species manifested different rates of emission enhancement. Although staining has been a broadly used technique for the identification of bacterial species, the kinetics of the staining process has not previously been examined. We hypothesized that the kinetic parameters can be utilized as "fingerprints" for detection and identification of bacterial species. We used three different vegetative bacteria and three different bacterial spores as model organisms to test our hypothesis. Kinetic emission assays with various concentrations of bacteria and fluorophores allowed us to determine the time constants of the fluorescence enhancement and the diffusion constant of the dye into the cell wall. These time constants reflect the migration of the dye from the surrounding media to the fluorogenic microenvironment within the bacterial cell wall. Development of this assay breaks a century old tradition of identifying bacteria using differential staining techniques and in addition it allows us to move us away from obtaining a strictly Boolean outcomes.

Quantifying Phagocytosis I:
An Engineering Approach

Cheng-Yuk Lee[#,!!], Jonathan Lam[#], and Volkmar Heinrich[#]

Departments of [#]Biomedical Engineering and [!!]Chemical Engineering and Materials Science, University of California Davis

From the perspective of engineering, perhaps the most important question regarding phagocytosis is: How do phagocytes coordinate the multitude of biochemical and mechanical processes that enable them to neutralize pathogens? Particularly intriguing, and much less studied than cellular signaling, are the mechanical feats that an immune cell routinely performs during target engulfment. For example, cell-adhesion molecules generate the required forces to hold on to a target. Cytoskeletal constituents maintain a delicate balance between the outward-growing cellular protrusions surrounding a target and the contractile elements that pull the target into the cell. All the while the cortical tension acts to return the cell shape to a sphere through its tendency to minimize the cell-surface area. It is processes like these that we aim to characterize in detail using our quantitative single-cell/single-target approach based on automated dual-micropipette aspiration.

We establish the time courses of key mechanical parameters of phagocytosis in the simplest geometrical configuration: isolated spherical cells that engulf opsonized spherical beads (diameter 2 to 10 μm). Experiments were performed on an inverted videomicroscope equipped with a motorized dual-pipette micromanipulation system. In each experiment, a passive phagocyte was chosen and lifted above the chamber bottom with a micropipette. Another micropipette was used to bring an opsonized polystyrene bead into soft contact with the cell. Images of the ensuing phagocytosis were recorded to computer hard-disk. Their analysis provided the time courses of cell morphology, cell surface area, cortical tension, and bead position.

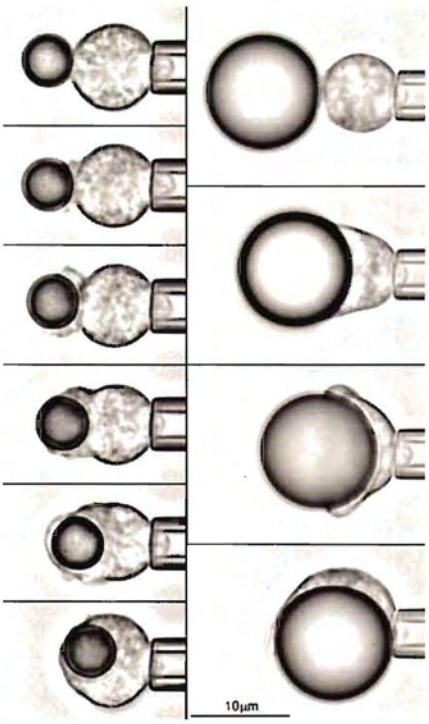

This approach is advantageous over traditional bulk assays because it allows us to manipulate single cells in an essentially axisymmetric configuration, as well as to monitor the cortical tension via the pipette-aspiration pressure. The application of this technique to different phagocytic cell types and/or phagocytosis pathways allows us to establish similarities and differences in the mechanistic programs governing phagocytosis.

Novel Net Charge Changing Fluorescent Protease Substrates for Rapid Disease Diagnostics in Whole Blood

Roy B. Lefkowitz[1], Che-Ming Hu[1], Jennifer Y. Marciniak[1], Geert W. Schmid-Schönbein[2], and Michael J. Heller[3]

From [1]UCSD, Department of Bioengineering, [2]UCSD, Department of Bioengineering and Department of Medicine, and [3]UCSD, Department of Bioengineering and Department of Nanoengineering

Increasing evidence suggests that physiological shock, diabetes, cardiovascular diseases, tumors, and other diseases are associated with an *inflammatory cascade*. This cascade is accompanied by elevated permeability of the endothelium and release of degradative enzymes that are targeted towards a variety of autologous proteins and lipids. Such evidence now provides a great opportunity to develop a variety of therapeutic interventions to ameliorate shock and treat inflammatory diseases. Unfortunately, such interventions will be highly dependent on the ability to diagnose and monitor a highly complex series of events which occurs rapidly in shock scenarios and more subtly in chronic inflammatory diseases. The goal of this work is to develop a novel monitoring and diagnostic system to meet this important clinical need.

We are therefore developing a novel protease activity detection system for the monitoring of clinically relevant inflammatory responses and for disease diagnosis. The basic premise for our approach is to use electric fields to actively concentrate fluorescent labeled peptide substrates when cleaved by a particular enzyme. Cleavage of the fluorescent peptide substrates will result in a change in the net charge on the complex and the cleaved products can then be separated from the intact peptide substrate by application of a directed electrophoretic field (see figure below). Subsequent detection is performed with a high sensitivity fluorescent detection device. These unique substrates will allow highly sensitive and selective rapid detection directly in clinical samples of the key enzymes (chymotrypsin, trypsin, elastase, matrix metallo-proteases, lipases, amylases) associated with the inflammatory cascade.

Thus far, we have designed and developed a fluorescent net charge changing substrate that can rapidly (1.5 hrs) detect low levels of activity of pancreatic α-chymotrypsin and trypsin (~20 mU/ml, ~400 ng/ml, ~20 pmole/ml) in 2-3 µl human plasma. The same levels of α-chymotrypsin and trypsin cleaved fluorescent fragments can be detected in 2-3 µl of whole blood. Substrates for MMP-2, MMP-9, MMP-14, elastase, as well as ones more specific to trypsin and α-chymotrypsin alone, have also been developed.

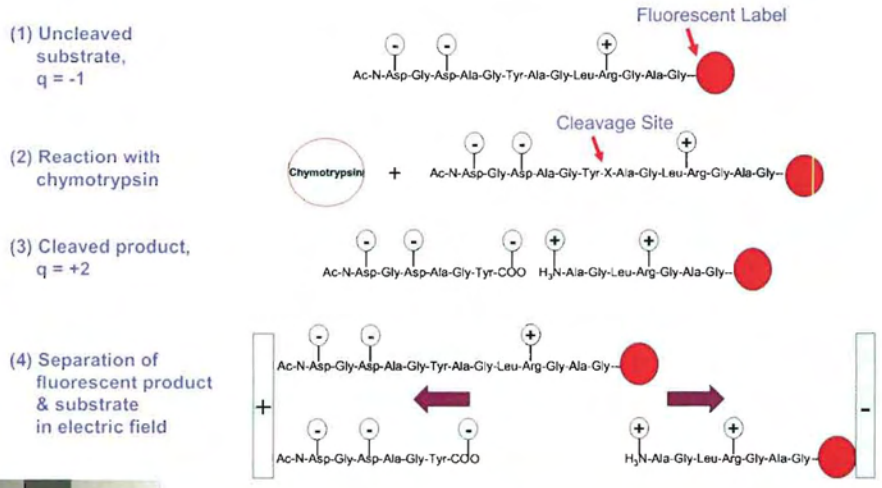

A Novel AC Electrokinetic Cell and Nanoparticle Separation Device for Cancer Diagnostics

Rajaram Krishnan[1], Benjamin D. Sullivan[1], Jason Steiner[2], Sergio Sandoval[1], Sadik C. Esener[2,3] and Michael J. Heller.[1,3]

Department of Bioengineering[1]. Department of Electrical and Computer Engineering[2]. Department of Nanoengineering[3]. University of California, San Diego. 9500 Gilman Dr., La Jolla, CA, 92093.

Our overall goal is the development of an advanced "ex-vivo" point of care (xv-POC) cancer therapy monitoring/diagnostics platform device. The device would provide near real time monitoring of patient blood for cancer cells, cell derived micro/nanoparticulates, high molecular weight DNA fragments, and carry out subsequent cancer related genotyping, gene expression and immunochemical analysis. A prototype AC Electrokinetic system has been constructed and tested. We have completed a number of initial experiments on cell, microscale particle and nanoparticle separations. We have achieved separation between different sized polystyrene beads and also between cells, DNA coated nanoparticles and DNA. Our most important result to date is the demonstration of rapid separation of DNA coated 40nm nanoparticles from larger 10 micron polystyrene particles in solutions with ionic strengths exceeding physiological levels. While still a model system, this in principle is exactly what we want to do with clinical samples i.e., separate DNA nanoparticulates of similar size from blood cells. Additionally, we have also separated and identified 40 kb DNA (150 ng/mL) from beads in high ionic strength fluids. We have also isolated human B-cell lymphocytes from mouse B-cell lymphocytes as well as other cells as a model for future cancer cell detection. Final performance goals for the system will be to carry out analysis of high molecular weight (hMW) DNA fragments with a sensitivity of <100 hMW-DNA fragments per 100 ul blood in less than 5 minutes. The secondary performance goals will be to carry out specific cancer cell isolation and subsequent related genotyping on DNA fragments (without amplification) along with antigen analysis within 15 minutes.

Bio-distribution of Nanoparticle Pollutants using Positron Emission Tomography

Heather A. Palko[1] and Angelique Y. Louie[2]

[1]Department of Chemistry, University of California, Davis, CA 95616
[2]Department of Biomedical Engineering, Chemistry Graduate Group, University of California, Davis, CA 95616

Trans-epithelial movement of inhaled particulate matter (PM) can result in PM accumulation in target organs based on endothelial cell-facilitated transport. The location of ultrafine PM accumulation in tissues could affect cardiac function, blood coagulation and the central nervous system. The aim of this work is to use Positron Emission Tomography and other radiotracer techniques to track the deposition and fate of model ultra-fine particles in vivo after delivery to the lungs. Polystyrene beads conjugated to DOTA-^{64}Cu were used as a model of ultra-fine particles to determine the location of PM in tissues. In these studies it has been shown that the polystyrene particles are capable of penetrating through the lungs to other target organs, in particular the heart, and that imaging and radiotracer techniques are useful tools in tracking this translocation. Future work will focus on how size, surface charge and composition affect translocation.

Novel Scintillation Detector for A Laboratory PET Scanner

Huini Du[1], Yongfeng Yang[1], Jarek Glodo[2], Yibao Wu[1], Kanai Shah[2] and Simon R. Cherry[1]
[1] University of California, Davis, [2] Radiation Monitoring Devices, Inc.

Preclinical molecular imaging using positron emission tomography (PET) is undergoing fast growth with applications in the areas of *in vivo* cell and molecular biology, studies in genetically-engineered mice, and in drug discovery and development. Contemporary preclinical PET scanners usually are designed to accommodate various mammalian species ranging from mice, rats to non-human primates. These scanners utilize large numbers of scintillation detectors and electronic channels to cover the required field-of-view (FOV). Statistics show that more than 90% of the mammals used in research are mice[1]. We therefore proposed to build a laboratory PET scanner specific to mouse imaging. Because of the small cross-sectional profile of a mouse, the ring diameter of such a scanner can be much smaller than current PET systems. Thus the number of detectors and electronic channels can be fewer. The laboratory scanner will be compact in size, low in cost and can be used for routine biological applications.

The major challenge in reducing the ring diameter is the parallax error, or the degradation of spatial resolution in the radial direction as the offset from the center of FOV increases. To solve this problem, the position of the interaction in the Z-direction, the depth-of-interaction (DOI), needs to be obtained. One major DOI detector design is phoswich detector which is a scintillator detector made of multiple layers of different scintillator with different decay time[2]. However, the DOI resolution of phoswich detector is defined by the thickness of the scintillator in each layer, and thus it only provides discrete DOI information. Another method usually used is to place photodetectors on both ends of the scintillation detector and to acquire DOI information based on the ratio of the energies detected on both photodetectors[3]. This dual read-out design can provide continuous DOI information but the number of utilized photodetectors doubles, so as the number of the electronic channels.

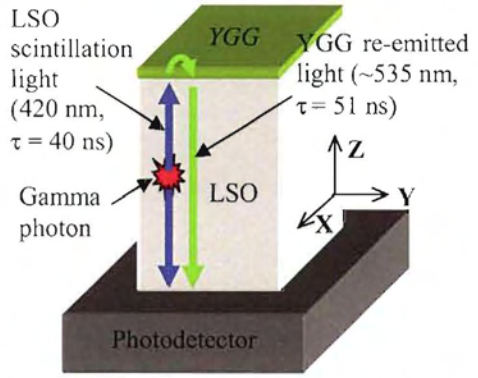

Figure 1 Illustration of an YGG-LSO detector

We propose a novel DOI detector using LSO (Lutetium Oxyothosilicate:Ce) scintillator and YGG (Yttrium Aluminum Gallium Oxide: Cerium, $Y_3(Al,Ga)_5O_{12}$:Ce) phosphor. The detector is single read-out and provides continuous DOI information as shown in Figure 1. The far end of the LSO scintillator is coated with a thin layer of YGG phosphor powder which absorbs some fraction of the LSO light and re-emits it with a longer decay time. The near end of the LSO scintillator is directly coupled to a photodetector. The photodetector detects a mixture of the LSO light and the light emitted by YGG. The ratio of the light re-emitted from the YGG coating to the unconverted LSO light depends on the interaction position. DOI information can be acquired by inspecting the light pulse decay time. Experiments were conducted to optimize the coating method. Around 19 ns decay time differences across the Z-direction of the detector were achieved experimentally when reading out a 1.5×1.5×20 mm^3 LSO crystal with unpolished surfaces and the end and half sides of the crystal coated with YGG phosphor. The same coating scheme was applied to fabricate a 4 by 4 LSO array with YGG phosphor. Pulse shape discrimination (PSD) methods were studied to extract DOI information from the decay time changes. The DOI full-width-half-maximum (FWHM) resolution was found to be 8 mm for 2 cm thick array. The detector design, the selection of scintillators and phosphors will be further optimized.

1 D. Malakoff, *Science* **288**, 248 (2000).
2 J. Seidel, J. J. Vaquero, S. Siegel et al., *IEEE Transactions on Nuclear Science* **46**, 485 (1999).
3 W. W. Moses and S. E. Derenzo, *IEEE Transactions on Nuclear Science* **41**, 1441 (1994).

Towards a Flexible, Conformal Medical Ultrasound Imaging System

Shyam Natarajan[1], Rahul S. Singh[1,2], Michael Lee[1],
Elliott R. Brown[2], Warren S. Grundfest[1], Hua Lee[2], Martin O. Culjat[1,2]

[1]Center for Advanced Surgical and Interventional Technology (CASIT)
University of California, Los Angeles
[2]Department of Electrical and Computer Engineering,
University of California, Santa Barbara,

A flexible, conformal ultrasound transducer array, system and image processing algorithms are being developed for use in medical imaging in a joint collaboration between the UCLA School of Medicine, and the UCSB School of Engineering. The transducer has been designed such that it can wrap conformally around curved body surfaces and provide volumetric imagery of soft tissue and hard tissue structures without mechanical scanning. Traditional ultrasound imaging, pulse-echo ranging, allows for the accurate reconstruction of a 2D image slice, but is limited to use by trained operators due to the skill involved in transducer placement and rotation. Flexible transducer arrays have the potential to improve usability and image quality. Rather than fixing transducer elements in a rigid plane, having flexible transducer elements that conform to the body and surrounds a particular vasculature, enables accurate bi-static data to be captured, improving image quality as a result. The portability and accessibility of this system enables remote operation by untrained technicians, increasing the viability and use of diagnostic ultrasound in rural and emergency situations.

The complete system includes a micro-machined flexible transducer array, a custom designed transceiver, and novel image processing techniques. In order to verify and fine-tune the behavior of the system, complex simulation data is modeled using PZFlex™, a finite element time domain piezoelectric solver. Simulations allow for the precise modeling of the transducer array beam curvature, and signal characteristics through heterogeneous media, providing feedback for the transducer design, image processing algorithm, and digital electronics. The transducer array is driven by a portable, lightweight transceiver, consisting of a digital signal processor, a microcontroller, and a capture interface. The return signals are captured by 14-bit analog-to-digital converters, and tomographic image reconstruction algorithms are applied to the resulting data in hardware. The created images are then transmitted via USB to a laptop computer, where software further processes the image, and displays it to the user.

This presentation covers the fabrication process for the flexible transducer array, an overview of the control and driver systems, and the utilization of PZFlex™ simulation data in system design.

Multi-Modal Approach for the Integrated Assessment of Activated Microglia with Plaques in Alzheimer's Disease Models

Erica Andreozzi, Ben Jarrett, Izumi Maezawa, Lee-way Jin, Angelique Louie

Department of Biomedical Engineering, University of California, Davis, 95616
UC Davis M.I.N.D. Institute, Sacramento, CA, 95817

Activated microglia, a macrophage-lineage cell located in the central nervous system (CNS), have been implicated to be important in the neuro-inflammatory response associated with Alzheimer's disease (AD). They are activated in the presence of senile plaques, current pathological hallmarks of AD, and this activation appears to be mediated by macrophage scavenger receptors. Since microglia have been identified as a target for anti-neuroinflammatory drugs as a possible treatment for AD, there is great interest for non-invasive *in vivo* methods to identify senile plaques as a way to confirm diagnoses of AD.

We plan to target novel imaging probes to a type of scavenger receptor (SR-A) that is highly expressed by microglia in AD but not in normal microglia, allowing *in vivo* visualization of activated microglia associated with senile plaques. We have developed two types of SR-A probes: 1) Iron oxide nanoparticles coated with dextran sulfate (SR-A ligand) and coupled to ^{64}Cu chelates; and 2) Maleylated BSA molecules (SR-A ligand), coupled to gadolinium (Gd^{+3}) and ^{64}Cu chelates. These probes are capable of both magnetic resonance imaging (MRI) and positron emission tomography (PET). While PET is utilized to assess general probe biodistribution, MRI will be investigated for labeling plaques too small to resolve by PET. This multimodal imaging approach will allow for the integrated assessment of activated microglia in relation to senile plaques in mouse models of AD using MRI and PET. In this way, we can attempt to correlate activated microglia with both senile plaque location and degree of neurotoxicity to more effectively monitor its role during AD disease progression as well as during therapeutic intervention.

Design and Development of Circumferential Image Reconstruction Algorithms for a Flexible, Conformal Ultrasound Array System.

Michael Lee (1); Rahul S. Singh, PhD (1,2); Martin O. Culjat, PhD (1,2); Shyam Natarajan (1); Elliott R. Brown, PhD (2); Warren S. Grundfest, MD (1); Hua Lee, PhD(2) 1: Center for Advanced Surgical and Interventional Technology (CASIT), University of California, Los Angeles. 2: Department of Electrical and Computer Engineering, University of California, Santa Barbara

This presentation describes the image reconstruction algorithms for a flexible, conformal ultrasound array imaging system. Traditional ultrasound imaging systems require large and rigid transducer arrays. In such systems, the ability to capture reflected, scattered acoustical power is limited by the surface area in contact with the subject, resulting in information loss. Flexible ultrasound arrays abate this problem by spanning large areas while maintaining full contact to curved surfaces. This concept combines advancements in medical imaging with light-weight, cost-effective systems with an emphasis on improved portability and versatility. With the promise of these benefits comes the cost of increased complexity in the image processing algorithms and a fundamental shift in the reconstruction techniques used.

In parallel with the hardware development phase of the flexible, conformal ultrasound transducer arrays, high-resolution image reconstruction algorithms are being developed. This allows for the reconstruction algorithms to develop in step with the hardware and allow for close integration and optimization of each. The conformal transducer array provides a solid environment in which to explore circumferential imaging in both 2-D and 3-D. In this presentation, the image reconstruction concept is presented using pulse-echo data. Using pulse-echo data provides a simpler signaling framework to develop the conceptual framework of the image formation process. With the basic image reconstruction technique established, the operating format is then extended to the frequency modulation coherent wave (FMCW) mode.

To accommodate the FMCW imaging modality, the image formation algorithm is modified to include additional FFT operations to obtain the range profiles. The ultimate ultrasound system will benefit from the improved signal quality provided by using FMCW. Preliminary image reconstruction experiments are described in the presentation, including trials based on both simulated data and phantom targets to demonstrate the resolving capability of the system. This presentation includes a system overview, theoretical study of the image formation procedure, extension to FMCW imaging modality, and experiments.

PERSONAL COMPUTER BASED MULTIMODAL TRAINER

Gurneet Singh[1,2], William J. Kaiser[1,3], Eric A. Savitsky[1,4]

[1]Center for Advanced Surgical and Interventional Technology, UCLA, [2]Biomedical Engineering IDP, UCLA, [3]Electrical Engineering, UCLA, [4]Department of Clinical Medicine, UCLA

Traditional education methods have been ineffective in teaching medical care-providers in a cost effective manner. More importantly, the care-providers without prior procedural training are forced to perform procedures for the first time on actual patients while learning. To provide a solution to this problem, a low cost PC-based medical procedure simulator is under development that fuses real-time, interactive task simulation with multimedia "hands-on" case-based scenarios. Content delivery is being linked to hands-on procedural training using well-integrated, simple to use, and proven hardware peripheral devices (e.g., a haptic device and an inertial sensor).

The focus of this presentation is the capture of real-time ultrasound streams from a medical ultrasound system at the UCLA Department of Radiology, and the linking of these streams to rotational information captured from a transducer-mounted tracking system. These data sets are being synchronized to an existing patient simulation system, and packaged together to allow an inexperienced ultrasound user to learn a series of ultrasound procedures from a single low cost training platform. The data collection from the ultrasound machine, and the retrieval of this ultrasound data into the GUI (shown in the Figure) from the database that we have created and are updating, is being automatized. The peripheral ultrasound probe, which is an inertial sensor and a part of the trainer kit, is being temporally synchronized with the virtual probe visible in the figure. The figure below shows a basic prototype for this system, which creates a simulating environment to perform an ultrasound on a patient. The functionality of the prototype is being expanded by automatizing the data-acquisition and accounting for more data points on the body.

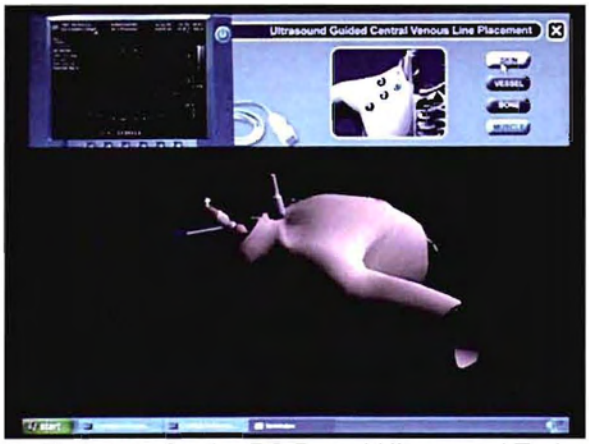

Fig: Prototype for the PC Based Ultrasound Trainer

The presentation elaborates on the Data Acquisition methodology where the data is acquired from the ultrasound machine, a database is created and the data is displayed in the simulating environment on a GUI. This hands-on procedural training aims to maximize educational value by being linked to realistic, graphic and case-based scenarios.

A Practical Double-tuned $^{1}H/^{13}C$ Birdcage Resonator for MRI/MRS at 7T

Chunsheng Wang, Bing Wu, Xiaoliang Zhang
Department of Radiology, UCSF/UC Berkeley Joint Graduate Group in Bioengineering,
University of California San Francisco, San Francisco

Introduction:

MRI/MRS at ultra high static magnetic field (>4T) is proving to be very successful since it yield increased SNR, allowing improved spatial resolution, and also provides better spectral resolution. Double-tune radiofrequency (RF) coils ensure spatial co-registration of signal from different nuclei without exchanging coils for imaging and spectroscopy examinations. In this work, a double-tuned birdcage coil, which was derived from the resonator introduced by Smain [1], was built and tested at 7T.

Methods:

A double-tuned $^{1}H/^{13}C$ Birdcage coil (Diameter: 4", Length: 5") showed in Fig. 1 was built with 16 copper tubes (OD: 0.25", Length: 5"). Compared with copper tape, copper tube has enlarged surface and hence has lower resistance because of skin-depth effect, which will reduce coil loss. Trimmer capacitors C1 and C2 (Johanson, Boonton, NJ) were placed between copper tubes and end-rings as shown in Fig.2. C3 are fix capacitors (ATC, NY). The rungs with C1 were tuned to resonant frequency of ^{13}C and the rungs with C2 were tuned to resonant frequency of ^{1}H. C The coil can be driven in quadrature for both frequencies. Each port was capacitively (Voltronics, Denville, NJ) matched to 50Ω while loaded with a cylindrical corn oil phantom (Diameter:2.5" , Length:6"). Baluns were used to reduce RF current leakage on the coax cable shield. The resonant modes were measured with a network analyzer (Agilent E5070B). The measured frequency responses of the double-tuned Birdcage

Fig.1 16-element double-tuned birdcage with Diameter=4" and Length=5"

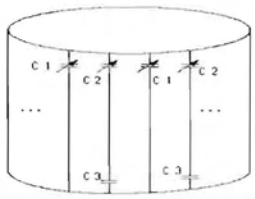

Fig.2 Schematic illustration of the double-tuned birdcage

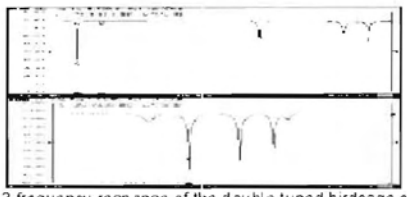

Fig.3 frequency response of the double-tuned birdcage coil for ^{13}C (top) & ^{1}H (bottom) with the frequency span of 70MHz

resonator were illustrated in Fig. 3. The useful mode (mode 1) for ^{13}C MRS and ^{1}H MRI were tuned to 75MHz and 298MHz respectively. The proton MR imaging and ^{13}C spectroscopy experiments were performed on a GE 7T/90cm MRI system (GE Healthcare, Waukesha, WI). Proton image obtained using a gradient echo sequence with TE = 7.3ms, TR = 500ms, Flip angle = 30°, FOV = 10cmx10cm, slice thickness=3mm, matrix size = 256x256, NEX=1, and bandwidth=15.63 kHz. ^{13}C spectrum of corn oil was acquired with single shot and TR = 2 sec.

Results and Discussion:

The unloaded Q is ~273 for ^{13}C and ~198 for ^{1}H by S11 measurement. Because the loading is corn oil, the loaded Q almost the same as the unloaded Q. Well-defined resonant mode peaks for ^{13}C MRS and ^{1}H MRI were easily identified. Compared with normal 4 res ant peaks for ^{13}C, the interesting thing is that there are five resonant peaks for ^{1}H (exclude the cable resonance), and the useful mode is corresponding the second peak which was verified by S21 measurement and reflected in MR imaging. Axial proton image of the cylindrical corn oil phantom acquired using the prototype birdcage coil was shown in Fig.4 (a). It demonstrated the relatively homogeneous intrinsic B1on field pattern generated by the prototype coil. Fig.4 (b) illustrated sufficient SNR for ^{13}C spectroscopy with single shot acquisition. Based on the bench test and MRI/S experiment, the double-tuned birdcage coil can be used successfully at 7T.

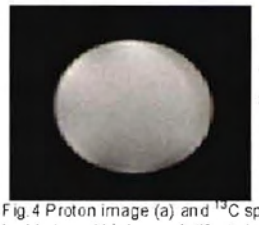

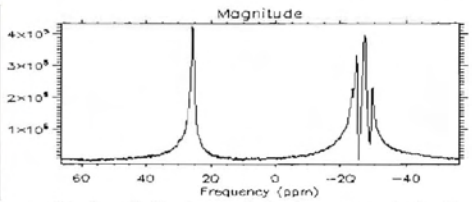

Fig.4 Proton image (a) and ^{13}C spectra (b) of a cylindrical corn oil phantom acquired using the double-tuned birdcage. Artifacts in (a) were caused by different chemical shift of protons in corn

Acknowledgement: This work was supported by NIH grant EB004453, QB3 Opportunity Award

References: [1] Samain Amari, etc "Multiple tuning of birdcage resonator", MRM 37: 243-251 (1997)

Multiple Reception Strategy and Extended GRAPPA for SNR Improvement at 7T

Bing Wu[1], Chunsheng Wang[1], Xiaoliang Zhang[1,2]

[1]Department of radiology, UCSF, San Francisco, CA. [2]UCSF/UC Berkeley Joint Graduate Group in Bioengineering, Berkeley/San Francisco, California

Introduction

A method by using multiple reception strategy and extended GRAPPA is presented to enhance signal-to-noise (SNR) for ultra-high field MRI. This method was demonstrated at GE 7T scanner. In comparison with a conventional 8-element array, around 41% SNR gain was achieved at the periphery of the human brain.

Method

The essential of this approach is to mount more coil elements into an array than the channel numbers. The elements are then divided into several groups, in each group the number of coil elements is equal or less than the number of receive channels so that multiple reception can be conducted by sequentially switching coil groups to receive channels. To speed imaging, reduced number of phase encoding steps is applied for each reception, and then extended GRAPPA is utilized for reconstruction. Figure 1 indicates the k-space filling scheme of extended GRAPPA. R and N represent reduction factor and reception times respectively. A 16-element commercial array (Nova medical, Wilmington, MA) was tested with R=2 and N=2. The image was compared to that from an 8-element array. Those arrays have almost the same dimension and specifically designed for GE 7T MR system (see figure 2).

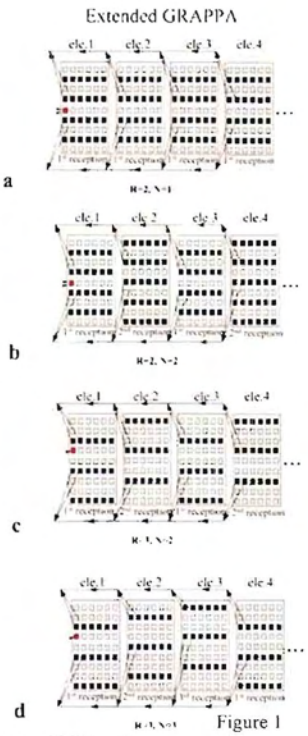

Figure 1

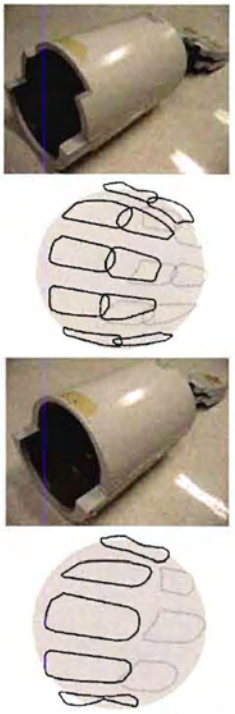

Figure 2

Results

Figure 3 shows the SNR comparison of human brain images in axial, coronal and sagittal planes. With 8 receive channels, we compare the SNR from 16-element array with N=2, R=2 (scan time is 137s) and 8-element array with NEX=1 and R=1 (scan time is 132s). The SNR from 16-element array is slightly lower (~4%) over 8-element array in the center of the brain, but has up to 41% gain at the periphery of the brain (figure 3a).

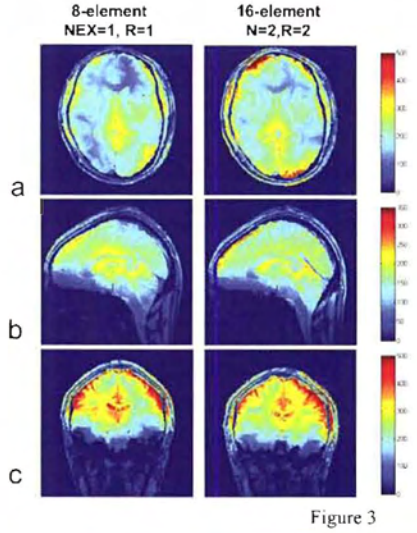

Figure 3

Conclusion and Discussion

This multi-reception strategy can be normally extended to various types of coil arrays and magnetic strengths for SNR enhancement at the periphery. It may be particularly useful for high and ultrahigh field MRI (≥3T) [1] where sample loss is dominant and with limited number of receive channels.

References and Acknowledgements

[1] Wiesinger F, et al. Magn Reson Med 2004; 52:376-390.

This work was partially supported by NIH grant EB004453 and QB3 Opportunity Award.

Correlation of Transepidermal Water Loss with Skin Barrier Function In Vitro and Comparison of Three Evaporimeters

Rania Elkeeb, Xiaoying Hui, Heidi Chan, Lilian Tian, Howard I. Maibach

Department of Dermatology, University of California, San Francisco, CA 94143

ABSTRACT

The purpose of this study was to investigate the relationship between transepidermal water loss and skin permeability to tritiated water (^3H_2O) as a rapid assessment of the integrity of the barrier properties of skin as part of in vitro skin permeation studies. Transepidermal water loss (TEWL) values before and during experimental period were measured using three different evaporimeters, Tewameter® TM210, VapoMeter™ and AquaFlux AF200, representing different measuring principles and technologies. Single application of tritiated water was dosed on dermatomed human skin samples collected from 12 donors in a flow through diffusion cell system. Samples (10 µl) of receptor fluid were collected every four hours to count radioactivity. The amount of radioactivity in each sample was calculated as percent administered dose by reference to standards prepared and measured simultaneously. These data were combined with TEWL values to analyze the correlation. The patterns of TEWL profiles from the three instruments were similar. However the measurement capacity of AquaFlux is significantly higher than those of VapoMeter™ or Tewameter® ($P < 0.001$). Baseline TEWL value was correlated with the thickness of dermatomed skin ($r = -0.44$, $p = 0.007$). It also correlated with fluxes of tritiated water ($r = 0.34$, $p = 0.04$). When TEWL and permeation data were compared in parallel throughout the experiments, the pattern of tritiated water expressed as percent dose permeated into receptor fluid was similar to that of TEWL values. These data indicate that transepidermal water loss can be ascribed to be a measure of skin barrier function.

Understanding cellular responses: multi-photon imaging of actin filament formation and mitochondrial energetics of ACBT gliomas

Yu-Jer Hwang[a], Edgar I. Sanchez, Chung-ho Sun[b] Tatiana B. Krasieva,[b] Bruce J. Tromberg,[b,c] Julia G. Lyubovitsky[a]* [a]*Bioengineering Department, University of California, Riverside, CA 92521* [b]*Laser Microbeam and Medical Program, Beckman Laser Institute, University of California, Irvine, CA USA* [c]*Biomedical Engineering Department, University of California, Irvine, CA USA*
E-mail: julial@ucr.edu

Reflectance-based multi-photon methods are potentially useful in non-destructively probing molecular processes on the tissue, cellular and sub-cellular levels within complex organisms *in situ* and in real time. The application of these techniques is hindered by a challenge of understanding the relationship between observed signals and structure/function of the systems under investigation. Using the multi-photon ratiometric redox fluorometry method, we created 3D metabolic state maps of ACBT glioma cells migrating deep within several types of hydrogels. Via the expanded sample set, we show that while the method is highly susceptible to noise, it is sensitive to cellular blebbing and leaking of cellular membranes both of which occur upon application of focused femtosecond NIR excitation. Since interactions of mitochondria with actin cytoskeleton have been implicated to play a key role in apoptosis and ageing, we established a 3D tissue staining protocol to probe distribution of different types of F-actin filaments in ACBT glioma cells. The 3D overlay of distributions of F-actin filaments and mitochondrial biomarkers provided a greater understanding of cell-to-cell and cell-to-substrate interactions and morphology.

TEMPERATURE MEASUREMENTS OF LASER IRRADIATION FOR TISSUE PROTECTION DURING CRYOSURGERY

L. Martínez-Suástegui[a], G. Aguilar[a], F. Godinez[a], A. M. Walker[b]

[a] Department of Mechanical Engineering, University of California, Riverside, CA 92521

[b] Department of Biomedical Sciences, University of California, Riverside, CA 92521

An experimental investigation is carried out to develop a novel approach to cryosurgery, where laser heating combines with cryogenic freezing to selectively freeze and better confine damage to cancerous tissue—an approach we refer to as Laser-Assisted Cryosurgery (LAC). Confining with precision the volume of frozen tissue within a lethal low-temperature isotherm is achieved by counteracting frozen tissue propagation upon application of a conventional cryoprobe with controlled laser heating. The advantage of this procedure relative to conventional cryosurgery assisted with cryoheaters is that controlled laser heating provides volumetric rather than superficial heating, which leads to deeper penetration and tissue protection. Furthermore, the limits of cell viability may be predefined regardless of freezing rate, duration at low-end temperature, number of freeze-thaw cycles, and thawing rate. To address this, histological changes and cell viability assays are correlated with the temperature histories after performing a LAC procedure on *ex vivo* mice hepatic tissue. Analysis of our experimental results show that reproducible and predictable volumetric temperature histories can be reliably produced by LAC.

An fMRI study to correlate objective brain activations with subjective survey responses.

Prashanthi Vandrangi[a], Angelika Dimoka[a]
[a] Department of Bioengineering, University of California at Riverside

Cognitive Neuroscience uses various brain imaging tools such as electroencephalogram, functional magnetic resonance imaging (fMRI) and positron emission tomography to study objective brain responses and understand human behavior. Social science tries to understand human behavior by employing subjective measures such as surveys, questionnaires and focus groups. We examine the correlation between the objective brain activations and subjective human responses.

In this study, the objective brain activations were measured using fMRI, an imaging technique that observes activation in the brain by measuring the level of deoxygenated hemoglobin in the blood. The level of the brain activations are determined by their corresponding t-scores which were mapped onto a template of the brain. The subjective social constructs used were trust, uncertainty, intention to purchase, ease of use, and usefulness. These constructs were measured using a Likert type scale, a widely used scale to define the level of agreement on surveys.

Six subjects were examined in this study. Before the fMRI scan, the subjects visited two e-commerce websites. The first website was user-friendly (easy to navigate) and trustworthy while the second website had the opposite characteristics, that is, it was not user-friendly and ignored basic functionality. The subjects were given some time to familiarize themselves with the two websites. In the fMRI machine, the subjects were asked to answer the set of survey questions for each website. A 3-point Likert type scale (labeled as agree, neutral, and disagree) was used to quantify the survey responses. An fMRI machine scanned the brain and recorded brain activations while the subjects were answering the questions.

The t-scores (in signal intensity) of each voxel of the scanned images that met a threshold of $p<0.05$ were mapped onto a canonical brain atlas using statistical parametric mapping. The brain regions activated were identified and found to be consistent with the literature. We correlated the t-scores obtained from the fMRI responses and the survey responses for each subject. The correlation of the objective brain activations and the subjective human responses are presented. We conclude this study by discussing the implications of functional brain imaging to social sciences and in particular to e-commerce.

Measuring Transepidermal Water Loss: A comparison between Conventional Bioengineering Techniques in vivo

S. Farahmand, L. Tien, X. Hui, and H.I. Maibach
Department of Dermatology, University of California San Francisco, San Francisco, USA

Since 1960s that Miller introduced unventilated-chamber method for measuring Transepidermal Water Loss (TEWL), two main systems have been utilized to measure this parameter: Open chamber & closed chamber. Although most of the commercially available instruments of this type are considered reliable and accurate, the values obtained from them generally differ due to calibration differences. Yet, further validation and standardization studies may be necessary to reveal the sensitivity, precision, & robustness of these instruments.

In the present study, three instruments are compared for their applicability to assess TEWL: Closed chamber Vapometer ® (Delfin Tecnologies Ltd, Kupio, Finland), Open chamber Tewameter® TM210 (Courage+Khazaka electronic GmbH, Köln, Germany) & Aquaflux® AF200 (Biox systems Ltd, London, UK).The comparative study carried out on human forearm skin (n=6), at the normal condition (baseline), and after 1) 10 tape strippings on both arms, 2) moisturizer cream & petroleum jelly application for 1 hr & 3) 1% Sodium Lauryl Sulphate (SLS) aqueous solution & distilled water (as control) application for 20 minutes.

Results showed that no statistically significant difference can be found in baseline TEWL mean values measured by three instruments ($p>0.05$). Aquaflux was the only device among these three that could show the effect of tape stripping on TEWL values as compared to baseline($p<0.001$).After cream & petroleum jelly application, the mean values obtained from the devices were not significantly different ($p>0.05$), however, only Aquaflux could reveal the change of TEWL values compared to the baseline ($p<0.05$).Besides, Aquaflux could also discriminate between the effect of cream & Petroleum Jelly on TEWL values ($p<0.05$). After SLS application, values measured by Aquaflux showed that there was significant difference between the treated site & the corresponding baseline ($p<0.05$), however none of the devices could differentiate between the effect of water & 1% SLS aqueous solution ($p>0.05$).The values measured by Aquaflux were significantly higher than Tewameter & Vapometer ($p<0.01$), but no significant difference could be detected between Tewameter & Vapometer ($p>0.05$).

The correlation between open chamber & closed chamber devices has been shown in previous studies. This study evaluates the sensitivity & capacity of the systems in detecting the effect of different variables on TEWL. The results highlight the differences between the conventional & newly invented closed chamber TEWL measurement instruments which are designed based on different measurement principles. This may give insights to manufacturers to find the best practice to improve the quality, precision & sensitivity of the measurements.

Prospective Study of the Effectiveness of Thermal Imaging in the Diagnosis of Arthritis

Can a radiometric thermal imager detect pre-clinical stages of arthritis in a quick and noninvasive test?

Shay Edwards
Norco High School

Objective: The objective of this study is to see if a radiometric thermal imager can detect preclinical stages of arthritis in a quick and noninvasive method.

Materials and Methods: To establish the effectiveness of thermography as a useful tool for diagnosis pre clinical stages of arthritis in participant's hands using a radiometric thermal imager a double blind test was performed. Forty-five participants filled out a medical history about general health, height, weight, diabetes, smoking, and known diagnoses of arthritis. Participants were then assigned an identification number. During the 16 minute test participants were asked to submerge their left hand and to keep it moving while it was in 63°F ± 2° water for 1 minute. The left hand would then be dried and placed on a wood surface. A thermal image was recorded of the left hand every 4 minutes starting with a preliminary test image.

Results: Inflammation in the interphalangeal joints is the first sign of arthritis. Inflamed joints are warmer. The distal interphalangeal (or DIP; the first knuckle), proximal interphalangeal (or PIP; the middle knuckle), and metacarpophalangeal (MCP; the knuckle at the base of the finger) were closely observed and evaluated, as shown in figure 1. All eight participants with medical history of confirmed cases of arthritis by conventional methods were detected by the use of the radiometric thermal imager showing an elevated temperature of 4°-5° in the interphalangeal joints.

Non Arthritic Hand Thermal Image

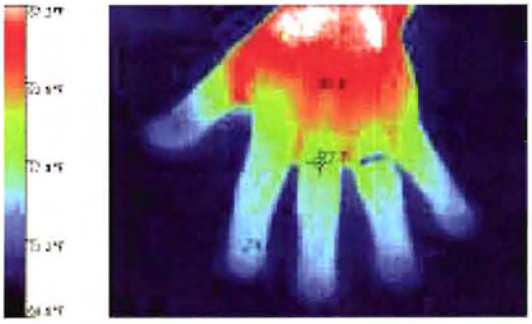

Arthritic Hand Thermal Image

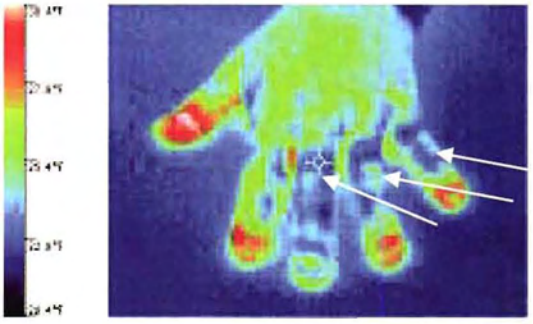

Figure 1. Thermal images after cold water stimulation test showing non arthritic and arthritic hand.

Conclusions/Discussions: The data from the test supports my hypothesis that thermal imaging can be a used to diagnosis arthritis. My data also identified five additional participants displaying preclinical stages of inflammation of the interphalangeal joints. This was a brief and simplified preliminary study designed to evaluate a cold stimulation test to learn whether it would be likely to yield valuable results.

Assembly of Micropatterned Co-Cultures on Conductive and Optically Transparent ITO Substrates

Sunny Shah, Ji Youn Lee and Alexander Revzin
Department of Biomedical Engineering
University of California, Davis

This study employed a combination of oxygen plasma-induced and electrochemical removal of non-fouling poly(ethylene glycol) (PEG) silane molecules from indium tin oxide (ITO) substrates to form micropatterned co-cultures of hepatocytes and fibroblasts. In these experiments, ITO coated glass slides were modified with PEG silane and patterned with photoresist. Exposure of this substrate to oxygen plasma resulted in selective removal of PEG silane from regions not protected by photoresist. Physical adsorption of cell-adhesive ligands such as fibronectin or collagen followed by photoresist lift-off created protein regions interspersed with PEG-silane on the conductive ITO substrate. Incubation of the micropatterned surface with hepatocytes or fibroblasts resulted in selective attachment of the cells on protein microdomains. Importantly, application of reductive potential to ITO substrates containing cell clusters led to removal of PEG silane and switching of the surrounding regions from non-fouling to cell-adhesive. Addition of the second cell type resulted in formation of hepatocyte-fibroblast co-cultures. Importantly, application of voltage did not affect pre-existing cellular patterns. Significantly, our surface engineering strategy allows us to construct co-cultures of cell types exhibiting similar adhesiveness and therefore does not depend on the sequence of cell seeding steps. Currently, this micropatterning approach is being used for co-cultivation of mouse embryonic stem cells with adult hepatocytes in order to drive stem cell differentiation toward hepatic lineage.

Aptamer based electrochemical biosensor for botulinum toxoid/type A

Fang Wei, Chih-ming Ho

Department of Mechanical and Aerospace Engineering, University of California, Los Angeles, CA

Botulinum neurotoxin (BoNT) is the most naturally occurring poisonous substances. Fast and highly sensitive detection of BoNT plays a critical role for bio-safety issue. Conventional detection of BoNT is limited by the specific human monoclonal antibody because of its high toxicity. Aptamer is the fragment of oligonucleotides, which could specifically bind to target protein with proper conformation. In comparison with antibody, the aptamer for the detection of BoNT is more convenient to be screened and obtained.

Herein, we propose a strategy combining electrochemical method with aptamer probe that couples an enzymatic amplification with a target-induced conformational change to detect BoNT/type A toxoid (BoNT/A). The electrochemical sensor is based on a DNA-dendrimer interfaced poly-pyrrole substrate to maintain the activity of aptamer. Aptamer is labeled with a reporting tag for the peroxidase. Without BoNT/A binding, aptamer is in closed state and the steric hindrance to the sensor surface inhibits signal amplification by preventing mediator access to the reporter. After binding with BoNT/A, aptamer is open which makes the reporter accessible and generating a current signal. Therefore, only the specific target can generate an amplified current (Fig. 1).

The key issue for the recognition of BoNT/A is the folding process of the aptamer. Misfolding of non-appropriate configurations will cause false-positive and false-negative. These misfoldings result in different quasi-stable intermediates during the reaction. Although the appropriate configuration is the most stable one and has the lowest Gibbs free energy ($-\Delta G$), trapping into these quasi-stable intermediates is still possible. In our work, short duration of folding (less than 3 hours) always has low signal-to-background ratio (SBR), while long duration (> 5 hours) gives good SBR. This phenomenon partly supports the assumption that there exists quasi-stable mis-folding conformation prior to the final status.

To drive the reaction into thermodynamically stable product, one of the important factors for correct folding is the ion composition. Since the aptamer is negatively charged, different ions guide into different folding conformation. Our experiment shows that the affinity of aptamer is dependent to the ion composition of the buffer. More interestingly, the folding process turns out to be not only related to single type of ion. Multiple types of ions result in better folding. With optimized combination of Na^+, K^+, Mg^{2+}, and Ca^{2+}, aptamer could bind to the BoNT/A with good affinity, and the limit-of-detection (LOD) of our sensor is about 40 pg/mL (400 fM).

Fig 1: Illustration of aptamer based BoNT/A electrochemical detection

One Dimensional Virus Templates for Hierarchical Nanofabrication – Hybrid Memory Devices

Faculty(PI): Cengiz Ozkan[1]
Researchers: Xiaoye Jing[2], Emre Yengel[2], Chunglin Tsai[2], Ricky J. Tseng[3*], Yang Yang[3*]
Mechanical Engineering Department[1], Electrical Engineering Department[2], Materials Science and Engineering Department[3*], UCR, UCLA[*]

Hybrid virus-inorganic nanomaterials are considered as important building blocks towards new types of functionality for electronic devices. We use Tobacco Mosaic Virus (TMV) templates 18 nm in diameter to assemble ZnS-capped CdSe quantum dots. The synthesis of TMV conjugated with ZnS-capped CdSe quantum dots (TMV-QD) is carried out with QD-COOH with 50 μL, and 2.4 nmol/mL solution was added with 200 μL 20 mM 1-ethyl-3-(3-dimethylaminopropyl) carbondiimide (EDC) to form a covalent bonding between carboxyl and amino groups to form a peptide bond. When EDC reacts with a carboxyl group, it forms an active ester leaving group, O-acylisourea, which will hydrolyze rapidly in aqueous solutions. Following the addition of EDC, the solution was then added with 200 μL, 50 mM N-hydrosulfosuccinimide (sulfo-NHS). The sulfo-NHS increases the half-life of the active intermediate from seconds to hours so that there is a higher probability to form a peptide bond between amino and carboxyl groups. Finally 500 μL TMV (~6mg/mL) was added to the solution under no lighting conditions. By forming a thin hybrid composite layer in a cross-bar device architecture, we show an electronic memory effect based on different electrical conductance states with large on/off ratio and long retention times. The mechanism in the memory device likely involves the transfer of charge from the RNA core of the TMV to the nanocrystals under the applied high electric field, which subsequently changes the conductivity of the material system (figure on the left). The electrical bistable behavior is shown in the Figure on the right. In the first scan, the current gradually increases as the voltage is increased to 3 V. A hysteresis in the current loop is observed with an on/off ratio of 262 at 1 V. The low and high conductivity in the first scan is termed as state 0 and state 1, respectively. In the second scan, another current loop is shown with an on/off ratio of 16. The high conductivity in the 2nd scan is termed as state 2. These states constitute multi-states that the device can actually store more than 2-bits of data. The retention time of these states can reach for about 1 day. Each state is stable during the stress testing at 1 V bias up to 5000 seconds as shown. State 1 and 2 are stable until an erase bias of -1.5 V is applied to turn to the state 0 once again. In conclusion, results indicate that devices fabricated based on TMV conjugated to core-shell QDs have the potential to store more than 2 bits of data. Such hybrid bio-inorganic nanostructures are promising for the development future bio-inspired nanoelectronics.

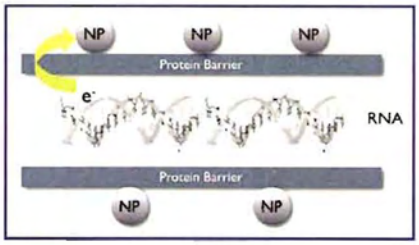

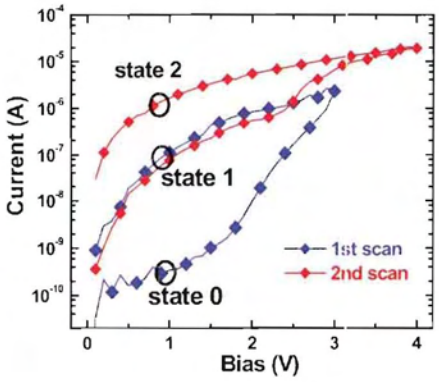

Electric Field Directed Fabrication of Active Bio/Chem Sensors from Enzyme Linked Nanoparticles

Alexander Hsiao[1], Dietrich Dehlinger[2], Michael J. Heller[1,3]
[1]Department of Bioengineering, University of California, San Diego
[2]Department of Electrical and Computer Engineering, University of California, San Diego
[3]Department of Nanoengineering, University of California, San Diego

Active transport atop an electrophoretic microarray allows for rapid concentration of nanoparticles onto individual electrode sites. We have previously demonstrated the fabrication of alternating layers of biotin and streptavidin derivatized nanoparticles on a CMOS microarray using electric field directed self-assembly. Our current research is focused on the construction of biological and chemical sensors using enzyme-linked nanoparticle layers. We believe that these nanoparticle layers will be superior to current surface bound sensors. The application of an electric field allows for rapid concentration of particles over individual electrode sites, allowing for efficient fabrication of enzyme-nanoparticle layers. Moreover, the increased surface area of multiple layers should enhance the recognition of analyte species. Our current method includes the alternate layering of glucose oxidase-avidin to 200nm biotin-polystyrene nanoparticles. Using the CMOS microarray we have fabricated constructs of up to 20 alternating layers of enzyme and nanoparticle. We further hope to activate these layers and observe chemiluminescence through the addition of glucose and luminol to the system, thereby producing a functional sensor. Furthermore, these structures can be customized to include multiple enzymes to allow for coupling between the layers as well as the incorporation of targeting or imaging moieties. In producing these active enzyme-nanoparticle layers we hope to develop efficient methods of fabrication of bio/chemical sensors that can be incorporated into small in vivo devices.

Antibody Microarrays for Immunophenotyping and Cytokine Profiling of T-Cells

Gulnaz Stybayeva*§, He Zhu*, Monica Macal**, Erlan Ramanculov§, Michael D. George**, Satya Dandekar** and Alexander Revzin*#

*Biomedical Engineering, University of California, Davis
**Medical Microbiology and Immunology, University of California, Davis
§National Center for Biotechnology, Astana, Republic of Kazakhstan
#Correspondence: arevzin@ucdavis.edu

ABSTRACT

Cytokine production by leukocytes in response to viral or bacterial pathogens correlates with disease outcomes and therefore carries significant diagnostic value. The goal of the present study was to develop a miniature device for detection of interleukin (IL)-2 and interferon (IFN)-γ produced by a small population of $CD4^+$ and $CD8^+$ T-lymphocytes. Microarrays of CD4-, CD8- and cytokine-specific Ab spots were printed onto poly(ethylene glycol) (PEG) hydrogel-coated glass slides and then were enclosed inside a microfluidic device, thus creating a miniature (3 μl) immunoreaction chamber. Introduction of the red blood cell (RBC) depleted whole human blood into the microfluidic device followed by washing at a pre-defined shear stress resulted in isolation of pure (>95%) $CD4^+$ and $CD8^+$ T-lymphocytes on their respective Ab spots. Importantly, the immune cells became localized next to anti-IL-2 and anti-IFN-γ Ab spots. Mitogenic activation of the captured T-cells was followed by immunofluorescent staining (all steps were carried out inside a microfluidic device) and revealed concentration gradients of IL-2 and IFN-γ emanating from an array of immune cells. Concentration of IL-2 and IFN-γ near $CD4^+$ T-cells was estimated to be 18 ng/ml and 60 ng/ml respectively while $CD8^+$ T-cells produced 32 ng/ml of IFN-γ and no IL-2. The production of cytokines by T-cells was confirmed using intracellular cytokine staining and flow cytometry. A microdevice described here is envisioned as a novel immunology tool for characterizing numbers and functions of T-cells from peripheral blood and may be used in vaccine development, HIV diagnosis or monitoring the effectiveness antiretroviral HIV therapy.

Microfluidic Formation of Lipid Vesicles

Shia-Yen Teh and Abraham P. Lee
University of California, Irvine

We present a novel microfluidic device capable of generating monodispersed lipid vesicles in a continuous manner while allowing encapsulation of a variety of materials and tunable surface properties. Liposomes were first discovered by Bangham et. al [1] in 1965, and since have garnered much attention for its use in a number of pharmaceutical and biological applications. Liposomes are spherical capsules ranging from nanometers to hundreds of micrometers in diameter that are formed by one or multiple lipid bilayers. However, current methods of liposome production such as lipid hydration result in liposomes of polydisperse size populations, unstable shelf life, and varying degree of multilamellarity. Droplet-based microfluidics has the potential to overcome many of these limitations with its ability to produce highly monodispersed droplets in the nanometer to micrometer diameter range and particles from a variety of materials. [2] We present a microfluidic platform that uses water-in-oil-in-water double emulsions to form lipid vesicles. As shown in figure 1, 40µm monodisperse water droplets are formed in a solution of the phospholipid 1,2-Oleoyl-sn-Glycero -3-phosphocholine (DOPC) dissolved in oleic acid. Due to the amphiphilic nature of lipids, DOPC lipids arrange themselves around the water droplet with the hydrophilic heads pointing inwards and hydrophobic tails pointing out into the oleic acid, thus forming a lipid monolayer over the droplet. As shown in figure 2, an ethanol solution consisting of 20% ethanol, 25% glycerol, and 5% Poloxamer 188 in water, shears the water droplet stream into 50µm monodispersed double emulsions. Oleic acid is miscible with ethanol, and over time dissolves into the ethanol, leaving behind a concentrated ring of lipid around the water droplet. (Figure 3) Exposure to aqueous environments on both sides forces the phospholipids to reorient into a bilayer, forming stable liposomes. In addition to quickly and controllably generating large number of liposomes, the device can further alter the membrane surface to include targeting ligands, and control the encapsulation of a variety of substances for drug delivery and other biological applications.

References

1. "Diffusion of univalent ions across the lamellae of swollen phospholipids" A. D. Bangham, M. M. Standish, J. C. Watkins, *J. Mol. Biol.*, ***13***, 238 (1965)
2. "Droplet Microfluidics", S.-Y. Teh, R. Lin, L.-H. Hung, and A. P. Lee, *Lab on a Chip*, **8**, 198 (2008)

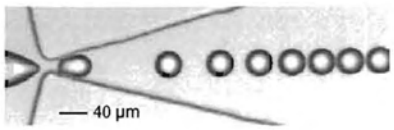

Figure 1. Formation of water droplets in DOPC/oleic acid

Figure 2. Generation of Ethanol/Oleic Acid/Water double emulsions

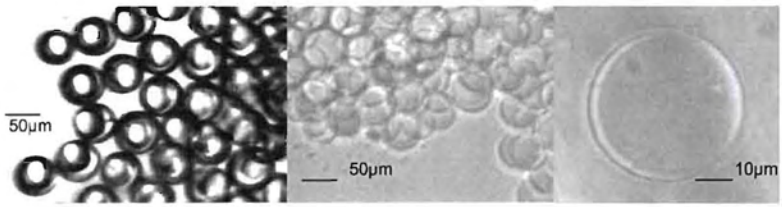

Figure 3. a)Stable double emulsion droplets suspended in ethanol, b) Over time oleic acid dissolves into the surrounding ethanol, resulting in the formation of liposomes, c) Single liposome at 40X magnification

Exploring the Interaction between Nanoparticles and Cells

Jennifer Reiber Kyle[1], Yu Zhang[2], Mihri Ozkan[1], and Cengiz Ozkan[2]
[1]Department of Electrical Engineering, [2]Department of Mechanical Engineering, University of California at Riverside

Nanotechnology promises a revolution of cancer diagnosis and treatment through multifunctional nanoparticles. In this research project, we probed the interaction between magnetic iron oxide nanoparticles and normal (MCF10A) and carcinoma (MCF7) breast epithelial cells. This information is vital in guiding the creation of iron oxide nanoparticles for drug delivery and provides insight into the differences and similarities between the normal and carcinoma breast epithelial cells. After incubating both types of cells with F3 peptide-conjugated, dextran-coated iron oxide (Fe_2O_3) nanoparticles, we analyzed the cells using zeta potential, confocal fluorescence microscopy, near-field scanning optical microscopy (NSOM), and atomic force microscopy (AFM). Zeta potential measurements show distinct signature patterns for the normal and carcinoma cells that change with nanoparticle incubation time. Confocal fluorescence images confirm the different uptake amount and timing for normal and carcinoma breast epithelial cells. Additionally, because fluorescence labels attached to the nanoparticles can change their interaction with the cell membranes, we have developed and demonstrated a method for identifying iron oxide nanoparticles within the cells without requiring fluorescence labels. This method uses the difference between the light absorption of the inorganic nanoparticles and the organic cell matter to identify the nanoparticles. NSOM, with its resolution of ~50nm, is capable of resolving the nanoparticles within the cell. Images we obtained with our custom NSOM/AFM hybrid system of an MCF7 cell incubated with FITC-labeled nanoparticles show the high correlation between transmitted light and fluorescence, demonstrating the accuracy of our method in detecting iron oxide nanoparticles without using fluorescence. Finally, highly interesting HP-91 peptide conjugated PLGA polymer nanoparticles and PEG-coated magnetic iron oxide nanoparticles were characterized using AFM phase and magnetic force microscopy (MFM) imaging respectively.

Near-field Scanning Optical Microscopy (NSOM) and Magnetic Force Microscopy (MFM): Two Advanced Fluorescence Labeling Free Imaging Methods for Studying the Nanoparticle Endocytosis by Cells

Yu Zhang[1], Vahid Yazdanpanah[1], Jennifer Reiber Kyle[2], Mo Yang[3], Mihri Ozkan[2] and Cengiz Ozkan[1]

[1]Department of Mechanical Engineering, University of California at Riverside, Riverside CA 92521, USA
[2]Department of Electrical Engineering University of California at Riverside, Riverside CA 92521, USA
[3]Department of Health Technology and Informatics, Hong Kong Polytechnic University, Kowloon, Hong Kong, China

Advanced fluorescence labeling free imaging methods to study the interactions between nanoparticles and biological cells are demonstrated using Near-field Scanning Optical Microscopy (NSOM) and Magnetic Force Microscopy (MFM). NSOM is capable of simultaneously recording topographic and near-field optical images. We examined the MCF10A normal and MCF7 carcinoma breast epithelial cells and their interactions with iron oxide nanoparticles using a hybrid AFM/NSOM system, which enabling simultaneous recording topographic information of the cell surface, as well as the near-field optical analyses of the cell interior. Specific nano-scale optical patterns of nanoparticle loaded vesicles inside the cells are observed and analyzed statistically. MFM has the capability to detect magnetic domains from a distance, which can get the magnetic force gradient image of the scanned samples and also simultaneously obtain topography AFM image and surface property Phase image. Magnetic iron oxide nanoparticles and their endocytosis by MCF7 carcinorma breast epithelial cells are examined. The magnetic nanoparticle spatial localization and topography of cells are directly visualized at the same time using MFM technique. By using the optical and magnetic properties of nanoparticles, these two advanced dual functional nanoscale-resolution microscopic techniques show the capabilities in label-free mapping the spatial localization of nanoparticles in/outside cell surface. Label-free detection is of considerable interest because the possible disadvantages associated with fluorescence labeling. And these nano-scale observations will provide very useful information for better design of new imaging, diagnostic and therapeutic nanomaterials in biomedical research.

Surface Charge Investigation of Interactions between Normal/Cancer Breast Epithelial Cells with Multifuntional Nanoparticles

Yu Zhang[1], Mo Yang[2], Jennifer Singelyn[3], Ji Ho Park[4], Nate Portney[5], Michael Sailor[4], Mihri Ozkan[6] and Cengiz Ozkan[1]

[1]Department of Mechanical Engineering, [5]Department of Mechanical Engineering, [6]Department of Electrical Engineering University of California at Riverside, Riverside CA 92521, USA
[2]Department of Health Technology and Informatics, Hong Kong Polytechnic University, Kowloon, Hong Kong, China
[3]Department of Bioengineering, [4]Department of Chemistry and Biochemistry , University of California at San Diego, San Diego, CA 92037, USA

A substantial understanding of the interactions between multifunctional nanoparticles and normal/cancer cells will enable the capabilities of improving diagnostic and treatment methods in cancer research, such as imaging and targeted drug delivery. Surface charge measurements of cells in terms of Zeta potential are demonstrated as a valuable biological characteristic and a promising approach in studying specific cellular function and cellular interaction of nanomaterials. A theoretical Zeta potential model was established to show the effects of binding process and internalization process during the nanoparticle uptake by cells and the possible trends of Zeta potential change is predicted for different cell endocytosis capacities. Then we reported the surface charge responses of human normal breast epithelial cells (MCF10A) and human carcinoma breast epithelial cells (MCF7) after incubated with untreated iron oxide nanoparticles, cowpea mosaic virus (CPMV) nanoparticles and tuomor homing F3 peptide conjugated dextran coated iron oxide nanoparticles over time. The interactions between different nanoparticles and normal/cancer cells led to distinct patterns in surface charge Zeta potential measurements. The results suggest a great potential for the surface charge measurements, which may be utilized as a streamlined method for gauging dynamic cell response and may aid in validating and developing novel candidates for diagnosis and therapeutics.

Fabrication and characterization for truncated tetrahedron nano-plasmonic biosensor

Bongsu Jung[1,2] and Wolfgang Frey[2]
[1]Department of Bioengineering, The University of California at Riverside, Riverside, CA 92521, USA
[2]Department of Biomedical Engineering and Center for Nano & Molecular Science & Technology, The University of Texas at Austin, Austin, TX 78712, USA

Localized Surface Plasmon Resonance (LSPR) is a label-free technique that is fast, highly sensitive to the dielectric environmental changes, suitable for high-throughput screening, nanoscale detection up to femto-molar, and can be detected by simple absorption and scattering measurement in a UV-Vis spectrometer or a dark-field microscopy. We developed new fabrication technique which is a carbon-based template stripping technique to create nano-textured ultraflat surface. This is called carbon-based ultraflat nanosphere lithography (c-UNSL). An increase in thickness of gold or silver nano particle causes the spectral peak to shift to the blue, but also leads to decreased sensitivity. However, as the length of the largest bisector on the tetrahedron particle is increased, the peak position shifts to the red, while increasing the sensitivity. Thus, highest sensitivity is achieved with particles that highly non-spherical this thin but elongated shapes. The peak position in the VIS-NIR spectrum is dependent on the environment of each particle, and each particle can act as its own sensor. Optimization of the non-spherical geometry of the metal nanoparticle leads to a strongly increased sensitivity to changes in the local refractive index, exceeding that of other LSPR configurations. The resulting arrays of silver or gold nanoparticles in the surface of a glass slide are capable of detecting thiol surface modification, protein binding, and their binding kinetics. Since each gold or silver particle principally acts as an independent sensor, on the order of a few thousand molecules can be detected, and the sensor can be miniaturized without loss of sensitivity. Our Finite-difference-time-domain (FDTD) and finite-element-method (FEM) numerical calculations show the influence of the sharp features on the resonance peak position. The simulation shows the local refractive index sensitivity of the gold truncated tetrahedron, which is in agreement with our experimental result. Both experimental and numerical calculations show that each particle can act as its own sensor for non-labeling array type assays.

Computational Prediction of Association Free Energies for the C3d:CR2 Complex and Comparison to Experimental Data

Alexander S. Cheung,[1] Jianfeng Yang,[2] Chris A. Kieslich,[1] Dimitrios Morikis[1]
Department of [1]Bioengineering and [2]Computer Science and Engineering
University of California, Riverside

The complement system is part of the innate immune system and functions to clear pathogenic threats. The association between complement protein C3d and B or T cell-receptor CR2 (complement receptor 2) represents a crucial link between innate and adaptive immunities. The goal of this study is to computationally predict association abilities of C3d and CR2 mutants by theoretically calculating electrostatic free energies of association with and without solvation effects. We demonstrate that incorporation of solvation effects is necessary to accurately predict previously published experimental data for the association abilities (relative to the parent proteins) of specific C3d and CR2 mutants. We show that a proportional relationship exists between the predicted solvation free energy differences and the experimental data. Additionally, an inversely proportional relationship is demonstrated between the calculated solvation free energy differences and previously calculated ionization free energy differences. Changes in the nonpolar free energies upon association were also calculated, but for the mutants considered in this study, are negligible. Our results yield new insights into the physicochemical properties underlying C3d:CR2 association. Our results can also be extended to any complex with excessively charged components. This basic study contributes toward developing a theoretical understanding of immune system regulation at the molecular level, and can be the groundwork for the design of regulators with tailored properties, vaccines, and biotechnology products in general.

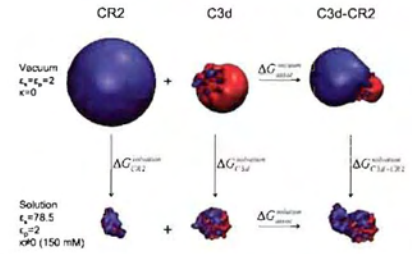

Hypothetical thermodynamic cycle and calculation parameters for the Poisson-Boltzmann equation.

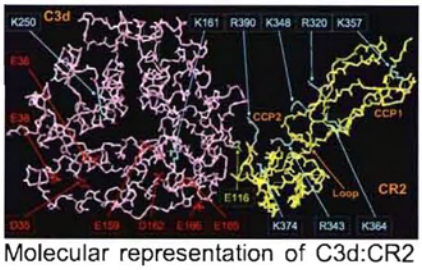

Molecular representation of C3d:CR2 demonstrating the topology of the mutated amino acids. Basic and acidic amino acids are shown in blue and red, respectively.

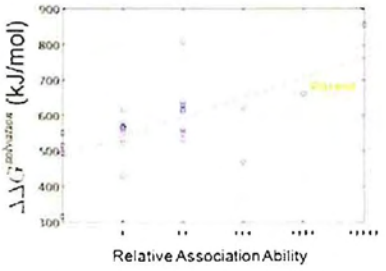

$\Delta\Delta G^{solvation}$ (calculated using the complete thermodynamic cycle) *versus* relative association ability with a linear fit drawn in red.

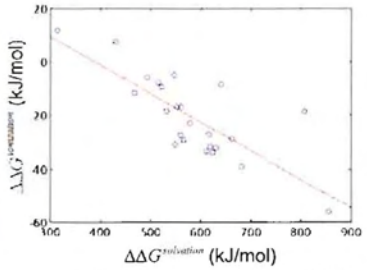

$\Delta\Delta G^{ionization}$ *versus* $\Delta\Delta G^{solvation}$. $\Delta\Delta G^{ionization}$ is from Zhang *et al* (2007). A linear fit is drawn in red.

[1]Clemenza L & Isenman DE (2000) *Journal of Immunology* 165:3839-3848.

[2]Hannan JP, Young KA, Guthridge JM, Asokan R, Szakonyi G, Chen XJS, & Holers VM (2005) *Journal of Molecular Biology* 346:845-858.

[3]Wu J & Morikis D (2006) *Fluid Phase Equlibria* 241:317-333.

[4]Zhang L, Mallik B, & Morikis D (2007) *Journal of Molecular Biology* 369:567-583.

Interactions of the V3-loop of HIV-1 gp120 and the N-terminal Domain of CCR5

Aliana López De Victoria, Chris A. Kieslich, Dimitrios Morikis
Department of Bioengineering
University of California, Riverside

HIV-1 involves binding of its envelope glycoprotein gp120 with the CD4 receptor and coreceptors CCR5 or CXCR4 in the host cell. The mechanism of cell infection by HIV is not well understood. The third variable region of gp120 forms a loop, called the V3-loop, which is composed of 31-39 residues. The V3-loop is responsible for determining HIV tropism and plays an important role in viral entry by selecting the appropriate coreceptor. Previous studies have demonstrated that the V3-loop interacts with the N-terminal extra-cellular domain of CCR5 (CCR5-Nt) and that electrostatics play the dominant role in this interaction.[1,2] The electrostatic attraction involves a highly positive V3-loop and a highly negative CCR5-Nt. The overall charge of CCR5-Nt is enhanced by the presence of a minimum of two sulfated tyrosines.

The V3-loop is excessively positively charged and is closed by a disulfide bridge formed by two cysteines. The V3-loop consists of three distinct regions: the base (closer to the core of the protein), the tip at the opposite end, and the stem between the base and the tip. Currently, there are two X-ray structures of gp120 complexes with the V3-loop intact, in which the V3-loop shows structural variability.[3,4] We have applied our high-throughput computational methodology[5] to delineate the contributions of each ionizable amino acid in the overall electrostatic potential generated by the V3-loop charges, using models from the available X-ray structures. We will discuss the calculated clusters with respect to visualized spatial distributions of electrostatic potentials and their importance for CCR5-Nt binding. We will also present docking models for the V3-loop:CCR5-Nt complex and calculated electrostatic and nonpolar free energies of association. These data will form the basis for future design of agonists and antagonists for the V3-loop:CCR5-Nt interaction.

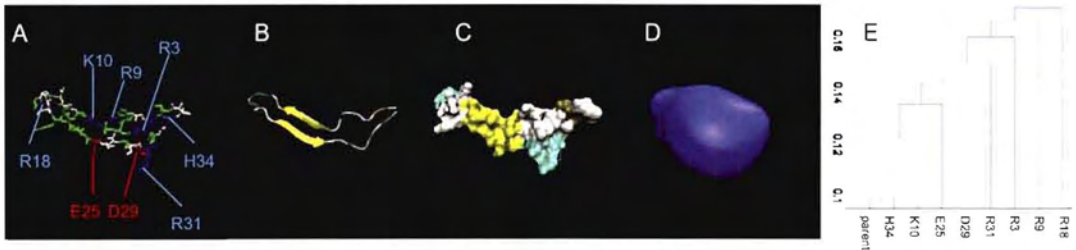

Molecular models of the V3-loop (PDB Code: 2QAD): (A) stick representation of backbone and side chains, with the ionizable amino acids marked; (B) ribbon representation of backbone; (C) molecular surface representation; (D) spatial distribution of electrostatic potential. The color code for (A) is: blue, positively charged amino acid; red, negatively charged; green polar; gray, nonpolar. The color code for (B) and (C) is according to secondary structure. The blue color in (D) demonstrates the presence of excessive positive charge. (E) Clustering of V3-loop mutants based on similarities of the spatial distributions of electrostatic potentials.

[1]Morikis D, Rizos AK, Spandidos DA, Krambovitis E (2007) *International Journal of Molecular Medicine* 19:343-5.
[2]Rizos AK, Tsikalas I, Morikis D, Galanakis P, Spyroulias GA, Krambovitis E (2006) *Journal of Non-Crystalline Solids* 352:4451-58.
[3]Huang C, Lam SN, Acharya P, Tang M, Xiang SH, Hussan SS, Stanfield RL, Robinson J, Sodroski J, Wilson IA, Wyatt R, Bewly CA, Kwong PD (2007) *Science* 317:1930-34.
[4]Huang CC, Tang M, Zhang MY, Majeed S, Montabana E, Stanfielg RI, Dimitrov DS, Korber B, Sodroski J, Wilson IA, Wyatt R, Kwong PD (2005) *Science* 310:1025-28.
[5]Yang J, Gunopulos D, Morikis D (2008) *In Preparation*.

Computational Investigation of Transient Heat Transport through a Porous Filled Heat Exchanger Applicable in Biological Sciences

Shadi Mahjoob

Mechanical Engineering Department, University of California, Riverside, CA92521, USA

Thermal management and temperature control have an important role in widely-used molecular biology techniques such as polymerase chain reaction utilized for nucleic acid amplification in vitro. This technique has a variety of applications such as structural genomics, generic fingerprinting, paternity testing, and cloning genes. Transient cyclic heat exchangers are required to set the nucleic acid temperature at each of the three steps of the process; denaturing (at 94-98°C), annealing (at 50-65°C) and elongation (at 72°C), respectively. After each three-step cycle, every nucleic acid is doubled and after n cycle, 2^n similar nucleic acid can be obtained. Between each two following steps, the temperature should change as fast as possible since the time increases the chance of primer dimmer formation and low quality amplified nucleic acids. Besides, temperature uniformity through the substrate where the nucleic acid is placed is a crucial issue to achieve high quality and similar amplified nucleic acids. In this work, fluid and heat transport are characterized through a designed miniaturized cyclic heat exchanger computationally. To enhance the thermal transport through the miniaturized heat exchanger, highly conductive porous materials, such as metal foams, are utilized. Temperature augmentation are investigated utilizing two types of cyclic heat exchangers; porous filled and plain heat exchangers. The results indicate a significant improvement in the temperature ramp (temperature change per heating/cooling cycling time) between each two step points, when the porous filled miniaturized heat exchanger is utilized. An optimized heat exchanger is obtained based on the effective parameters in order to have a faster temperature ramp, more uniform temperature through the substrate and less required power for pumping the working fluid. The results are presented and discussed based on the temperature distribution, velocity vectors and streamlines within the heat exchangers.

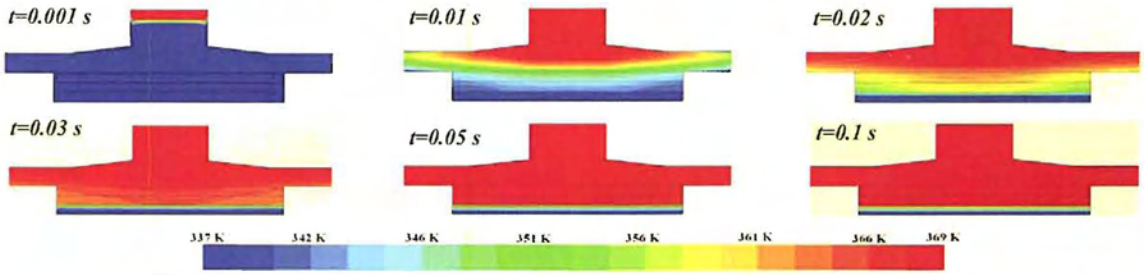

Fig.1. Temporal temperature contour in the miniaturized porous filled heat exchanger.

Novel Tissue Mimicking Materials for the Development of Hard Tissue Ultrasound Phantoms

Priyamvada Tewari [1], David Goldenberg [1], Rahul Singh [1,2], Warren Grundfest [1], Shane White [3], Martin Culjat [1,2]

[1]Center for Advanced Surgical and Interventional Technology,
University of California, Los Angeles,
[2]Department of Electrical and Computer Engineering,
University of California, Santa Barbara,
[3]School of Dentistry,
University of California, Los Angeles

Ultrasound is very effective in detecting density or acoustic impedance changes in tissues, such as those that occur within air- or water-filled organs, at bone/soft tissue interfaces, and with foreign objects in soft tissue. Ultrasound imaging of soft tissues is well developed, but the ultrasound imaging of hard tissue surfaces and abnormalities has not found widespread clinical application in the United States. Hard tissue ultrasound imaging systems are currently under development; however, phantoms that mimic the acoustic properties of human tissues are required to better understand the interaction of acoustic waves with bones and joints. While many studies have demonstrated accurate soft tissue phantoms, investigation of hard tissue mimicking materials has been limited.

The pre-requisite for a bone phantom mimicking material is that it should acoustically mimic the properties of ultrasound in bone within the operating frequency range. A variety of materials have previously been studied for potential development of ultrasound cortical bone phantoms, including polyvinyl chloride, acrylic, ebonite, and epoxy. However, due to lack of validated data there is still no widely adopted bone mimicking material. For this purpose, we have explored a number of hard polymers like acrylic, polyethylene, polypropylene, nylon, Teflon, polystyrene and polycarbonate as potential cortical bone mimicking materials. The density of each material was measured mechanically, and the acoustic velocity and acoustic impedance were evaluated from acoustic time of flight measurements. Finally, these parameters were compared to the published values for cortical bone.

Nanoscale Memory Characterization of Virus-Templated Semiconducting Quantum Dots

Alfredo A. Martinez-Morales[1], Nathaniel G. Portney[3], Cengiz S. Ozkan[2], Mihrimah Ozkan[1]

[1]Deparment of Electrical Engineering, [2]Department of Mechanical Engineering, [3]Department of Bioengineering, University of California Riverside.

Icosahedral viruses are promising building blocks for enabling the self-assembly of next-generation nanoelectronic devices. In this work, we have developed a substrate based bottom-up approach to assemble two different color emitting CdSe/ZnS (core/shell) quantum dots on the surface of a novel Cowpea mosaic virus mutant, CPMV-T184C. This technique provided successfully production of individual hybrids and enabled single hybrid characterization. Electrical characteristics of individual hybrid were investigated by conductive atomic force microscopy (CAFM) for potential digital memory applications (*i.e.*, RAM). These individual 40 nm CPMV-QD(1,2) hybrids exhibited reversible bistable electrical behavior during repeatable writing-reading-erasing processes at the nanoscale. The observed conductance switching is attributed to an E-field induced charge transfer mechanism between the highly aromatic CPMV and the QD core leading to a memory effect. Detailed study of the conduction mechanism in both the low and the high conductivity states shows that thermionic emission is responsible for conductance in the low conductivity state, whereas a Poole-Frenkel emission is likely to be the conduction mechanism in the high conductivity state. In light of these results, we can hypothesize that the current conduction changes from an injection dominated mechanism in low conductivity state to a charge-transport-dominated mechanism in the high conductivity state. It is, therefore, believed that the charge transfer process is the result of the charge donating ability of the CPMV's aromatic residues which enables the observed bistability behavior while it also provides a direct pathway to the charge transfer phenomenon. This work depicts the possibility of using each individual hybrid of 40nm as a single addressable memory element applicable to a random access memory. This unique composite system opens the possibility of extending organic-QD hybrid applications beyond photovoltaics and organic LEDs to encompass high density digital memory. The results are significant in showing that organic-QD hybrid nanostructures are very promising for application in memory-based nanoelectronics.

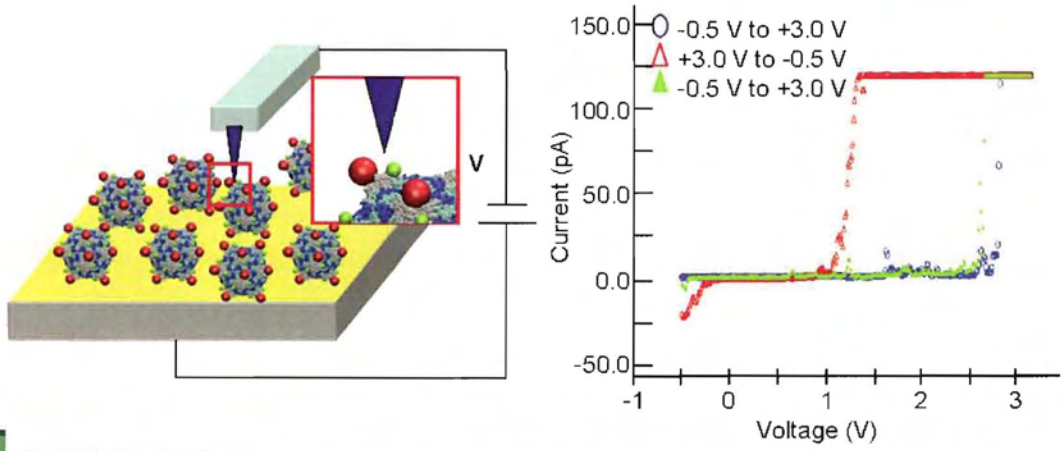

Quantitative Conversion of Alcohols to Aldehydes Using Alcohol Dehydrogenase

Sean Guthrie and Valentine Vullev
Department of Bioengineering, University of California, Riverside

Due to their reactivity, aliphatic aldehydes are important precursors for a range of coupling reactions broadly used in organic and bioorganic synthetic procedures. Aldehydes are usually prepared by selective chemical oxidation of the corresponding alcohol derivatives. Such chemical procedures, however, can readily lead to overoxidation and formation of carboxylic acids, decreasing the yield of aldehyde production. Enzyme catalysis allows for highly selective control of chemical transformation under mild conditions in aqueous media. We utilized alcohol dehydrogenase (AD) for the development of homogeneous and heterogeneous procedures for quantitative transformation of aliphatic alcohols into the corresponding aldehydes. We demonstrated the AD-catalyzed conversion of hydroxyl-terminated polyethylene glycol (PEG) into PEG-aldehyde conjugates. PEGs are versatile materials for preparation of bioinert (i.e., non-fouling) interfaces. Furthermore, PEGs are susceptible to chemical and enzymatic oxidation, placing high demands on the types of reaction used for their chemical transformations. Selective oxidation of this family of hydroxyl-terminated polymers conveys the utility of our enzyme-catalyzed conversion methodology.

Print-and-Peel Fabrication of Microelectrodes

Duoduo Bao, Connie Hong, Marlon S. Thomas, Joseph M. Clift and Valentine I. Vullev*
Department of Bioengineering, University of California, Riverside, CA 92521

Our laboratory plays a leading role in the development of nonlithographic, i.e., *print-and-peel* (PAP), fabrication methodologies, which proved essential for fast and expedient prototyping of microfluidic devices. We have already demonstrated the application of PAP for microfabrication of continuous-flow biosensors. Due to the enormous importance of interfacing microfluidic with electronic devices, we developed a PAP method for fabrication of arrays of microelectrodes on flat substrates. Computer-aided-design patterns of microelectrodes were printed directly onto polyester transparency films using regular office equipment. Casting polydimethylsiloxane (PDMS) prepolyer over the film produced PDMS components with negative-relief imprints, which reversibly adhered to glass surfaces to form microfluidic assemblies. Utilizing Tollen's reaction, metal silver was deposited onto the walls of the microchannel, transferring designed patterns of electrodes onto the substrate surface. Removing of the PDMS components followed by electrodeposition of copper over the silver patterns allowed us to prepare micrometer-thick electrodes that are significantly less susceptible to mechanical damages than the Ag deposits. We used PAP-fabricated microelectrode arrays for preparation of capacitance sensors, which were characterized using impedance spectroscopy. Triangular waveform (TW) measurements allow for fast extraction of the capacitance component of the complex impedance. Therefore, we employed TW for monitoring fluids with various dielectric properties. We believe that the presented PAP methodology offers an expedient and facile alternative for fabrication of impedance-spectroscopy biosensors.

Bioinspired Molecular Rectifiers

M. K. Ashraf,[1] Roger K. Lake[1] and Valentine I. Vullev[2]

[1]Department of Electrical Engineering, University of California, Riverside, CA 92521.

[2]Department of Bioengineering, University of California, Riverside, CA 92521.

Correspondance: Email: mashraf@ee.ucr.edu

Polypeptide α-helices possess an enormous intrinsic dipole moment (4 to 5 Debye per residue) that has been demonstrated to cause rectification of charge transfer processes. In α-helices, the intrinsic dipole moment results from the orientation of the amide bonds in an ordered direction and the collective shift in electron density upon formation of an internal network of hydrogen bonds between the amide groups. Polypeptide helices, however, mediate charge transfer via tunneling through sigma, hydrogen and amide bonds, which is inefficient for distances beyond 1.5-2nm. Synthetic polymers with narrow band gaps can mediate long range charge transport. Aromatic poly-ortho-amides have extended π-conjugation along their backbones. These polymers are bioinspired in a sense that their secondary conformation is held together by a network of hydrogen bonds between amide groups with ordered direction. We determined that the codirectional orientation of the amide bonds and the collective shift in electron density, resultant from the hydrogen-bond formation, produces an intrinsic dipole moment that is comparable to the dipole moment of polypeptide α-helices.

Using ab initio density functional theory calculations, we modeled oligoanthranilamide derivatives with different lengths. All structures were optimized using the B3LYP exchange correlation functional with the 6-311G** basis set. Dependence of the electronic properties of the oligomers on their lengths revealed that each residue contributes about 3 Debye to the macromolecular dipole moment. We also investigated n- and p-doping of the oligomers by attaching electron donating and electron withdrawing groups, respectively, to various positions of the aromatic ring of the residues. As expected, n-doping (using diethylamine and ethoxy groups) lead to shift of the level of the frontier orbital (FO) to higher energy. Similarly, the energy levels of the FO decreased upon p-doping (using nitro and pthalimide groups). In addition to these expected energy shift, we observe two other effects from the doping that significantly impacted the electronic properties of the bioinspired system: (1) Proper positioning of the electron donor and withdrawing groups further polarized the aromatic residues, increasing the intrinsic dipole moment to about 5 Debye per residue. (2) Extension of the π-conjugation by the doping groups narrowed the band gap with as much as 1.1eV. We believe that the investigated bioinspired systems offer perspectives for the development of broad range of organic electronic materials with non–linear properties. The expected rectification properties of the oligoanthranilamide present venues for improved photovoltaics and molecular-electronics application.

Microfluidic Devices for Luminescence Lifetime Measurements with Submillisecond Resolution Using Solely Steady-State Excitation and Detection

Brent Millare and Valentine I. Vullev

Emission lifetimes of photoexcited species provide invaluable information that is complementary to their steady-state spectral characteristics. For example, terbium (III) has been employed in emission-enhancement assays for detection of bacterial endospores through complexation with dipicolinic acid (DPA), a natural product found solely in spores.(*Anal. Chem.* **1997**, 69, 1082; *ibid* **1998**, *70*, 1755.) As we have shown, while only minimal perturbation in the emission bands reflects changes in the state of ligation of terbium ions, a four-fold increase in the luminescence lifetimes accompanies the increase in the number of DPA ligands, from 0 to 3.(*J. Am. Chem. Soc.* **2006**, *128*, 16062; *J. Phys. Chem. A* **2002**, *106*, 8213; *Photochem. Photobiol. Sci.* **2002**, *1*, 925.) Time-resolved techniques, necessary for measuring emission lifetimes, however, require pulsed (or frequency-modulated) light sources and/or fast detectors. Herein, we will present an inexpensive alternative for emission time-resolved measurements based solely on steady-state excitation and detection. The dynamic nature of flows in microchannels provided the temporal resolution of the described technique. A light-emitting diode (LED), coupled to a microfluidic (mF) chip through an optical fiber, illuminated a small area of a channel. Despite the relatively small flow rates used in mF devices (e.g., in the order of mL/s), the linear rates of flows through microchannels can easily be in the order of meters per second. As the chromophores carried by the laminar microflows with such large linear rates pass through the LED-illuminated area, they experience pulsed excitation. The "pulse width" depends on the size of the illuminated spot and the flow rate. As the flow carries them away from the illuminated area, the photoexcited species decay to ground state by leaving luminescence traces along the mF channel, that are readily imaged using a CCD camera. Deconvolutive conversion of the distance from the points of illumination into time after the excitation (by using the linear flow rates), resulted in emission decay curves, from which the luminescence lifetimes are readily extracted. Using the described mF time-resolved measurements we investigated the luminescence properties of DPA chelates of Tb (III) and Eu (III). The obtained lifetimes were in an excellent agreement with lifetimes measured using time-correlated single-photon counting techniques. We believe that the described mF technique will provide means for facile and inexpensive incorporation of time-resolved measurements in lab-on-a-chip devices.

Flow Restrictions and Fluid Turbulence in Microfluidic Channels

Joseph M. Clift, Marlon Thomas and Valentine Vullev
Department of Bioengineering, University of California, Riverside, California 92521

The objective of this study is to broaden the capability of non-lithographic fabrication by developing an approach for generating features smaller than the resolution limit of the currently used printers. Our research demonstrates techniques for reproducible fabrication of small restrictor channels (gates) for limiting fluid flows. Evaluations of the printed restricting channels have shown that at the junction point angles at 30° and 60° separated by distances of twenty microns yield small connections. These small restrictor channels have connection widths of approximately 100 μm.

Since photolithography and the printing of channels on transparencies are limited to two dimensions, a need has developed for methodologies that produce three-dimensional microstructures in a single casting step. A non-lithographic methodology developed in our laboratory allowed for fabrication of cylindrical channels with spiral grooves along their walls. These channels produce twists in the flow directions that result in fast mixing. Tests at flow rates 2, 20 and 200 μl/min demonstrated that the presence of spiral grooves in the channels results in mixing superior to that of smooth-walled channels fabricated via the existing procedures.

Modulating hepatic gene expression using shRNA-aptamer construct

Nazgul Tuleuova*§, Chung-Il An*, Erlan Ramanculov§, Yohei Yokobayashi*# and Alexander Revzin*#

*Department of Biomedical Engineering, University of California, Davis, CA

§National Center for Biotechnology, Republic of Kazakhstan

#Correspondence: yoko@ucdavis.edu, arevzin@ucdavis.edu

The ability to modulate gene expression in mammalian cells leads to improved understanding of genetic regulation of cell function and therefore has important applications in cell biology and therapeutics. RNA interference (RNAi) has emerged as a powerful technology to silence arbitrary genes by designing small RNA constructs to target messenger RNA (mRNA) sequences. This presentation will describe a gene silencing strategy that allows dose-dependent modulation of an endogenous gene expression. This strategy utilized short hairpin RNA (shRNA) to silence expression of a liver-specific gene, albumin. In order to regulate gene expression in a dose-dependent fashion shRNA designed to silence albumin was fused with an RNA aptamer which was selected *in vitro* to bind a small molecule theophylline. Transfection of shRNA-aptamer expression vector into hepatic (HepG2) cells resulted in silencing of albumin gene expression through posttranscriptional degradation of albumin mRNA. However, addition of theophylline into cell culture media and its subsequent interaction with the shRNA-aptamer construct prevented RNAi and had the effect of rescuing gene expression in a dose-dependent fashion with increase in protein and mRNA levels corresponding to an increase in concentration of this small molecule. The modulation of gene expression was verified using ELISA and real-time RT-PCR and was shown to be specific to albumin. In the future, dose dependent regulation of hepatic gene expression may be used to investigate molecular events underlying liver fibrosis and may also be applied in driving embryonic stem cells towards hepatic lineage selection.

Development of photo-crosslinker for lipid ligand

Yongfeng Zhao, Jiayu Liao
Department of Bioengineering, Bourns College of Engineering, University of California-Riverside, Riverside, CA 92507, USA

Lipids are a diverse group of compounds that have many key biological functions, such as acting as structural components of cell membranes, serving as energy storage sources. It is interesting that lipid also widely participate in signaling pathways. Lipid pathway is a vital part of cell signaling.

Recent deorphanization effects have paired a series of G-protein-coupled receptors (GPR) with fatty acids as endogenous ligands. While the fatty acids were traditionally known to serve as nutrient resources and biomarkers of disease, these studies show that fatty acids can act as signaling molecules at the cell-surface level. GPR40, activated by long-chain free fatty acids, is highly expressed in the beta cell of pancreatic islets, and enhances glucose-stimulated insulin secretion. These result suggested that GPR40 is possible novel target for the treatment of type 2 diabetes and obesity.

Although a lot of data indicate that fatty acid act as ligand for GPR40, binding experiments using proper synthetic compounds with high affinity are required to analyse the direct interaction between fatty acid and GPR40. To investigate the interaction with the ligand and GPR40, lipid ligand with photo-crosslinker were designed and synthesized. Figure 1 shows the principle of this novel approach. Figure 2 list two typical lipid ligands we have synthesized. We believe that our research will provide new insight into insulin secretion mechanism and the treatment of diabetes.

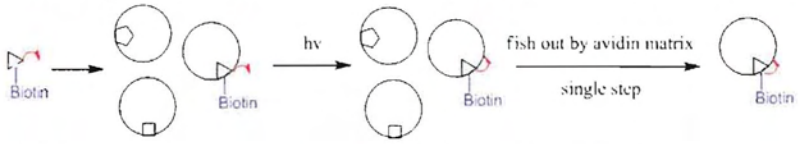

Figure 1. Indentify and evaluate the interaction between the ligand and protein.

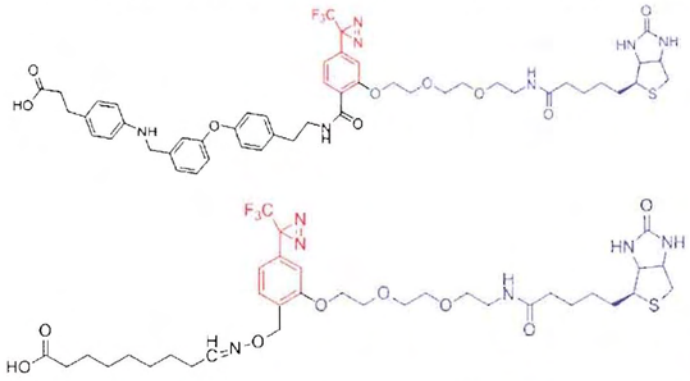

Figure 2. Structure of biotinylated diazirinyl lipids ligands.

Effect of shear stress on the inflammatory potential of endothelial cells

Ying Wang, R. Michael Gower, Scott I. Simon
Department of Biomedical Engineering, University of California, Davis, CA

Atherosclerosis is a chronic inflammatory arterial disease characterized by atheromas frequently developed in some specific arterial geometries, such as posterior aorta and arterial branch points. Local hemodynamic studies have recently revealed that flows in these apparent athero-prone areas are disturbed flows (DF), with high oscillatory shear index (OSI), while flows in athero-resistant areas are mostly undisturbed laminar ones, suggesting a potential role of the local flow profile in regulating vascular response. On the other hand, the inflammatory responses to atherosclerotic stimuli of endothelial cells, which line the inner wall of arteries, have been recognized as important early-stage events in atherogenesis. This study aimed to explore how shear stress affects endothelial cell inflammatory response. Human aortic endothelial cells (HAECs) were pre-exposed to oscillatory shear stress, and the inflammatory potential of HAECs were investigated through stimulation by TNF-α. Cell adhesion molecule expression was evaluated by immunofluorescence microscopy and flow cytometry. Hele-Shaw flow chambers were further introduced to provide a wide linear range of shear stress. Our results showed significantly greater upregulation of E-selectin, VCAM-1 and ICAM-1 in HAECs, when they were pretreated with oscillatory flows, indicating that oscillatory shear stress enhance the inflammatory potential of endothelial cells.

Recombinant mussel adhesive protein as a gene delivery material

Dong Soo Hwang[1,2], Hyung Joon Cha[2], Matthew Tirrell[1]

[1]*Material Research Laboratory, University of California, Santa Barbara, CA 93106, United States*

[2]*Department of Chemical Engineering, Pohang University of Science and Technology, Pohang 790-784, Korea*

Abstract

Efficient target gene delivery into eukaryotic cells is important for biotechnological research and gene therapy. Gene delivery based on proteins, including histones, has recently emerged as a powerful non-viral DNA transfer technique. Here, we investigated the potential use of a recombinant mussel adhesive protein, hybrid fp-151, as a gene delivery material, in view of its similar basic amino acid composition to histone proteins, and cost-effective and high-level production in *Escherichia coli*. After confirming good DNA binding affinity, we transfected mammalian cells (human 293T and mouse NIH/3T3) with foreign genes using hybrid fp-151 as the gene delivery carrier. Hybrid fp-151 displayed similar or higher transfection efficiency in both mammalian cell lines, compared to the widely used transfection agent, Lipofectamine™ 2000. Our results indicate that this mussel adhesive protein can be successfully used as a protein-based gene-transfer mediator.

Keywords: mussel adhesive protein; hybrid fp-151; DNA binding; gene delivery ma terial; transfection; mammalian cells

ATR Analysis of Nucleic Acid-Lipid Self-Assembling Complexes for Drug Delivery on Biochips

Thorsten Neumann[1,3], Surekha Gajria[1,3], Wirasak Smitthipong[1,2], Luc Jaeger[1,3] and Matthew Tirrell[1,2]
[1]Materials Research Laboratory, [2]College of Engineering, [3]Department of Chemistry and Biochemistry; University of California, Santa Barbara, CA 93106, USA

Please submit all queries by email to tirrell@engineering.ucsb.edu and by phone to (805) 893-5302

In order to better manipulate the properties of our self-assembling nucleic acid-lipid films, it is essential to determine the different melting temperatures and temperature-dependent reorganization processes that occur with different complexes, as well as their rate of biodegradation and drug release. To do this we have built a homemade ATR (attenuated total reflectance fluorescent reader) that in combination with biochips can measure many reactions at once in real time. We have used this technique to determine the biodegradation of these materials in blood serum and their melting temperatures in buffer using nucleic acid-intercalating fluorescent dyes. Daunorubicin, which is a fluorescent intercalating cancer drug, was also used as a model for a drug delivery system. We have shown that by changing the type of nucleic acid used in the lipid complex we can vary the degradation rate and the rate of drug release.

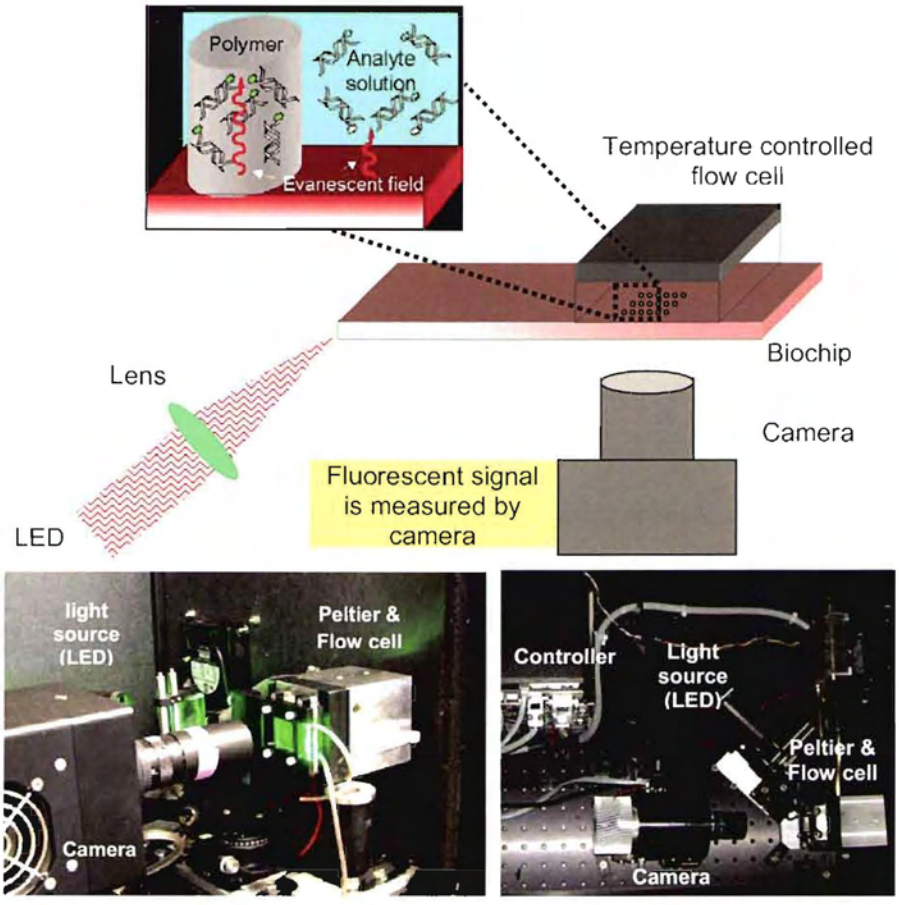

A Pneumatic Balloon Actuator for use in Refreshable Braille Displays

Adam M. Feinman[1,4], Chih-Hung King[1,2], Miguel L. Franco[1,2], James W. Bisley, PhD[1,5], Erik P. Dutson, MD[1,3], Martin O. Culjat, PhD[1,3], Warren S. Grundfest, MD,[1,2,3]

[1]Center for Advanced Surgical and Interventional Technology (CASIT), [2]Biomedical Engineering IDP, [3]Department of Surgery, [4]Computational and Systems Biology IDP, [5]Department of Neurobiology, University of California, Los Angeles, Los Angeles, CA 90095

Since the 1970s, researchers have been struggling to improve the functionality and economy of refreshable Braille displays. Many attempts to create new ways to display refreshable Braille have been attempted, but few have worked and/or become popular amongst commercial users. Amongst the ones that have worked well, one of the cheaper Braille displays sold commercially, which uses piezoelectric crystals, still use Braille cells that cost about $35 dollars a cell. A pneumatic balloon actuator has been developed for use in refreshable Braille displays that is small, easy to produce, and requires little power. Each actuator consists of a molded PDMS block with cylindrical channels bound to a 200-μm spin-coated silicone membrane. Pneumatic valves apply pressure to the membrane via the cylindrical channels. The deflections in the membrane caused by the pneumatic pressure form a 2 x 3 balloon array. Previous studies have been done using blinded subjects to characterize the actuator with different balloon diameters and balloon spacing to characterize the structural stability of the actuator as well as the deflections of different balloons diameters under different levels of pneumatic pressure. It was determined that an actuator that approximated the dimensions of standard American Braille would be structurally stable. The actuator applies 13 psi to balloons with a diameter of 1.5 mm spaced 1.0 mm apart to achieve about 0.5 mm of deflection. Standard American Braille uses dots with diameter 1.45 mm and height 0.48 mm spaced 0.89 mm apart. Further work will need to be done to compare the readability of this actuator as well as research into less costly pneumatics for this Braille cell.

The Atheroprotective Pulsatile Flow Activates the AMP-activated Protein Kinase-Krüppel-like factor 2 in Vascular Endothelial Cells

Wei Wu[1], Angela Young[2], Wei Sun[1], Yi-Shuan Li[2], John Y Shyy[1], and Shu Chien[2]

[1]Division of Biomedical Sciences, University of California, Riverside, CA, 92521, [2]Department of Bioengineering, University of California, San Diego, La Jolla, CA

Vascular endothelial cells (ECs) provide athero-protective functions in the straight part of the arterial tree under pulsatile laminar shear flow (PS) with a high shear stress and a large net forward direction. AMP-activated protein kinase (AMPK) plays a central role in controlling energy and metabolism homeostasis in various organs. The transcription factor Kruppel-like factor (KLF2) is a critical integrator of multiple endothelial functions, including inflammation, vascular tone, blood vessel development. We showed that PS flow can activate AMPK and induce KLF2 expression in ECs. AMPK inhibitor Compound C had a significant blocking effect on the downstream target of AMPK, i.e. acetyl-CoA carboxylase phosphorylation, as well as the induction of KLF2 by PS flow. The induction of KLF2 gene expression by PS flow led to the augmentation of anti-inflammatory gene endothelial nitric oxide (eNOS) and the suppression of pro-inflammatory gene endothelin-1 (ET-1). KLF2 knockdown significantly reduced the PS-induced KLF2 and eNOS expressions, as well as ET-1 suppression. In addition, PS can induce phosphorylations of ERK5 and MEF2 to enhance KLF2 expression. Blocking AMPK caused the reduction of PS-indunced ERK5 and MEF2 phosphorylations. The phosphorylation levels of ERK5 and MEF2, as well as the expression of KLF2, were significantly reduced in the aorta of AMPKα2 knockout mice in comparison with control mice. In conclusion, our findings suggest that PS regulates anti-inflammatory functions in ECs via the AMPK-ERK5-MEF2-KLF2 pathway.

Translocation of ATP synthase β chain by laminar versus oscillatory flow

Yi Fu[1,2], Yingjian Hou[2], Yi Zhu[2], and John Y-J. Shyy[1]

[1]Division of Biomedical Sciences, University of California, Riverside, [2]Department of Physiology & Pathophysiology, Peking University Health Science Center, Beijing, PRC

Shear stress plays an important role in endothelial function and can be a major pathogenic factor of atherosclerosis, depending upon flow patterns. ATP synthase β chain is the enzymatic center of this synthase and locates either in mitochondrion or on the cell membrane. In addition to playing a key role in ATP synthesis, ATP synthase β chain also exerts other functions such as the receptor for apoA-I and apoA-I can bind to T cell γ/δ receptor. In this study, we examined whether shear stress affects cellular cholesterol metabolism and thus induces the translocation of ATP synthase β chain in bovine aortic endothelial cells (BAECs). Our results showed that laminar flow caused a decrease in membrane cholesterol in BAECs with attendant increased translocation of ATP synthase β chain from membrane to mitochondrion. As a result, ATP synthesis was increased in the EC cytosol. In contrast, oscillatory flow increased the cholesterol content membrane and decreased the translocation of ATP synthase β chain in ECs under oscillatory flow was marginal, compared to these events in ECs exposed to laminar flow. The incubation of ECs with cholesterol or depletion of EC cholesterol with β-cyclodextrin mimicked the respective effects of laminar and oscillatory flows. The inhibition of caveolin-1 expression by caveolin-1 siRNA prevented the translocation of ATP synthase β chain in ECs responding to laminar flow. Our results provide some molecular evidence underlying the cholesterol metabolism in ECs exposed to athero-protective versus athero-prone flow patterns.

Electrostatic Contributions in Binary Protein Ultrafiltration

Yiheng Wang, Bioengineering, University of California, Riverside, CA 92521
Victor G. J. Rodgers, Bioengineering, University of California, Riverside, CA 92521

The current research investigates, both experimentally and theoretically, the important electrostatic effects on binary protein ultrafiltration (UF) performance via factors such as system pH and ionic strength.

Experimental method: Four proteins were used in this study: α-lactalbumin (αLA, 15 kDa), hen egg lysozyme (HEL, 15 kDa), cytochrome C (CytC, 15 kDa) and bovine serum albumin (BSA, 69 kDa). Cross-flow UF experiments were conducted for three binary protein systems: αLA/BSA, CytC/BSA and HEL/BSA. These systems were chosen due to their similar protein/protein size ratio however different charge properties, so they were ideal systems to study the non-solute-size effects, especially electrostatic effects, in binary protein UF. The membrane used in all experiments was 30,000-MWCO composite regenerated cellulose (CRC) membrane, selected for its low extent of fouling. The experiments were conducted at various pH values (pH 4.7, pH 6, pH 7, pH 8 and pH 10), and low to moderate ionic strengths (0.0015 M, 0.015 M and 0.15 M). During the experiments, the applied operating hydraulic pressure was varied randomly in the range from 0 to 145 kPa, and the permeate flux versus pressure dependence profiles, as well as the corresponding protein sieving behaviors, were recorded.

Experimental result analysis: The pH and ionic strength dependences of the permeate flux were first observed in the single BSA UF experiments that served as controls. The permeate flux generally increased with increasing pH (which corresponds to the increase of BSA net charge), and decreased with increasing ionic strength. For the binary protein UF experiments, the permeate flux behaviors differed largely from system to system, as expected. For the αLA/BSA system in which αLA was similarly charged as BSA at all pH values studied, the flux-pressure behaviors were almost identical to those of the control experiments with BSA only. On the other hand, for the HEL/BSA system consisting two proteins that were always oppositely charged at the pH values studied, the permeate flux-pressure behaviors differed largely from control experiments. At lower ionic strengths, the significant pH dependence as well as unusual patterns in the permeate flux-pressure profiles strongly suggested reversible formation of HEL-BSA complex caused by electrostatic interaction. Though less significantly, the CytC/BSA system showed similar flux behaviors as the HEL/BSA system. The observed sieving coefficient (as a function of the permeate flux) of the 15 kDa proteins for all three binary protein UF systems also demonstrated clear pH, ionic strength and system dependences.

Theoretical modeling: The free solvent-based model (FSB), which successfully predicts and characterizes of the flux behavior in protein UF with moderate electrostatic "screening", was modified to include electrostatic contributions, and was applied to the theoretical modeling of the observed experimental observations. The modified film theory [Ref. 2], which includes a permeate flux contribution resulted from the electrostatic forces on the solute particles in the concentration polarization layer, was used to study the pH and ionic strength dependences observed in single BSA UF flux behaviors. Through this approach, the regressed protein surface potential values for each solution condition agreed with the literature reasonably well; however, the limitations of this approach were also recognized. Hindered transport theory [Ref. 3] with electrostatic contribution was used to study the electrostatic interaction effects on the sieving behaviors in binary protein UF. For the αLA/BSA system that only contains repulsive interactions, the model calculations agreed well with the experimental observations. For the other two systems that contain attractive interactions, theoretical modeling is currently on-going.

[Ref. 1]: Y. Wang, and V.G.J. Rodgers, J. Membr. Sci., in press.
[Ref. 2]: R.M. McDonogh, A.G. Fane, and C.J.D. Fell, J. Membr. Sci., 43 (1989) 69-85.
[Ref. 3]: W.M. Deen, AIChE Journal, 33 (1987) 1409-1425.

Pump-probe imaging of nanosecond laser-induced bubbles in agar gel

F. Pérez-Gutiérrez[1], R. Evans[2], S. Camacho-López[2], and G. Aguilar[1]
1. Department of Mechanical Engineering, University of California, Riverside
2. Department of Optics, Centro de Investigación Científica y Educación Superior de Ensenada, México.

We show results of Nd:YAG laser-induced bubbles formed in a one millimeter thick agar gel slab. The nine nanosecond pulse duration with a wave length of 532nm was tightly focused inside the bulk of the gel sample. We present for the first time a pump-probe laser-flash shadowgraphy system that uses two electronically delayed Nd:YAG lasers to image the bubble formation and shock wave fronts with nanosecond temporal resolution and up to nine seconds of temporal range. The shock waves generated by the laser are shown to begin at earlier times within the laser pulse as the pulse energy increases. The shock wave velocity is used to infer a shocked to unshocked material pressure difference of up to 500MPa. The bubble created reaches a quasi-stable size that has a linear relation to the maximum bubble size. The energy stored in the bubble is shown to increase nonlinearly with applied laser energy, and corresponds in form to the energy transmission in the agar gel. We show that the interaction is highly nonlinear, and most likely is plasma-mediated.

Energy-Aware Heart Rate Monitoring During Stair Climbing

Navid Amini, Mahsan Rofouei, William J. Kaiser, Majid Sarrafzadeh
University of California, Los Angeles

Stair climbing is one of the most energy-burning sports, requiring individuals to move their entire body weight vertically, instead of horizontally. Stair climbing exercise has been shown to be very effective in improving cardiovascular fitness, reducing cholesterol levels, decreasing body fat, and increasing the strength of the lower limbs. Besides the above mentioned benefits, being able to provide accurate estimates of the amount of energy expenditure during stair climbing motivated us to monitor the heart rate changes during ascending stairs. Although previous studies have determined the caloric cost of stair climbing, none of them has been conducted on an actual staircase with a large number of stairs. Accordingly, the purpose of this study is to determine the heart rate response during the stair climbing exercise for different intensities of constant-load exercise (see Figure 1). To this end, we used the stepmill (Figure 2) since it excellently performs like a real stair climbing exercise.

Two healthy male volunteers with an average level of cardiovascular fitness carried out two different intensities of exercise on a stepmill for three times in three different days and their heart rates were measured using a Bluetooth pulse oximeter (Figure 2). In this work, we attempted to fit the heart rate trends induced by constant exercise loads of different intensities to a second-order exponential function:

$$HR = \alpha_1(e^{\beta_1 t}) + \alpha_2(e^{\beta_2 t}) \qquad (1)$$

Through employing the least-squares method in MATLAB we compared the results with fitting of the heart rate changes to first-order exponential curves. The second-order exponential function suitably fitted the heart rate responses induced by two different intensities of loads for stair climbing (see Figures 3 and 4): moderate (91.5 W: correlation coefficient, r = 0.9732 ± 0.01), high (149.2 W: r = 0.9684 ± 0.02). However, the first-order exponential curve to some extent fitted the moderate case only (91.5 W: correlation coefficient, r = 0.8737 ± 0.03).

The presented results indicate that the second-order exponential function fitted the heart rate response for both the moderate and high loads and is more reliable than first-order exponential function to analyze the heart rate response during climbing stairs, however, this function includes many regression coefficients whose relation to factors like age and gender needs to be determined.

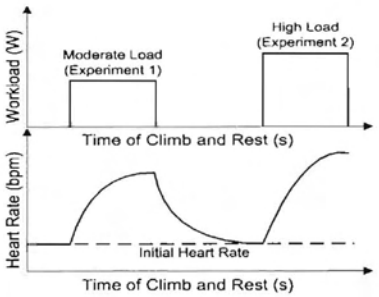

Figure 1: Heart rate changes versus time during stair climbing with different climbing speeds (workloads).

Figure 2: The Stairmaster stepmill 7000PT and Nonin's pulse oximeter.

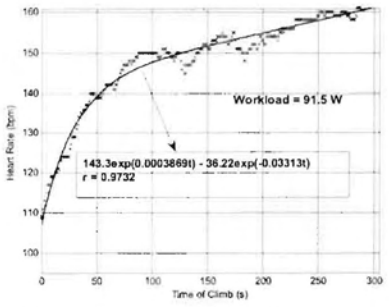

Figure 3. Heart rate versus time in the first experiment (Climbing a 14-story building in 5 minutes).

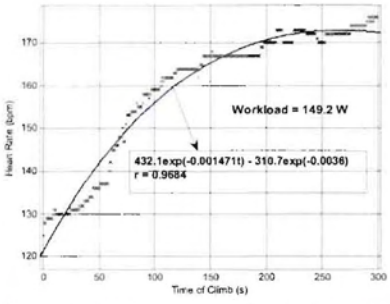

Figure 4. Heart rate versus time in the second experiment (Climbing a 24-story building in 5 minutes).

Addressable Shrinky-Dink Hanging Drops for Stem Cell Culture and Differentiation

Chi-Shuo Chen, Bing Xia, Anthony Grimes, Diep Nguyen, Jesus Luna, and Michelle Khine
School of Engineering
University of California, Merced

Abstract:

The most common way currently to create embryoid bodies (EB), aggregates of embryonic stem cells, is the hanging drop method. This laborious approach involves pipetting an arbitrary number of cells into well plates. Generation of EBs is promoted by the interactions between the stem cells when forced in close proximity of one another. However, because the media in each of the wells has to be manually exchanged every day, this approach is manually intensive. More critically, because EB size can be a function of environmental parameters (including cell-cell, cell-soluble factor interactions, pH, and oxygen availability), cell populations obtained from traditional hanging drops can vary dramatically even when cultured under identical conditions. Recent studies have indeed shown that the initial number of cells forming the aggregate can have significant effects on stem cell differentiation. Finally, large scale screenings of chemical cues, such as growth factors, to differentiate the EBs, under identical conditions is challenging with the traditional approach. While microfluidic approaches enable perfusion of chemical cues in a large scale array, it is typically difficult to remove the cells from the microsystem for further off-chip analysis.

To address these limitations, we have developed a simple, rapid, and scalable culture method to: load pre-defined numbers of cells into microfabricated wells, control the size of the wells, maintain the cells for embryoid body development, subject the EBs to various chemical cues by perfusion, and provide easy access for further analysis and experimentation.

This method is amenable to any lab and requires no dedicated equipment. We create microfabricated wells without any photolithography by using the children's toy Shrinky-Dinks. Shrinky-Dinks are essentially pre-stressed, printable, polystyrene sheets that shrink upon heating. We use this to replace the silicon wafer as a mold for PDMS. To load the cells into the wells, we centrifuge different cell concentrations into the wells. We verify the average number of cells per well by optical inspection. After the EBs develop, we can add our reversibly-bondable perfusion chamber on top of the EBs to subject the cells to various chemical cues.

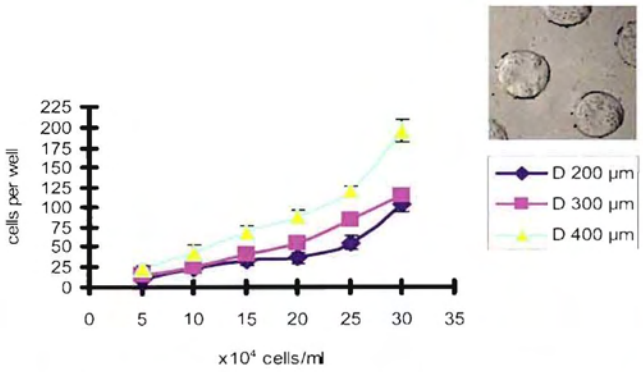

Figure 1. Graph of # of cells per well as a function of concentration (left) and representative picture of cell loading (right).

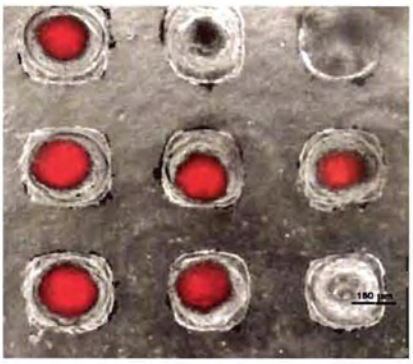

Figure 2. Picture of EBs.(red fluorescent mouse cell line (129S6B6-F1) growing in wells at 4 days.

Digital Holographic Microscopy: A Unique Tool for Analyzing the Mechanical Properties of Cell and the Extracellular Matrix

Kaveh Azartash, Enrico Gratton
University of California Irvine

Principles of digital holography are applied to study the dynamics of cell and its extracellular matrix. Digital holographic microscopy (DHM) has appeared as a unique tool to study the shape and deformation at the nano-scale by resolving differences in refractive index. A digital holographic microscope with the ability to interchange between transmission and reflection mode is designed and built to record two–dimensional holograms on a CCD camera. The digitally recorded holograms are numerically reconstructed based on the angular spectrum method (ASM) providing a better signal to noise ratio in comparison with the traditional Fresnel method. The graphical user interface developed with matlab based on the ASM method outputs the intensity and phase images. The phase images are unwrapped to eliminate the 2pi ambiguity applying the Flynn's discontinuity algorithm. The unwrapped phase images are employed to perform quantitative phase-contrast imaging. The importance of conducting quantitative phase analysis rises up when one needs to reveal the optical thickness profile of a transparent specimen with sub-wavelength accuracy. Digital holography not only offers a simplified and easy to use technique but also has the advantage of yielding quantitative analysis of the phase distribution introduced by the biological samples. The goal of this study is to measure cell-migration induced deformation of collagen matrix. Quantitative phase information concerning cell morphology and volume along with those of the extracellular matrix could be obtained with digital holographic microscopy. One of the major advantages of DHM is that this method is completely non-invasive and there is no need to dissect the sample or to stain it.

Quantifying Phagocytosis II: Comparison of Neutrophils and Macrophages

Jonathan Lam,[1] Cheng-Yuk Lee,[1,2] and Volkmar Heinrich[1]
Departments of [1]Biomedical Engineering and [2]Chemical Engineering and Materials Science, University of California, Davis

A variety of cell types are capable of target engulfment by phagocytosis, which raises a critical question: Do all phagocytes follow the same mechanical program of phagocytosis, or are there quantitative or even qualitative differences between the mechanistic schemes across different phagocytes and/or phagocytic pathways? Answering this question will allow us to evaluate, for example, to what extent insights obtained from experimentally more amenable cell lines can be generalized to phagocytosis in humans. Here, we aim to establish similarities and differences in the phagocytosis of antibody-coated beads by human neutrophils and murine macrophages (J774 cell line).

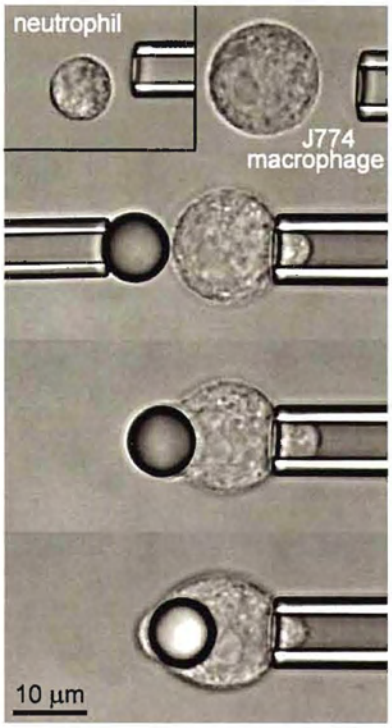

As a first step, we compared the baseline mechanical properties of passive cells. Micropipette-aspiration experiments were used to characterize the cortical tension and cytoplasmic viscosity of both cell types. The cortical resting tension of passive macrophages and their viscosity were found to be higher than the respective values of neutrophils, revealing that overall, the J774 macrophages are mechanically stiffer than human neutrophils.

Moving on to phagocytosis experiments using our dual-micropipette manipulation system, we discovered a number of differences between the mechanical parameters characterizing target engulfment by the two cell systems. Both neutrophils and macrophages were able to call upon an immense reservoir of membrane during phagocytosis; however, macrophages were able to utilize these reserves at a much lower energetic cost than neutrophils. We observed macrophages ingesting beads larger than the cells without increasing the cortical tension. The maximum area increase in macrophages was >3.5 fold of their resting surface area, compared to ~2.6 fold for neutrophils. Additional differences were observed in the timing of different characteristic phases of phagocytosis. For example, neutrophils generally began engulfing their targets earlier than macrophages. Furthermore, the presence of a nucleus in macrophages hindered the inward movement of larger target beads during engulfment. These and other results indicate that different phagocytic cell types may not follow a universal mechanistic program of target engulfment.

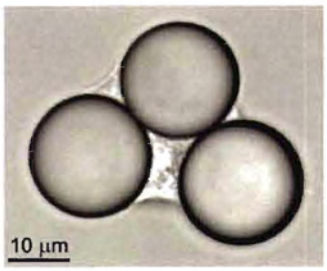

Concentrating DNA with Aqueous Complex Fluid Solvents for Cancer Diagnosis

Foad Mashayekhi, Aaron S. Meyer, Stacey A. Shiigi, Vu Nguyen, Daniel T. Kamei
Department of Bioengineering, University of California, Los Angeles, CA 90095

Cancer is the second leading cause of death in the United States. Studies suggest, however, that early diagnosis and treatment of cancer significantly increases the chances of survival [1]. The efforts directed at identifying biomarkers for robust cancer diagnosis has yielded promising results in recent years. Nevertheless, early detection of cancer still remains a challenge due to the low concentrations of biomarkers that are present during the early stages of various cancers [2, 3]. Accordingly, lowering the detection limit would prove useful, and this may be accomplished by improving either the sensors and/or the sample preparation. In this presentation, we focus on the latter method by developing a concentration step that can increase the concentration of mammalian genomic DNA fragments prior to detection. Specifically, we are investigating two-phase aqueous micellar systems in a liquid-liquid extraction process, since these systems have the advantage of both phases being primarily comprised of water, which can provide a mild environment for the biomolecules.

Two-phase aqueous micellar systems are composed of mainly water and surfactants. Increasing the temperature can induce a macroscopic phase separation, where a homogenous micellar solution separates into a bottom, micelle-rich phase, and a top, micelle-poor phase, as shown schematically in Figure 1. DNA fragments partition unevenly between the two phases based on their physico-chemical characteristics. Our recent results demonstrate that two-phase aqueous micellar systems can indeed be used to concentrate mammalian genomic DNA fragments. Moreover, the partitioning behavior of these molecules were determined to be primarily driven by steric, repulsive excluded-volume interactions that operate between the micelles and the DNA fragments, while being limited by the entrainment of micelle-poor, DNA-rich domains in the macroscopic, micelle-rich phase.

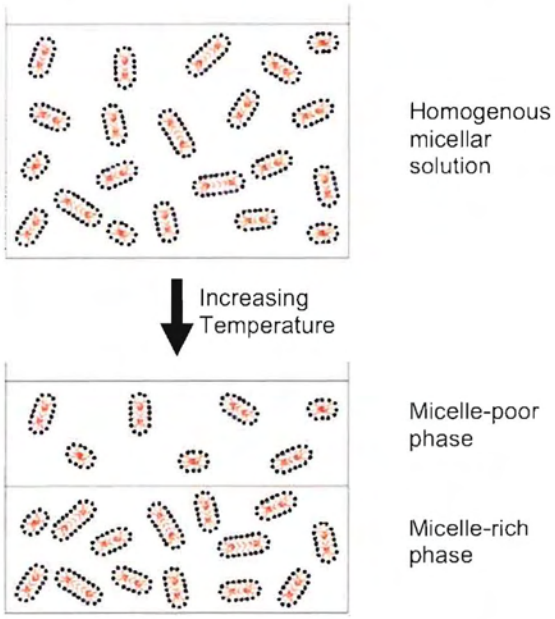

Fig. 1. Schematic representation of the phase separation associated with a Triton X-114 aqueous micellar system.

REFERENCES

1. Surveillance, E., and End Results (SEER) Program (www.seer.cancer.gov), 2007.
2. Fournie, G.J., *et al. Cancer Lett* 1995. **91**(2): p. 221-227.
3. Li, J., *et al. Clin Chem* 2002. **48**(8): p. 1296-1304.

Self-Assembly and DNA Binding Properties of bZip Peptide Amphiphiles

Rachel Marullo, Raymond Tu, Matthew Tirrell
Materials Research Laboratory, University of California, Santa Barbara

The GCN4 protein is a well-studied transcription activator in yeast. bZip, a thirty-eight amino acid peptide derived from GCN4 that retains the DNA-binding ability, contains a leucine zipper dimerization segment and a basic binding region. Conjugating a hydrophobic tail to bZip promotes the formation of cylindrical micelles in aqueous solution. Circular dichroism has shown that the peptides adopt a high degree of α-helical secondary structure in the aggregated state compared to the monomer. This enhanced secondary structure facilitates DNA binding in a fashion similar to the native protein, in contrast to the typical binding saturation curve of the unmodified peptide. Binding studies were performed using gel electrophoresis and fluorescent intercalator displacement assays. Future work will include *in vitro* cell assays of bZip peptide amphiphile micelles to determine cellular uptake and nuclear targeting. Biofunctional bZip constructs may have applications as artificial transcription factors or gene delivery vehicles.

Name	Page	Location
Heller, Michael J.	79,80,98	Podium IV, A4
Hettiarachchi, Kanaka	65	Podium III
Ho, Chih-Ming	96	A2
Hsiao, Alexander	98	A4
Hu, Simon	39	Podium I
Huang, Carlos	68	Podium III
Hwang, Dong Soo	118	A18
Hwang, Yu-Jer	73,90	Podium IV, B9
Jaeger, Luc	57	Podium II
Jeon, Noo Li	68	Podium III
Jing, Xiaoye	97	A3
Jung, Bongsu	104	A10
Jung, Woonggyu	40	Podium I
Kamei, Daniel T.	58,58,63,129	Podium III, B23
Karplus, Kevin	34	Podium I
Kastantin, Mark	55	Podium II
Khine, Michelle	43,69,126	Podium I, III, B25
Kieslich, Chris A.	47	Podium II
Kim, Min-Ho	61	Podium III
Krishnan, Rajaram	80	Podium IV
Kyle, Jennifer Reiber	101	A7
Lam, Jonathan	128	B22
Lee, Abraham P.	65,100	Podium III, A6
Lee, Chang Won	76	Podium IV
Lee, Cheng-Yuk	78	Podium IV
Lee, Hua	85	B4
Lee, Michael	85	B4
Lefkowitz, Roy B.	79	Podium IV
Lemoyne, R.C.	66	Podium III
Levesque, Marshall J.	36	Podium I
Li, Rong	45	Podium I
Liao, Jiayu	59, 116	Podium II, A16
Lopez De Victoria, Aliana	106	A12
Louie, Angelique	81,84	Podium IV,B3
Lowengrub, John	49	Podium II
Lyubovitsky, Julia G.	73,90	Podium IV,B9
Mahjoob, Shadi	107	A13
Maibach, Howard I.	89,93	B8,B12
Martinez-Morales, Alfredo A.	109	B14
Mahjoob, Shadi	107	A13

Name	Page	Location
Singh, S.	51	Podium II
Song, Yang	59	Podium III
St. James, Sara	71	Podium IV
Stybayeva, Gulnaz	99	A5
Sun, Feng	52	Podium II
Sun, Victor Z.	63	Podium III
Tan, Robert	42	Podium I
Tanner, Kandice	53	Podium II
Teh, Shia-Yen	100	A6
Tewari, Priyamvada	108	A14
Thomas, Marlon	77	Podium IV
Tirrell, Matthew	55,62,64,118,119, 130	A18,A19,B24 Podium II, II, IV
Trent, Amanda	64	Podium III
Tromberg, Bruce J.	72	Podium IV
Tsourkas, Philippos	46	Podium II
Tuleuova, Nazgul	115	A15
Vandrangia, Prashanthi	92	B11
Vasquez, Jacob M.	56	Podium II
Vigneron, Daniel B.	39	Podium I
Vullev, Valentine	56,77,110,111,112, 113,114	B15,B16,B17 B18, Podium II,IV
Walker, A. M.	91	B10
Wang, Chunsheng	87	B6
Wang, Yiheng	123	A22
Wang, Ying	117	A17
Wei, Fang	96	A2
Wilson, Noah A.	74	Podium IV
Wu, Bing	88	B7
Wu, Wei	121	A20
Yang, Yang	97	A3
Yoon, Dennis J.	58	Podium III
Zhang, Xiaoliang	87,88	B6,B6
Zhang, Yu	102,103	A8,A9
Zhao, Yongfeng	116	A16